Verification and effects investigation of FS Marine+ technology on-board Bravenes

I. Iakovou

TU Delft

Verification and effects investigation of FS Marine+ technology on-board Bravenes

by

I. Iakovou

This thesis (MT.21/22.048.M) is classified as confidential in accordance with the general conditions for projects performed by the TU Delft.

To be defended publicly on Wednesday 21 September 2022 at 14:00 PM

Thesis exam committee

Chair/Responsible Professor:	dr. ir. P. de Vos,	TU Delft, supervisor
Independent member:	dr. ir. R D. Geertsma,	Netherlands Defence Academy
Company Member:	ir. J. Voormolen,	Van Oord, supervisor
Staff member:	dr. ir. M. Ramdin ,	TU Delft, Assistant Professor
Staff member:	ir. K. I Kiouranakis ,	TU Delft, PhD candidate

TU Delft

Summary

New vessels need to remain fuel flexible in order to handle the uncertainties of the future regarding the available alternative fuels aiming to lower their environmental impact. On the other hand, it is even more challenging for existing vessels which are not fuel flexible to successfully improve their carbon impact.

The current study examines the combustion characteristics of alternative maritime fuels including methanol and hydrogen in the compression-ignited internal combustion engines of Bravenes that burn diesel fuel, as well as the implications these fuels have on the environment and on safety when used onboard ships. The diesel fuel still acts as the main fuel but also as the ignition fuel for the injected additives. The purpose of the additives is for the substitution of diesel and to offer a more complete combustion in the cylinders. Van Oord is already implementing the Fuelsave Marine+ technology on board of Bravenes. This technology aims to reduce harmful emissions like NO_x and greenhouse gases while also increasing engine efficiency in order to effectively contribute to the overall energy transition. Therefore, the primary goal of this research is to examine if there are any potential impacts of the technology on the efficiency, emissions, and fuel consumption of Bravenes engines.

The existing literature review showed limited to none existing technologies like Fuelsave which enables the injection of low quantities of methanol-water mixtures and hydrogen in the scavenging area of a marine 4-stroke diesel engine. In this master thesis, since no literature material was available for the applied technology, a research was performed for the combination of diesel with methanol, diesel with methanol-water mixture and diesel with hydrogen to investigate their effects on the performance of the engine. Combined with the literature study, documentation from on-board of Bravenes while sailing was used to simulate and calibrate the M32E engines of the vessel in a mean value engine model.

The model used is able to characterise the combustion of the engine using the Seiliger combustion shape parameters a, b and c. These parameters take into account the combustion efficiency, the ignition delay and also the heat fractions of the potential heat for the appropriate stages. The effects of the additives small quantities can be seen in the combustion duration and the ignition delay of the combustion. In order to properly model the additional fuels effects some of the diesel mass needed to be substituted with methanol mass to provide the same energy content in the cylinder. Attention was also given on the proper selection of the X_a&X_b parameters impacting the combustion shape parameters and the pressures and temperatures in the engine.

The results of the model for the diesel and diesel with additives operation predict a decrease in the diesel fuel consumption which is a good indication of CO_2 emissions reduction. The peak cylinder pressures have increased with the additives injection and the peak temperatures as well which indicate an increase of NO_x emissions. The increase of the temperatures is not something expected in reality and could be due to a modelling effect. The indicated work of the engine combustion cycle also improved for the Fuelsave technology but due to the increase in peak pressures the mechanical efficiency decreased resulting in a reduced effective efficiency. The selection of the Seiliger settings, which allowed for a higher heat loss efficiency than was realistically anticipated, is another factor contributing to the decrease in effective efficiency. All in all, proper measurement campaign needs to be performed to show the clear effects of the technology as a retrofit solution on-board existing vessels for efficiency and emission reduction.

Preface

With this report I conclude my studies in the Marine Technology master program at the Delft University of Technology. I am presenting my graduation research about the effects investigation of Fuelsave technology on-board of Bravenes.

I would like to express my appreciation to my TU Delft daily supervisor Peter de Vos and my company supervisor Job Voormolen. I sincerely thank both of them for their guidance, advises and support during the project. I would like to extent my acknowledgement to Van Oord for providing me a workplace and the opportunity to contribute in their project while also getting involve with such an interesting technology.

Last but not least, I would like express my gratitude to my dear friends and family for their positive feedback and support since the beginning of this journey and thank them for following me until the end of this chapter of my life.

I. Iakovou
Delft, September 2022

Contents

List of Figures

List of Tables

1 Introduction

At present, the maritime industry is responsible for a large contribution to harmful and greenhouse emissions including nitrogen oxides, sulphur oxides and particulate matter. Therefore, it is crucial to take action to lower emissions and increase the vessels' energy efficiency. In 2018, the International Maritime Organization set an ambitious GHG strategic plan aiming in the decarbonization of the shipping industry. The aims include the total greenhouse gas emissions reduction by 50% by 2050 compared to year 2008 while at the same time decrease the CO_2 per tonne-mile in international shipping by 40% and 70% by 2030 and 2050 respectively, [6]. Due to the major accountability of the shipping sector in the worldwide emission levels measuring around 2.5% of the global greenhouse gas emissions [44], the need for environmental solutions is present and getting essential as more and more regulations and policies, investors and ship owners pressure for improvements, [8], [9].

The effects of the IMO's strategy are already having an impact on the operation and design of new vessels in order to fulfil the minimum requirements. The standards are high although since the poor performers could be missing their chance in the charter market due to commercial pressure, [7]. It is expected that a period with rapid changes about technology and energy transition will impact the values of assets, the costs and the turnover for ship owners.

It was normal practice in the past for the shipping industry to switch from wind propulsion to fossil fuels, but things are now changing as more options are available with the same objective in mind: the transition to zero emissions. One can comprehend the variety of alternatives by taking into account the alternative fuel sources and engine technologies that are currently available but also in piloting stages. It can be understood that the future for shipping will be highly dependent on the fuel market itself and needs to be interconnected with the energy production and industry of the different regions,[9].

The shipping industry also needs to maintain an open mind and adapt to fuel flexible solutions in order to be fuel ready for the oncoming advancements, as the future still holds many uncertainties about the problems stated above ,[8]. To meet the decarbonization expectations shipowners are required to invest in new fuels and technologies to reduce emissions and improve efficiencies while also prioritizing safety. This is the main topic of the current thesis, the research of a new retrofit technology on-board Bravenes to enable the energy transition to the future of Van Oord.

1.1. Motivation

Van Oord as a family-owned company sets high standards and aims for a net-zero emission future by 2050. One of the current problems faced is the gap between the existing vessels and how to make them future proof since they are valuable assets and are expected to return back profits, thus they should not be left as stranded assets.

In order to successfully transition from the present to the future starting with short-term solutions, one can take into consideration many available options depending on the situation. The current study focuses on a retrofit solution aiming to increase the efficiency and harmful emissions reduction on the current engine power-plant of Bravenes without performing major modifications on main engine components. Figure 1.1 describes the four M32E diesel generators supplying power to the vessel. While sailing the vessel can be operated by the 2 8 cylinder M32E engines providing power to the main

thrusters 5 and 6. Bravenes is a DP3 type vessel which is characterised by high redundancy enabling it to remain in operation even in case of a active or static components failure,[48].

The engagement with regulations and certifications, given that the engines are already approved and that this process would take time, was one of the reasons Van Oord rejected retrofitting solutions that required engine component modifications. Avoiding engine component adjustments also eliminates the danger that they won't work well with the ship's current systems, offering a risk- and error-free solution.

Van Oord has already chosen the FUELSAVE MARINE+ module as their short-term solution in this transition and thus the thesis will focus on the performance assessment of this new technology. Some of the reasons that made this choice ideal is the module's compact size and can be considered as a secondary device modification that does not require any changes in the current engine components and thus does not compromise the technology on the vessel. In addition, the claimed benefits of the system are very attractive since the efficiency, fuel consumption and emissions can be improved.

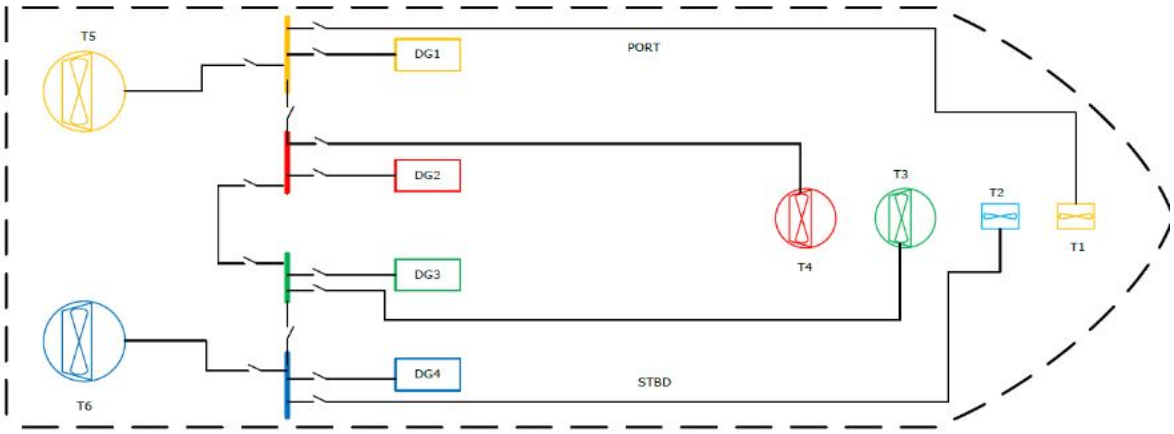

No.	Type & Model	Power (kW)
T1	BRUNVOLL FU93LTC2500	1500kW
T5	SCHOTTEL SRP 4040FP -CPL	3100kW
T4	BRUNVOLL AR100LNA2600	2000kW
T3	BRUNVOLL AR100LNA2600	2000kW
T2	BRUNVOLL FU93LTC2500	1500kW
T6	SCHOTTEL SRP 4040FP -CPL	3100kW

No.	Engine Model	Engine (kW)	Alternator Model	Alternator (kVA/kW)
DG1	MaK 8M32E	4400kW	Indar GBLS1210	4689kVA
DG2	MaK 6M32E	3300kW	Indar GBLS1110	3332kVA
DG3	MaK 6M32E	3300kW	Indar GBLS1110	3332kVA
DG4	MaK 8M32E	4400kW	Indar GBLS1210	4689kVA

Figure 1.1: Bravanes diagram, [28]

1.2. FuelSave Marine+

FuelSave company has set high goals for the maritime markets to provide in the energy saving and emission reduction with their technology. Along with Van Oord, the installation of the Marine+ will be installed on Bravenes, a DP3 subsea rock installation vessel, equipped with four CAT M32E diesel generator engines, 2 8 cylinders and 2 6 cylinders, paired in 8 and 6 cylinder configurations as can be seen in figure 1.1.

1.2.1. Working principle

The FuelSave Marine+ can be considered as a secondary device that does not require any engine modifications in any major components. The module itself introduces to the existing engines on-board the vessel small quantities of hydrogen, oxygen, methanol and water in the air scavenge area. The way FuelSave bypassed the hydrogen storage concerns was by using an electrolyzer producing on-demand hydrogen and oxygen. Methanol on the other hand, is stored in storage tanks on the ship and is merged with pure water before injection in a mixture of 30%-70% methanol-water although according to the company depending on the engine and weather conditions this can change. In addition, the system is equipped with two pumps which are responsible for the injection of the water-methanol mixture into the two pairs of engines thus the quantity of each pump is divided into the two engines in each pair. The injection location of oxygen is before the turbo compressor while methanol-water and hydrogen are injected in the hottest part of the intake which is before the air charge cooler to ensure that liquid methanol-water vaporize sufficiently in order to reach the cylinder chamber in small droplets [11]. Once the module is installed, an experimental phase will be conducted in order to fine tune the Marine+ for the needs of Bravenes. Things like the additives quantities and the methanol-water injection location and number of injections still need to be investigated in real life in order to have the best possible results in the operation of the project.

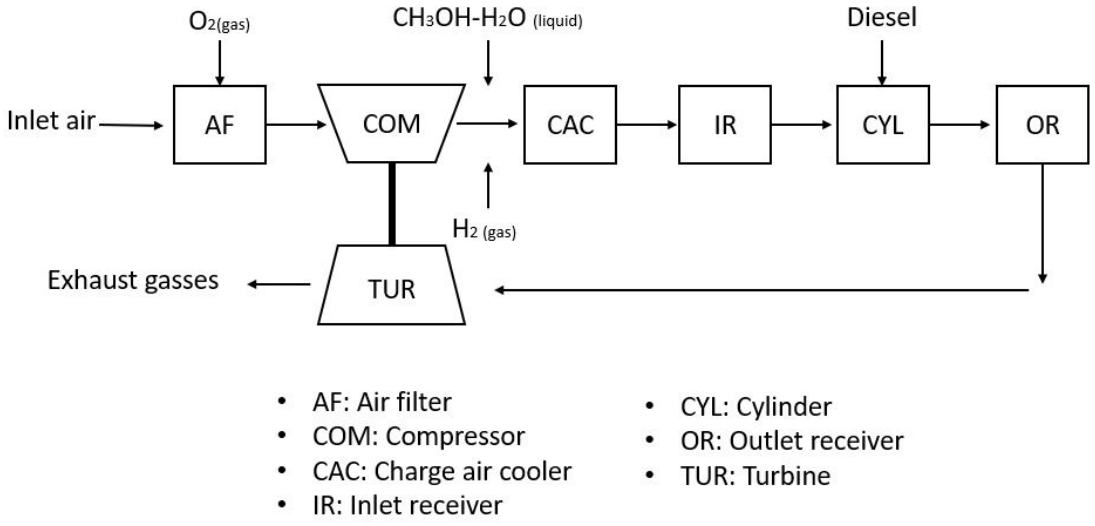

Figure 1.2: FuelSave Marine+ working principle

1.2.2. Aim of the project

FuelSave Marine+ primary aims are to replace some of the diesel quantity with methanol in order to act as a combustion catalyst as well as a cooling agent to reduce the NO_x emissions from the engine. By mixing methanol with water the company also aims to reduce further the temperature in the cylinder. Last but not least, the hydrogen and oxygen addition are introduced to have a more complete combustion which can further reduce CO_2, BC and PM emissions.

1.3. Thesis objective

FuelSave Marine+ has a very interesting concept due to the combination of four additives in marine diesel engines which is innovative and with only one current application in the marine industry the MV Annette heavy-lift crane ship. The installation on board of Bravenes will be the second installation worldwide that offers promising benefits.

The objective of the current thesis is to investigate whether the Marine+ with the addition of small quantities of hydrogen, methanol-water and oxygen can benefit the engine combustion efficiency, fuel consumption and emissions and in which percentage. The initial aim of the thesis was to have measurements with the module on and off in a controlled environment comparing the impact of the installation.

Post-processing of the results would be able to conclude on the impact of the module. Due to supply chain delays and other issues the installation was not possible thus the investigation will be mainly focus on available information and literature sources.

Ideally, a mean value first principle model will be adapted and verified based on the specific engine on-board of Bravenes with measurements to capture the combustion process. The goal will be to get the model ready for all the necessary adjustments needed for the model calibration for the diesel and Fuelsave operation while the verification and validation can be postponed until measurements are available in the event that they are not available by the project's conclusion.

1.4. Research questions

The main research question of the thesis is if the Fuelsave Marine+ installation aboard Bravenes can improve engine efficiency, fuel consumption and/or minimize hazardous emissions, with a particular focus on NO_x, which is also the main area of interest for Van Oord. To provide sufficient conclusions an investigation on the combustion performance of the engine needs to be completed. The research question can be answered by the the following sub-questions:

- What are the main differences of hydrogen and methanol compared to marine diesel oil with regards to fuel and combustion properties?
- Which performance parameters of the diesel engine are affected by the methanol-water and hydrogen properties?
- What are the effects of hydrogen, methanol-water addition on the engine's combustion parameters and emissions?
- How does the model's results for diesel operation compare with the available engine measurements from Bravenes?
- Which modifications and assumptions are necessary for the engine B model in order to accommodate the hydrogen, oxygen, methanol-water characteristics along with the diesel operation in the combustion process?
- How does the diesel operation compare to the Fuelsave operation based on the changes and assumptions selected in terms of efficiency, fuel consumption and emissions?

1.5. Research method

Initially an introduction to the subject needs to be made in order to understand the fundamentals and the purpose of the project. This step is completed with the literature study where the fuel properties, the working principle of the FuelSave and the effects to the diesel engine and engine modelling are investigated based on theoretical knowledge and experiments performed by others. With the completion of the literature study a clear understanding of the project is achieved and the first research questions are answered.

The next step after the literature study will be the research phase. The first part of the project development will be to explore the TU Delft engine B model and include the CAT M32E engine of Bravenes to the model's environment with pure diesel operation. Once the specific engine is introduced and the results of the model are acceptable the next step will be to understand how to FuelSave operation can be included in the model.

The second part of the research will be to adapt the model to accommodate the hydrogen and water-methanol properties with the diesel operation. For this step the model choices will be based on the gained knowledge from the literature study and the FVTR measurements. According to those expectations the calibration of the model will be performed and the outputs will be discussed whether they are meeting the expectations or not.

In the last phase of the thesis, the modified model hosting the Fuelsave operation is compared to the original diesel model for the Bravenes' engine followed by a discussion regarding the performance differences between the two.

I

Literature study

2

Compression ignited engine

Conventional compression ignited (CI) engines rely on the auto-ignition of an injected liquid fuel into high-pressure and high-temperature cylinder conditions near the top dead center producing effective work. In this chapter some of the important parameters of the compression ignited engines will be described and how some fuel properties can affect the combustion performance and smooth operation. In this thesis as explained in the FuelSave section, the conventional compression ignited engine of Bravenes will be retrofitted to accommodate small quantities of hydrogen and methanol-water before the charge air cooler. The retrofit solution will impact the combustion performance of the engine and some of the parameters which are expected to have the greater effect are described.

2.1. Engine performance

2.1.1. BTE

Brake thermal efficiency (BTE) expresses the output brake power to input fuel power ratio of the engine describing the conversion of heat into work. H. Koten et al. [20] mentions that the BTE can be used to compare how efficient the transition of the energy stored in the fuel is converted to mechanical output.

2.1.2. Brake specific fuel consumption

Brake specific fuel consumption, bsfc, can be expressed with the relationship, bsfc = $\frac{\dot{m}_f}{P_b}$, and relates the fuel consumption and the effective power generated in return. The lower the result, the lower the fuel consumption of the engine for the generated power. According to Stapersma [39] and equation 2.1 when fuels with lower values of LHV are used the sfc increases.

$$sfc = \frac{1}{\eta_e \cdot h^L} \tag{2.1}$$

2.1.3. Ignition delay

Ignition delay can be described as the time between the start of fuel injection in the cylinder and the start of combustion. In the conventional compression ignited (CI) engines the quality of the injected fuel serves an important role in the smooth operation of the engine. Furthermore, depending on the ignition delay length the combustion process and the engine performance can be affected. As can be seen in figure 2.1 three ignition delays values are presented showing the difference is occurring pressure depending on the situation. In the early ignition the occurring pressure is before the TDC meaning that while the piston is moving upwards the gasses in the cylinder are pushing it downwards reducing the effective work done while also in the late ignition the piston is far away from the TDC thus again reducing the effective work which could be produced. This explains the importance of the ignition delay, [18].

The ignition delay (ID) can be also be affected by the engine load and engine type. For example, a high speed engine as can be observed in the 2.2 needs more time than a slow speed engine to

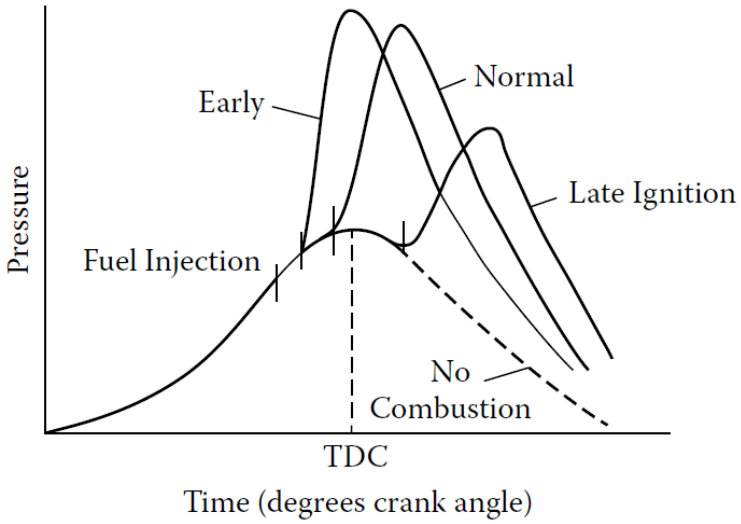

Figure 2.1: Ignition delay variation [18]

ignite thus the injection timing needs to be appropriate for each engine to obtain the most out of the combustion process, [40].

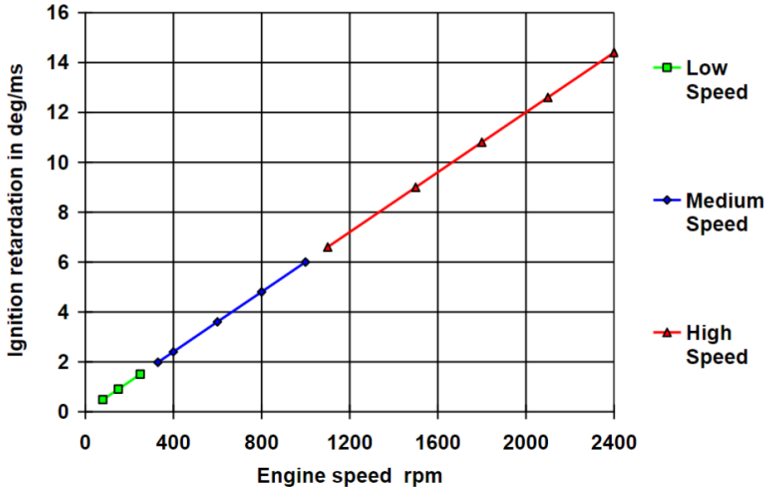

Figure 2.2: Ignition delay based on engine speed, [40]

2.1.4. Cetane Number

Worth mentioning is that the ignition delay is highly affected by the fuels' cetane number (CN). According to Stepersma [40], CN describes the auto-ignition properties of fuels. In CI engines where the main fuel is auto-ignited due to the high in-cylinder temperatures and pressures, the cetane number is critical to maintaining combustion. Ideal fuel values of CN are between 40 to 60, while values less than 40 worsen the quality of ignition.

2.1.5. Combustion Duration

Combustion duration can be described as the period in crank angles required to complete the burning of the mixture from the start of combustion to the end of combustion. Fuels with a higher flame speed will result in a shorter combustion duration since the mixture will burn at a higher rate. A shorter combustion duration means that most of the fuel is burned in less cranks angles, near the TDC, therefore it could result in higher engine efficiencies and higher heat release rates, [22]. Further down, it will

be discussed in greater detail how the hydrogen, methanol-water additions in the diesel engine could affect the ignition delay and combustion duration.

2.1.6. Heat Release Rate

The heat release rate is the heat per crank angle (CA) delivered in the engine's cylinders due to the combustion of fuel mixtures inside the cylinder. Heat release shape is highly dependent on the fuel properties injected in the engine and can describe the combustion performance of the engine. Pure diesel combustion usually can be expressed by two-stage combustion phases. The premixed combustion and the diffusive combustion. The premixed combustion phase in pure diesel applications can be identified by the sudden heat release peak which is due to the rapid combustion of the premixed fuel inserted until the start of combustion. The diffusive phase is later on the premixed phase and is following the fuel injection rate, [40].

2.1.7. Cylinder Pressure

The cylinder pressure is highly affected by the combustion process. After the premixed combustion takes place and near the TDC, the cylinder pressure usually takes the maximum value forcing the piston down in the expansion stroke and performing work. As mentioned before in figure 2.1 the cylinder pressure can alter depending on the ignition delay.

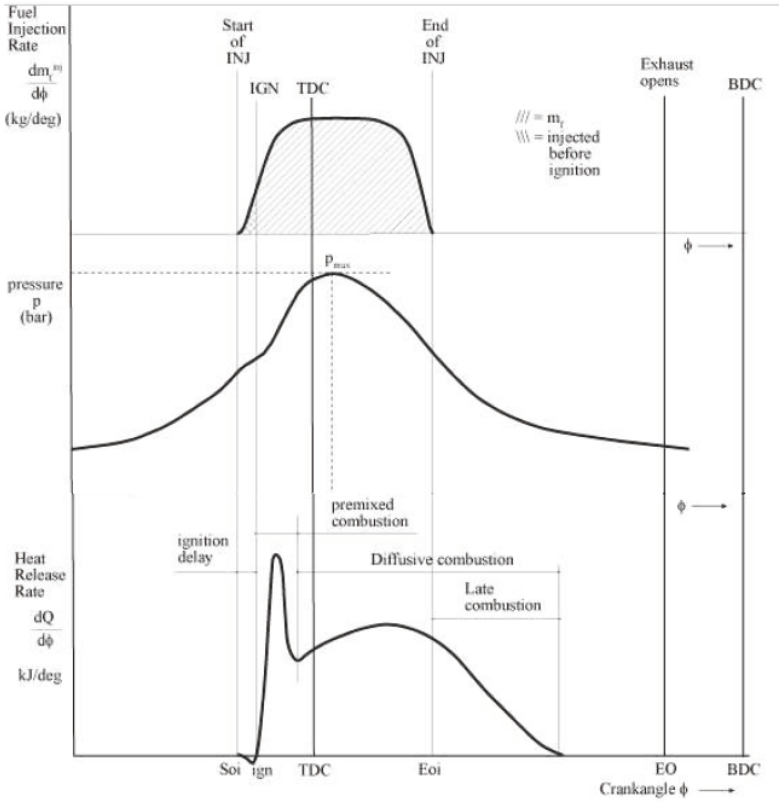

Figure 2.3: Heat release rate and cylinder pressure ,[40]

2.1.8. Heat of vaporization

The latent heat of vaporization describes the heat required to convert 1kg of liquid to vapour without any temperature rise of the substance [kJ/kg]. The heat is absorbed from the hotter environment where the liquid is injected in. Under normal operation, diesel is injected in liquid form in the cylinder chamber where the higher cylinder temperature will transfer heat to the diesel in order to evaporate. In addition to this, in this thesis injection of methanol-water mixture and hydrogen is taking place in the hottest part of the intake which is before the intake charge cooler. By doing this the liquid methanol-water absorbs heat from the hotter intake area after the turbocharger compressor and is assumed to become fully

vapour thus providing a cooling effect reducing the temperature.

2.1.9. Heating value

Heating value or calorific value expresses the amount of heat released when 1kg of fuel is under combustion. The heating value can be defined by the higher and lower heating values. The difference between the two regards in taking into consideration the assumption that all the water is in vapour form and thus the condensation heat by the water vapour is not included for the lower heating value (LHV). On the other hand, the higher heating value (HHV) is taking into consideration the condensation heat, [40].

2.1.10. Flammability limits

Flammability range describes the volume percentage in the air of flammable mixtures to combust. The range can be defined by a lower and higher flammability limit. Below the lower limit, the mixture is too lean to burn while for the high limit the mixture is too rich to burn [22], [18].

2.1.11. Stoichiometric air/fuel ratio and air excess ratio

Stoichiometric air/fuel ratio, $\sigma = \frac{m_{a,min}}{m_f}$, describes the minimum quantity of air required to the fuel quantity to have a complete combustion. The higher the σ the more air is required to burn all the fuel while the lower the σ the more fuel is needed to have a complete combustion. The air excess ratio, $\lambda = \frac{m_a}{m_{m_a,min}}$ describes the actual air quantity used for combustion to the minimum air quantity from the stoichiometric conditions. Another way to measure the air excess ratio is by using the $\lambda = \frac{afr}{\sigma}$ equation which affects the engine performance and emissions. When the λ equals unity this means that we are at stoichiometric condintions while when above 1 the conditions are lean meaning that oxygen will be present in the exchaust gasses. On the other hand when the λ is less than 1 the conditions are rich meaning that not enough air, oxygen is present and the combustion is incomplete thus unburned fuel traces will be in the exhaust gasses and the fuel consumption increases, [39].

2.2. Engine emissions

2.2.1. CO_2 and CO

Carbon monoxide (CO) is dangerous for people and other living organisms since it is extremely toxic. CO is produced in the process of CO_2 reaction due to shortage of hydroxyl (OH) radicals and thus is a result of incomplete combustion. In equation 2.2, the oxidation of CO can be seen and additional the CO and CO_2 are in equilibrium [42].

$$CO + OH \Leftrightarrow CO_2 + H \tag{2.2}$$

Carbon dioxide ($C0_2$) emissions are part of the greenhouse gas (GHG) emissions affecting climate change which is a major concern and has toxic effects on humans' health. Compared to the CO emissions which were results of incomplete combustion CO_2 emissions are the result of complete combustion and are fuel related. In addition CO_2, in the next sections, it will be discussed how they are affected by the reduction of diesel and addition of other fuels like hydrogen and methanol, [42].

2.2.2. NO_x

Nitrogen oxides emissions are products of the reaction of nitrogen and oxygen in the air, the high gas temperatures in the engine's cylinders during combustion and the concentration of oxygen during combustion. Nitrogen oxides emissions range from a variety of nitrogen oxide groups like N_2O, NO_2, NO, and can be referred to as NO_x in a more general term. Quantity wise N_2O accounts for the least percentage, 1%, while NO account for the most and the remaining is the NO_2 accounting for around 10% - 5%, [42].

The NO emissions are governed by the Zeldovich formation mechanism and consist of three chemical reactions which are reversible which are shown in equations 2.3, 2.4, 2.5 :

$$O + N_2 \Leftrightarrow NO + N \tag{2.3}$$

$$N + O_2 \Leftrightarrow NO + O \tag{2.4}$$

$$N + OH \Leftrightarrow NO + H \tag{2.5}$$

The NO_2 emissions formation can be described by the equation 2.6, 2.7 mechanism:

$$NO + HO_2 \Leftrightarrow NO_2 + OH \tag{2.6}$$

$$NO_2 + O \Leftrightarrow NO + O_2 \tag{2.7}$$

2.2.3. HC

Hydrocarbons (HC) are products of incomplete combustion in the cylinder chamber. Once the diesel is injected into the cylinder it mixes with the trapped existing air from the inlet stroke. The mixture of air-fuel depending on the local position in the cylinder will contain different air fuel ratios in the fuel spray zones which can be either too rich containing more fuel than the ideal mixture, for example near the fuel injection, or too lean containing more air than the ideal mixture, further away from the fuel injector and somewhere in the middle will be the ideal stoichiometric ratios. This uneven distribution will contribute to in some cases, slow reaction or even no ignition thus resulting in incomplete combustion and traces of hydrocarbon emissions can be detected in the exhaust systems, [42].

3

Alternative Fuels

This literature review will research based on relevant sources how the addition of hydrogen, methanol and methanol-water addition in small quantities in the air intake can improve the operation of compression ignited (CI) diesel engine. Based on the research results, an expected hypothesis can be drawn regarding the performance and emission benefits or drawbacks from the FuelSave Marine+ effects on the CAT MAK 32E engine.

3.1. Hydrogen

3.1.1. Why hydrogen is an ideal additive in the marine diesel engines

Hydrogen is of the lightest chemical elements with no carbon atoms avoiding any greenhouse gas (GHG) emissions when ignited. It consists of a wide flammability range (% volume in air) and high combustibility characteristics which are why hydrogen is considered to be dangerous especially on board of ship. Hydrogen is characterized by a high auto-ignition temperature, 858 K, which makes it more ideal for spark-ignited engines rather than compression ignited. On the other hand, the low minimum ignition energy of hydrogen, 0.02 mj, makes it suitable for ignition when paired along with higher reactivity fuel, like diesel but it could lead to knock or self-ignition when high temperatures and pressures are present. In addition, the good diffusivity in the air creating a homogeneous mixture could potentially affect the combustion performance and the efficiencies of the engine [35].

The heat of combustion of hydrogen delivers almost three times the energy released from diesel but due to the lower density, the storage capacity for the equivalence diesel energy requirements would be a challenge. As mentioned above the FuelSave working principle adds hydrogen by continuously injecting it in the air intake area of the MAK 32 engine before the charge cooler so it can mix uniformly with the inducted air before arriving in the engines' cylinder and ignite from the diesel injection.

When hydrogen is introduced in the compression ignited (CI) engines in small quantities with diesel fuel it can increase the H/C ratio and due to its high diffusivity it can create a more uniform air-hydrogen

Property	Units	Diesel	Hydrogen
Chemical formula	[-]	$C_{12}H_{26}$	H_2
Density(gas)	[kg/m^3]	-	0.081
Lower heating value	[mJ/kg]	42.6	120
Flame speed	[m/s]	0.38	2.92
Auto-ignition temperature	[k]	483	858
Min ignition energy [mj at ϕ=1]	[-]	0.23	0.019
Flammability limit (% volume in air)	[-]	0.6 - 5.5	4 - 75
Stoichiometric A/F	[-]	14.6	34
Cetane number	[-]	50	-
Diffusivity in air	[cm^2/s]	[-]	0.63

Table 3.1: Hydrogen properties compared to diesel fuel, [45]

mixture decreasing the heterogeneity of diesel and having better combustion. In addition, hydrogen's high flame propagation speed can help to have faster combustion which can increase the indicated efficiency by combusting under constant volume conditions. The wide flammability limits of hydrogen can lead to leaner mixture operations impacting the resulting emissions and the engine's fuel consumption since fuel residuals in the cylinder will be less due to the lower equivalence ratios (ϕ) required. [30]

3.1.2. Safety concerns, storage and production

Hydrogen even though has been tested in the automotive industry, in the maritime industry is still in development steps as can be also seen in figure 3.1. According to DNV,[8] it is expected that hydrogen commercial application on internal combustion engines is somewhere between 2025 and 2030. One of the main reasons for the slow adoption to the specific area is the highly explosive characteristics of hydrogen which yield safety concerns and the difficulties in storage or production onboard the ships.

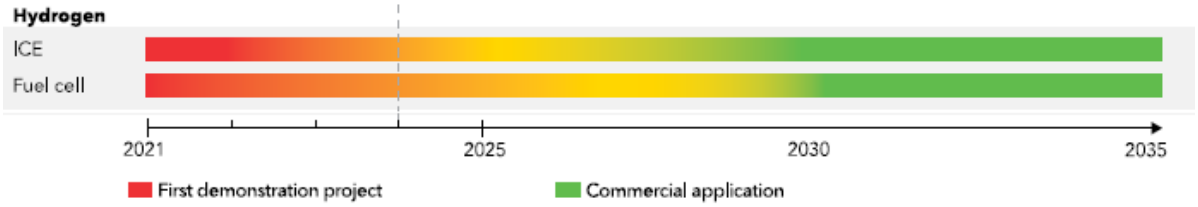

Figure 3.1: Hydrogen availability for on-board use [8]

Even though hydrogen when released in the atmosphere is non-toxic its wide flammability limits and combustible characteristics are major concerns in the ship's working environment since any leaks in contained spaced can become serious hazards for fire spreading. Hydrogen is characterized by invisible flames making them difficult to detect without proper equipment, [30].

Storage

The low energy density per volume of hydrogen is a challenge that needs to be addressed. Hydrogen can be stored as a gas in pressures around 350 - 700 bars, could be stored as cryogenic liquid with temperatures as low as -253 C which can offer greater energy density compared to compressed hydrogen but still is lower than conventional diesel fuel thus will require more space for the same equivalent energy density [35].

Production

Hydrogen is an ideal fuel for the future as it can be produced using renewable energy for electrolysis. Currently is commonly converted from coal or natural gas and other fossil fuels. Hydrogen production methods can be categorized into 4 groups, brown, grey, blue and green hydrogen. Brown hydrogen is when hydrogen production is by using coal while grey hydrogen is when the production is by using natural gas or other kinds of fossil fuels. Blue hydrogen is when the brown and grey hydrogen production methods are combined with methods for emission control like carbon or storage and utilization. Lastly, the green hydrogen is when renewable sources are being used to power water electrolysis. Grey hydrogen is currently accounting for around 75% globally with the brown hydrogen be second with 23% while only 2% globally is green hydrogen. The last category, blue hydrogen, is still very low in the global scale [35].

3.1.3. Hydrogen-Diesel operation in CI internal combustion engines

According to O. Ghazal [12], hydrogen addition in gaseous form is expected to have reduced heat transfer losses to the cylinders' chamber walls due to the enhanced air-fuel mixing, thereby lower peak gas temperatures and the lower fuel inertia having fewer issues with wall spray impingement. In the experiments of G. Lilik et al. [25], with the addition of hydrogen the recorded needle lift height for the diesel injection seemed to be reduced meaning less diesel fuel is injected through the injectors.

Cylinder pressure

C. Liew et al. [23] researched how the usage of H_2 addition in the intake for three engine loads, 15%, 30%, 70%, at 1200 rpm can affect the cylinder pressure. The quantity of added hydrogen was

expressed in the volumetric fraction of the rest of the intake mixture, $\frac{H_2}{Air+H_2}$. At the higher engine load, 70%, the addition of 2-3% hydrogen increased slightly the cylinder pressure before combustion, while with increasing amounts of hydrogen, >4% the pressure prior combustion had decreased. Meanwhile, after the combustion initiation the cylinder pressure increased with all the hydrogen addition, while a significant increase was recorded with the amount of 6% hydrogen. For the 30% engine load a similar behavior was observed with the higher load condition but with reduced effects. Worth to be mentioned is that for the lower engine load, 15%, the addition of hydrogen in all levels reduced the peak cylinder pressure compared to the pure diesel operation. The results of G. Lilik et al. [25] agree with the C. Liew et al. [23] regarding the cylinder pressure measurements. During the experiments at high engine load conditions the addition of hydrogen leads to higher peak pressures while also advancing compared to the diesel baseline operation. As mentioned before hydrogen in CI engines requires a pilot fuel for ignition which in our case is the diesel injection. When diesel ignites in the premixed phase the existing hydrogen-air mixture in the cylinder ignites as well resulting in a rapid pressure rise due to the higher flame speed which could help in having more complete combustion.

Willem Kes [19] in his thesis investigated the effects of small hydrogen additions in a MAN 4L20/27 medium-speed engine. According to his experiments he concluded that hydrogen effects at low load conditions are not as significant as for higher engine loads something which is supported by the mentioned literature. For the higher engine loads, 1000 rpm and 300 kW, as can be seen in figure 3.2, the peak cylinder pressure near the TDC increased slightly for the 2.5% and 5% hydrogen addition.

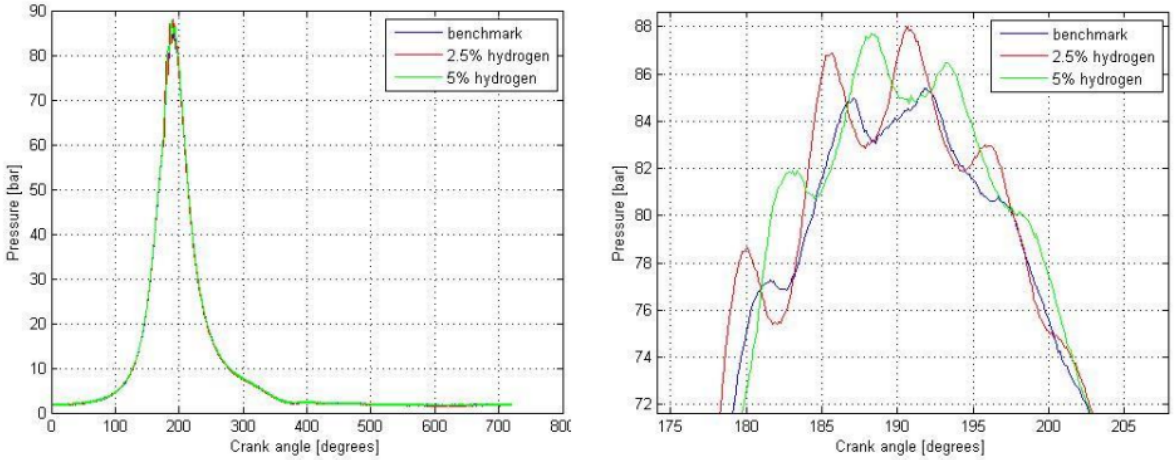

Figure 3.2: Cylinder pressure measurement for 1000 rpm and 300 kw [19]

Based on the knowledge from the literature it can be observed that hydrogen addition in the diesel engines for the peak cylinder pressure is load and quantity dependent. It can be assumed that for this thesis in the low engine loads operation the pressure in-cylinder reduces or remain unaffected while for the higher load conditions it is expected to have a slight advancement and increase of the peak pressure.

Heat release rate

In the same experiment of C. Liew et al. [23] the heat release rate was also monitored for the same conditions mentioned above. It was observed that for the high engine loads, a slight delay at the premixed combustion phase was present and an increase in the diffusion phase. The most significant effect was recorded with the 6% hydrogen addition which advanced and enhanced the heat release rapidly due to the faster burning characteristics of hydrogen and the better mixing with air. With hydrogen addition <3% the peak heat release rate curve followed the pure diesel operation with a slight increase of the peak heat release value. Worth mentioning is that with the increasing amount of hydrogen the diffusion phase of combustion is reduced.

For the 30% engine load condition, the heat release rate with the hydrogen addition showed less significant effects on the diffusion phase combustion while recording a slight enhancement and retardation of the premixed combustion phase. In even lower engine load the increasing addition of hydrogen reduced the peak heat release rate.

The results from P. Sharma et al. [31] show similar findings with C. Liew et al. [23]. In the low load conditions, 25%, modest retardation of the premixed heat release rate phase is recorded with the peak heat release almost constant. For the higher engine loads conditions, 75%, minor retardation is present while the peak heat release increases.

Willem Kes [19] in his thesis concluded that a small amount of hydrogen addition in low load conditions shows insignificant effects on the heat release rate while for the higher load conditions an increase in the early combustion was recorded while also a late combustion increase.

Brake thermal efficiency

S. Bari et al. [33] using an on-board H_2-O_2 generator injected them in the air intake recorded the increase of the brake thermal efficiency (BTE) in three different engine loads. Increasing the percentage of hydrogen-oxygen increased the BTE as well. This can be explained by the higher flame speed of the hydrogen, nine times the diesel flame speed, which results in faster and more complete combustion. The improved combustion results in higher peak cylinder pressure closer to the top dead center (TDC) which enhances the work produced on the piston improving the efficiency. H. Kose et al. [13] in their experimental investigation injected hydrogen in different engine speeds, 1000-2500 rpm but a maximum load condition. It was observed that the addition of 2.5% hydrogen increased the most the BTE efficiency at 1000 rpm and kept the improved efficiency until 2500 rpm. Interestingly the 7.5% hydrogen addition showed very small gains at the 1000 rpm compared to the diesel baseline while increasing until the 2500 rpm but still was less than the 2.5% and 5% hydrogen levels. Reasons have been the higher flame speed of hydrogen and the higher lower heating value (LHV) which helps in an improved combustion. The poorer results of the 7.5% hydrogen addition are believed to be due to the replacement of air in the intake from hydrogen resulting in richer mixture conditions in the cylinder chamber. H. Koten et al. [20] in a constant rpm engine with varying loads and varying hydrogen addition levels again confirmed the increase of BTE explained by the better mixture formation and higher flame speed of hydrogen which result in more complete combustion.

Brake specific fuel consumption

Following the experiment of S. Bari et al. [33] the brake specific fuel consumption (bsfc) of the diesel engine with the H_2/O_2 addition reduced in all three engine loads with the increase of the additives. The more complete combustion and the uniformed hydrogen-air mixture due to hydrogen's smaller high diffusivity with air help to reduce the bsfc. In addition, hydrogen-oxygen addition helped to have leaner combustion thus reducing the needed fuel. Hydrogen normally displaces some air when inserted into the air intake of the engine but in this experiment due to the addition of oxygen the air fuel ratio (AFR) increased slightly along with the increase of the additives. According to H. Kose et al. [13] adding small amounts of hydrogen can minimize the specific fuel consumption of the operation due to the better mixing of hydrogen with air.

Combustion duration and ignition delay

C. Liew et al. [23] compared the combustion duration in the three engine loads mentioned above with different hydrogen addition levels. According to figure 3.3 from their research for the higher engine load after the introduction of 2% hydrogen addition the combustion duration (CD) reduced while for the 30% engine load the CD decreased after 3.5 % hydrogen addition. Worth mentioning is that for the lower load, 15% the addition of 4.5% hydrogen resulted in a significant increase of CD. Combustion duration is highly connected with the better mixing of hydrogen with air and the higher flame speed of propagation.

Emissions

S. Bari et al. [33] in their experiments noticed also the behavior of engine emissions with the addition of H_2/O_2. According to the results the NO_x emissions increased in all three engine loads. This could be a result of the higher temperatures occurring from the hydrogen combustion and the increased availability of oxygen in the cylinder. Continuing on the NO_x effects from hydrogen addition G. Lilik et al. [25] performed separate measurements on NO_2 and NO. As reported by the measurements the NO_x levels increased with the addition of hydrogen with the greatest effects taking place at low loads. Additionally, the effects on NO show a reduction with the increase of H_2 while the lower loads show smaller NO values than the higher loads due to the increased combustion temperatures. On the other

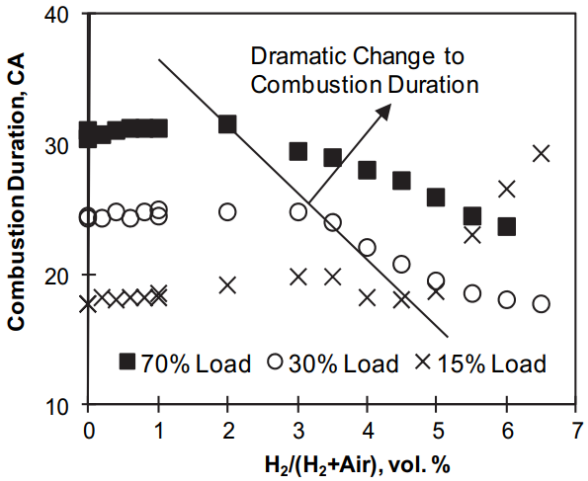

Figure 3.3: Combustion duration and hydrogen addition effects [23]

hand, the NO_2 levels increased with the additional H_2 levels in all loads while the highest effect on the lower loads. They concluded that the increasing levels of H_2 increase the HO_2 levels enhancing the conversion of NO to NO_2.

Hydrocarbon emissions in the S. Bari et al. [33] showed a reduction with the addition of H_2/O_2 in all engine loads since both fuels lack carbon bonds and the improved combustion. In line with the above measurements, H. Kose et al. [13] confirmed that the introduction of hydrogen can reduce the HC due to the carbon absence and the improved combustion occurring from the superior flame speed of H_2.

S. Bari et al. [33] continuing with the emissions experiments also noted that CO_2 and CO emissions reduced with the related additives. This was expected since either H_2 or O_2 contain carbon which reduces the overall concentration in the fuel-air mixture. The reduction of CO could also be due to the leaner mixtures that H_2/O_2 form. Confirming the results of S. Bari et al. [33], H. Koten [20] concluded that increasing the hydrogen addition results in lower CO and CO_2 emissions compared to diesel operation due to the absence of any carbon atoms nor hydrocarbon molecules in hydrogen.

3.2. Methanol

Methanol, according to DNV [8], is one of the promising alternative marine fuels which can contribute to the energy transition with commercial applications in internal combustion engines (ICE) before 2050. As can be seen in figure 3.4 methanol is already in the first steps for commercial application on ICE since the technologies are more mature [[8]].

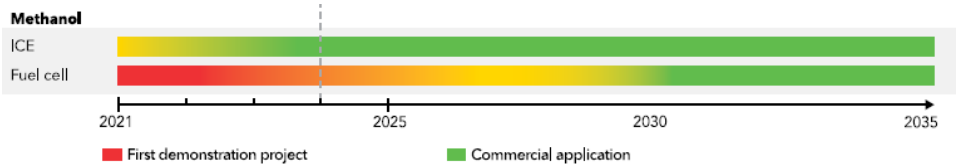

Figure 3.4: Methanol expectation for on-board use [8]

3.2.1. Why methanol is an ideal alternative fuel

Methanol's liquid form at ambient conditions and historical usage in the chemical history provides enough knowledge and experience to handle it and have an easier transition to the marine industry in terms of worldwide availability.

Methanol as a fuel compared to diesel is described by almost half the lower heating value for the same quantity which can lead to specific fuel consumption increase as described in equation 2.1. On the other hand, methanol has no sulfur or carbon to carbon bonds reducing any particulate matter or SO_x emissions during combustion. Furthermore, methanol contains the highest hydrogen to carbon ratio

Property	Units	Diesel	Methanol
Chemical formula	[-]	$C_{12}H_{26}$	CH_3OH
Density	[kg/m^3]	830	793
Lower heating value	[MJ/kg]	42.6	20
Heat of Vaporization	[kJ/kg]	250	1089
Flame speed	[m/s]	0.38	0.5
Flash point	[k]	326-370	285
Auto-ignition temperature	[k]	483	744
Min ignition energy	[mj at ϕ=1]	0.23	0.21
Flammability limit	(% volume in air)	0.6 - 5.5	6 - 36.5
Stoichiometric A/F	[-]	14.6	6.5
Cetane number	[-]	50	4
Oxygen content	[wt%]	-	50

Table 3.2: Methanol properties compared to diesel fuel, [45]

compared to other liquid fuels which could lower the CO_2 emissions during combustion. In addition, the cetane number of methanol is quite low compared to diesel fuel which can affect the auto-ignition characteristics of the engine performance. Methanol's high latent heat of vaporization results in cooling effects since it absorbs heat from the hotter environment is injected in to become vapour and also could affect the thermal stratification on the cylinder. The decrease of the temperature can potentially help in less NO_x formation [4], [36].

The introduction of methanol in diesel operation can be performed by either direct injection of methanol in the cylinder chambers along diesel injection. This would require the modification of the engine to accommodate a second injector in each cylinder which may not be possible in some cases due to space limitation and increased risk of modifications. Another way to perform dual fuel operation is by blending the methanol to diesel and using the existing fuel lines and injectors. The drawback of this method is the necessity of additives, emulsifier agents because methanol and diesel are immiscible. Last but not least, the method which is also used in the current thesis is the injection of methanol in the intake area which is commonly called port injection or fumigation. Using this method no modifications are required for the engine itself but the addition of an injector in the intake area which is ideal for retrofit solutions [36].

3.2.2. Safety concerns and challenges

Methanol is considered a low flash point fuel meaning that it can burn quite easily and accumulate at the lower points of pipes or tanks urging the need for proper ventilation and warning systems. In addition, it could cause asphyxiation in high concentrations of vapor which is of major concern on board a ship for the crew members since also vapour is heavier than air and the inhaling risk is higher and proper ventilation and measurements for detection need to be arranged.

Another concern regarding methanol is the nearly invisible flame with no smoke traces burning at low temperatures. Moreover, when methanol is installed in vessels due to its corrosive properties to some materials, special attention needs to be given to the fuel supply lines, storage tank and other components that come in contact with it. When methanol is released into the environment it could produce less damage compared to gasoline or crude oil spill due to the rapid degradation by biodegradation processes and photo-oxidation in salt and fresh water, sediments and groundwater. On the other hand, when methanol comes in touch with the human organism, even in small quantities 10-100 ml, it is poisonous to the nervous system which could cause blindness even death. It is challenging to detect with the human senses with concentrations below 2000 ppm which is dangerous in close working environments in case of leakage thus proper detecting equipment and warning systems shall be considered [4],[36].

Storage

Methanol at ambient conditions is in liquid form which makes it easier to store compared to hydrogen and liquefied natural gas. The supply chains of methanol already exist due to the variety of other applications for example in the chemical industry. Changes will need to take place on board the ships since

the corrosive behaviour of methanol to a certain type of materials will deteriorate engine components faster and take into account changes regarding the lower energy density compared to diesel [36].

Production
Nowadays, the most common production technique is using natural gas feedstock which is an energy intensive production process and can be separated in three steps:

- natural gas reforming to syngas, with steam addition, including CO, CO_2 and H_2
- methanol synthesis using hydrogen by products and water
- methanol distillation/purification from water using boiling

Methanol has the potential to be produced from renewable sources, like electrolysis or biomass using renewable power from solar or wind energy and the application of carbon capture technologies to decrease further the greenhouse gas emissions during production also known as well-to-tank emissions [36].

3.2.3. Methanol-Diesel operation in CI internal combustion engines

Pressure cylinder
C. Xu et al. [3] in a set of experiments performed for different methanol-diesel combustion ratios in different engine loads showed that in low loads conditions the in-cylinder pressure increased slightly while following the baseline curve. For the higher engine load the pressure was lower than the diesel baseline operation until the premixed combustion phase and then increased slightly recording a higher late combustion pressure. For the medium engine loads the increase of cylinder pressure compared to the diesel operation had recorded the highest change.

According to Zhang et al. [49], who experimented with methanol fumigation the results for the cylinder pressure indicate a reduction of the pressure for the low to medium engine conditions while an increase for the higher engine loads. In all cases the increasing amount of methanol fumigation had a greater impact on the cylinder pressure measurements. Although the results from the two references do not agree on the lower engine load conditions is it expected that the pressure will either remain stable or reduce slightly while for the higher engine loads an increase is expected.

Heat release rate
The heat release rate with the methanol addition according to literature has significant effects on the medium-high engine loads. According to C. Xu et al. [3], methanol addition on the low load conditions has insignificant effects while for the higher engine loads it enhances the cylinder heat release rate after the premixed combustion phase as a result of the higher cylinder temperatures which counteract the high latent heat of vaporization of methanol and the high oxygen concentration of methanol leading to boost combustion.

In addition to C. Xu et al. [3] results, Zhang et al. [49] concluded that methanol fumigation can increase the heat release rate independent of the engine load. Worth to be mentioned is that in the low load conditions the low gas cylinder temperatures, the prolonged ignition delay due to methanol latent heat of vaporization and the leaner mixture of air-methanol cause the heat release to retard away from the TDC and thus reduce the in-cylinder pressure since the piston will be already in the expansion stroke. On the other hand, for the higher engine load conditions the increased gas temperatures reduce the ignition delay. In the higher engine loads, the premixed mixtures of methanol-air become richer in the cylinder, burning faster and thus increasing the heat release rate in the premixed phase combustion. As can be observed in figure 3.5 from Zhang et al. [49] it is clear that methanol effects are load and quantity dependent on the engine performance.

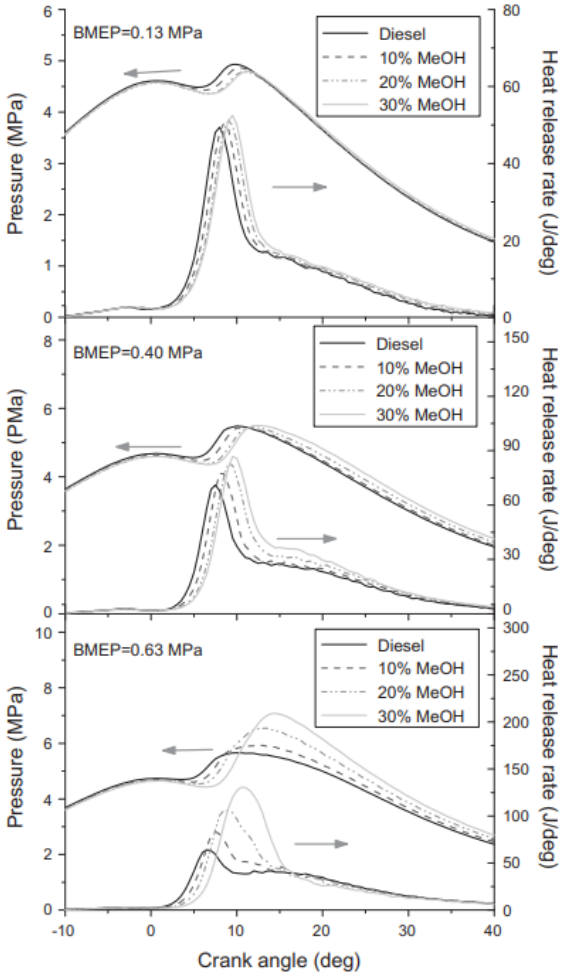

Figure 3.5: Methanol influence on diesel engine operation [49]

Ignition delay

Ignition delay is prolonged with the addition of methanol fumigation in the diesel engine due to the higher latent heat of vaporization that subtracts energy in the form of heat from the system to vaporize causing a cooling effect and lowering the intake temperatures and reducing the low temperature oxidation rate of injected diesel. In addition, the lower cetane number of methanol compared to diesel slows down the overall reactivity of the combustion. This can be confirmed by C. Xu et al. [3], where the ignition delay is prolonged in all engine conditions. It is interesting though that in the higher engine loads the ignition delay is less than the medium engine load as a result of the higher cylinder temperatures taking place. The increasing levels of methanol addition increase the ignition delay as well. One of the side effects of higher ignition delay is that more time is available before ignition thus more diesel is injected into the cylinder which along with the existing methanol-air mixture can cause sudden, sharp increases in the heat release rate which depending on the engine load could even lead to knock. Zhang et al. [49], during experimentation concluded that ignition delay increases for all the engine load conditions with the increasing amount of methanol as can be verified by figure 3.6 Another possible explanation that connects the methanol to the increase of ignition delay is provided by H. Xu et al. [14] research where results showed that methanol acts as an intermediary converting active OH into non-active H_2O_2 at temperatures lower than 1000 k reducing the system's reaction activity while when above 1000 k they begin to decompose back into OH.

Combustion duration

The effects of methanol addition on diesel engine operation depending on engine load can be seen from C. Xu et al. [3] experiments. According to them on low load operation the combustion duration increases

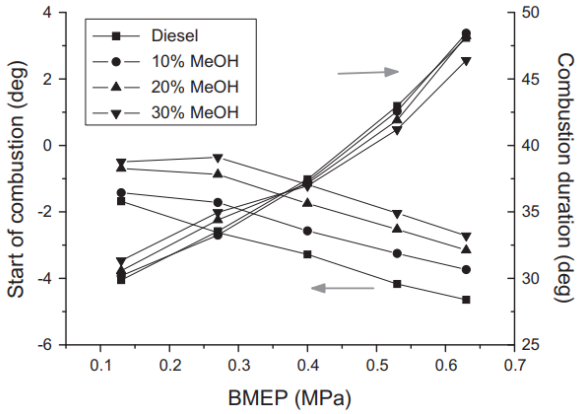

Figure 3.6: Methanol and load effects on ignition delay and combustion duration, [49]

while for the medium and high engine loads there is a decrease with the methanol addition increase. On the other hand, experiments performed by Zhang et al. [49], concluded that small amounts of methanol fumigation have no significant effects the on combustion duration independent of the engine load. Figure 3.6 describes that for the lower load conditions the only visible change is due to the 30% methanol increasing slightly the combustion duration while for the higher loads the combustion duration reduces marginally for the same fumigated level. Although the Zhang et al. [49] results it can be expected that the higher flame speed of propagation of methanol and the high oxygen content can lead to improved combustion and thus to reduce the combustion duration in the diffusive phase.

ITE
Based on C. Xu et al. [3] results, the indicated thermal efficiency (ITE) increased in all engine modes with the increasing amount of methanol addition. The greatest effects although were recorded for the lower load conditions in which the methanol's high oxygen content and lean mixture improved the combustion and the ITE.

BTE
L. Wei et al. [24] observed that small additions of methanol had minor effects on the brake thermal efficiency (BTE) on the engine while increasing methanol levels reduced it. The high latent heat of vaporization delays the ignition which could lead to deteriorated combustion due to the piston already in the expansion stroke phase thus 'losing' effective work. C. Cheng et al. [1] concluded that methanol impact on BTE can be load dependent. For the lower load operation the fumigation of methanol had a slight increase while as the load increases the increasing effects of BTE were more significant. Cheng explains that methanol can affect diesel combustion in two contradicting ways. The first one is the increase of ignition delay providing more time for the diesel injection and thus more mass fuel in the cylinder burning in the premixed phase increasing the BTE. On the other hand, the high latent heat tries to decrease the cylinder temperatures reducing the BTE. Depending on the engine type, load and specific operating conditions one of the two ways can dominate the other.

BSFC
Brake specific fuel consumption (bsfc) is expected to increase with methanol addition due to the lower heating value. According to C. Cheng et al. [1], in general bsfc decreases with the increase of the engine load. When methanol is fumigated in the engine the bsfc for the low load condition is higher compared to the baseline operation while for the higher engine load the effects are similar to the baseline operation. The same results were confirmed by Z. Zhang et al. [50] which the increase of methanol addition increase the bsfc as well. The reason is the low lower heating value of methanol which in large quantities can have significant impacts on the bsfc due to the replacement of the higher lower heating value of diesel reducing the overall LHV of the mixture.

NO_x
According to Saxena et al. [27] the NO_x emissions can be affected by the methanol fuel properties like the latent heat of vaporization, cetane number, oxygen content, calorific value, substitution rate and the

engine load condition. NOx emissions are highly temperature and oxygen concentrations dependent. Many solutions for their reduction include the lowering of the combustion temperature. Methanol with the high latent heat of vaporization and lower heating value manages to subtract heat from the system to convert from liquid to vapour reducing the gas temperature in the cylinder. C. Xu et al. [[3]] concluded that the methanol addition in low, medium and high loads can reduce the NO_x emissions significantly.

HC

Based on the experiments of C. Xu et al. [3] the increasing amount of methanol rates increased the unburned hydrocarbons emissions for different engine loads. On the other hand, when the methanol substitution rates remained near the 10%, for the low loads the effects were not significant while for the medium to high loads a minor increase was recorded. Methanol's addition with the high latent heat of vaporization in higher quantities especially for the low load conditions could reduce the reaction temperature and thus increase unburned hydrocarbons emissions. It is also possible, that the high flame speed of propagation of methanol could reduce the combustion duration and increase the in-cylinder temperature decreasing the unburned HC.

CO

C. Xu et al. [3] concluded that the increase of methanol may lead to CO emissions increase in every engine load condition. This can also be confirmed by W. Pan et al. [46] where the methanol addition for different air intake temperatures increased the CO emissions significantly while the temperature increase reduced the CO emissions. Since CO emissions are temperature related and methanol can result in quenching effects which can decrease the oxidation of CO and decrease the combustion temperature it is explained why CO emissions increase with the increasing methanol levels. On the other hand, the higher oxygen content of methanol and higher air intake can help accelerate the oxidation of the carbon oxides.

3.3. Methanol-Water

3.3.1. Cylinder pressure and heat release rate

According to the experiment of C. Xu et al. [2] with the addition of methanol-water mixture the heat release rate and the cylinder pressure peaks increased due to the micro-explosions of water during the evaporation process which enhanced the premixed combustion. It can also be noted that the heat release rate is delayed due to the methanol's high latent heat of vaporization which explains the increase of the cylinder pressure and the delayed maximum cylinder crank angle. As can be seen in figure 3.7 during the smallest addition of water-methanol addition of the experiments, when pure methanol-diesel was in operation the heat release rate was slightly delayed, had a higher peak and a higher diffusion phase. With the methanol-water-diesel operation for the 30%-70% mixture the heat release peak was even higher with a similar late combustion phase. On the other hand, the cylinder pressure reduced up to the premixed combustion phase and then increased marginally.

3.3.2. ITE

C. Xu et al. [2] using different methanol/water blends injected on constant load and constant engine speed before the air charge cooler, observed that the indicated thermal efficiency (ITE) increased compared to pure diesel operation. According to the author, the increase is due to the micro-explosions of water enhancing the combustion. Worth mentioning is that diesel-methanol and diesel-water performed slightly better in terms of ITE compared to the pure diesel operation with the increasing of quantities having greater effects. Compared to the diesel-methanol and diesel-water operation, methanol-water-diesel operation on the specific experiments proved to be the most efficient.

3.3.3. Brake specific fuel consumption

On the same set of experiments of C. Xu et al. [2] the brake specific fuel consumption decreased the most with the pure methanol-diesel operation while water-methanol-diesel also reduced the bsfc slightly. The increase of the additives' quantities from 10% to 40% volume substitution leads to decreasing the bsfc even more.

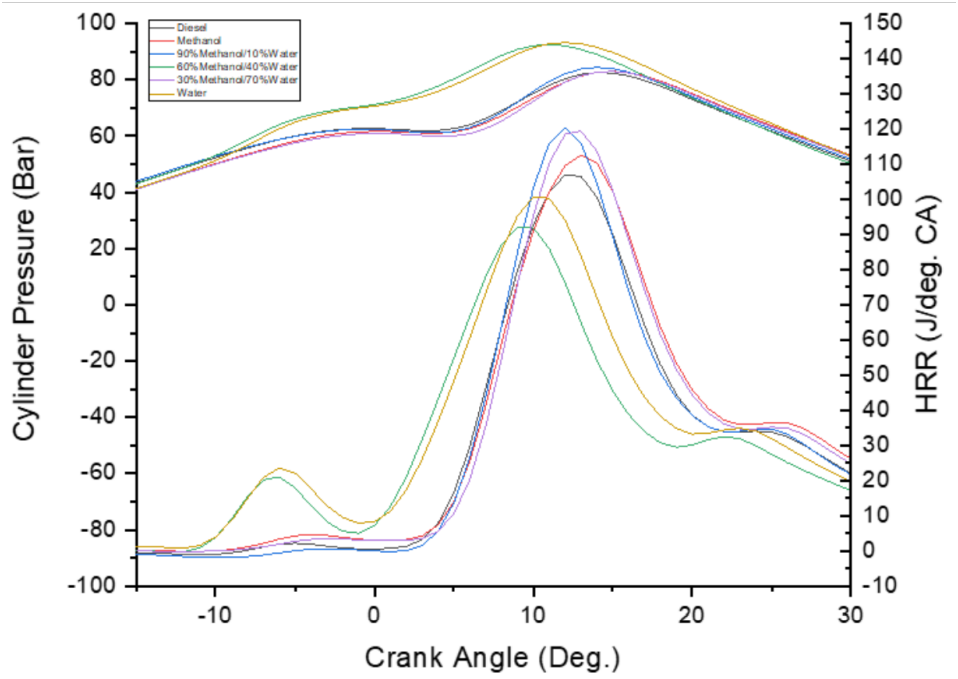

Figure 3.7: Methanol-water mixture effects on diesel engine [2]

3.3.4. Ignition delay

Water-methanol mixture was also investigated by C. Xu et al. [2]. Ignition delay is affected by the hydroxyl (-OH) free radical. As the experiments show, methanol addition suppresses the growth amount of OH radicals in lower temperatures. On the other hand, with the water addition due to the hydrophilicity of OH, the free radicals contacted water first and reduced ignition delay compared to the methanol-diesel operation. This is due to methanol instead of suppressing the OH growth in the reaction to 'snatching' OH from the molecules of water.

3.3.5. Exhaust gas temperature

According to the same experiments as above, the exhaust gas temperature (EGT) was reduced with the addition of water-methanol mixture by approximately 10 degrees. This is due to the greater amount of work during the heat transfer and expansion process which managed to extract more energy from the gas, thus reducing the heat losses and exhaust temperature. In addition, the higher latent heat of vaporization of the mixture could potentially have absorbed large amounts of heat decreasing the cylinder temperature and thus the exhaust gas temperature.

3.3.6. CO

C. Xu et al. [2] during experimentation for the emissions found out that the addition of water-methanol reduced the CO emissions due to the influence of the water micro-explosions and the oxygen excess promoting the conversion of CO to CO_2 thus reducing the carbon monoxide emissions. On the other hand, when only methanol was inserted in the diesel engine the CO emissions increased while water-diesel had the lowest emissions. This concludes that water-methanol mixture could potentially reduce the CO emissions of diesel engines.

3.3.7. HC

For the hydrocarbon emissions the results were similar to the carbon monoxide. Methanol-diesel operation on the specific conditions increased the HC while water-diesel operation had performed the best. The reason for the methanol-diesel fuel having the highest hydrocarbon emissions is due to the richer mixtures which resulted in possibly incomplete combustion while the water with the micro-explosions managed to improve combustion due to the leaner mixture. When the water-methanol mixtures were inserted in the diesel engine the hydrocarbon emissions were reduced, [2].

3.3.8. NO_x

Nitrogen oxides emissions had the most beneficial impact from the water-methanol addition. Water vapor when introduced in the cylinder helped to reduce oxygen's partial pressure during combustion while also surrounding heat is absorbed, reducing the maximum cylinder temperature through the vaporization process. The high molar heat capacity of water managed to increase the heat capacity of the total mixture in the cylinder reducing the NO_x formation. Furthermore, the high latent heat of vaporization of the water-methanol mixture reduced the cylinder maximum temperature even though the heat release rate for the specific mixture, 30% methanol and 70% water percentage was high as seen in figure 3.7, [2].

3.4. Hydrogen & Methanol-Water-Diesel in CI internal combustion engine hypothesis

The addition of methanol-water is expected to act as an emission reduction technique in the engine performance by lowering the temperatures of the gas in the cylinder and effectively reducing NO_2 emissions. In addition, methanol can act as a fuel that can replace small quantities of diesel in the combustion chamber. The benefit of this substitution would be the creation of a leaner mixture since methanol contains no C-C bonds and higher oxygen concentration which could decrease the CO and CO_2 emissions and improve combustion quality. Furthermore, methanol's higher flame speed of propagation could reduce the combustion duration and increase the engine efficiency since the combustion will take place nearer the TDC. On the other hand, the high latent heat of vaporization of methanol could result in prolonging ignition delay which provides time for more diesel to be injected in the cylinder and could possibly lead to a sharper increase of the heat release rate and in some cases knocking could be observed. This behavior on the engine performance could be counteracted by the water addition and the hydrogen addition which are expected to advance the ignition delay. Hydrogen addition with the higher lower heating value, low auto-ignition energy and high flame speed of propagation is expected to reduce the prolonging of ignition delay caused by methanol addition but could increase the in-cylinder gas temperature and thus the NO_x emissions. The effect of methanol-water although could restrain that increase and the overall operation of the additives could potentially lead to fewer emissions, increase engine efficiency and less fuel consumption. These expectations will be confirmed or not during the measurement and post-processing of the data after the installation on-board the Bravenes is completed.

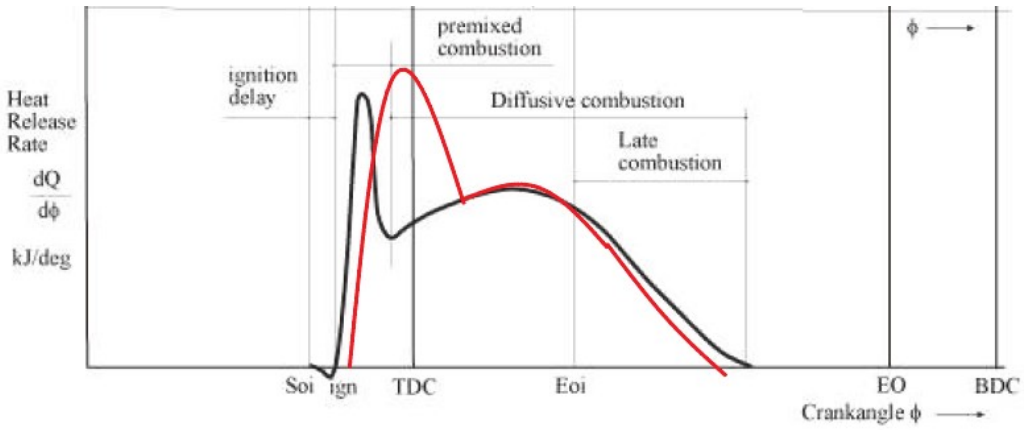

Figure 3.8: Heat release rate curve expectation based on literature study

Figure 3.8 describes a potential heat release curve that shows an increase in ignition delay caused by the higher latent heat of methanol vaporization, rapid combustion that may result from sudden hydrogen ignition with a higher flame speed, and a reduced late combustion phase caused by the need for less diesel fuel in the cylinder to produce the same amount of heat over a shorter combustion time or an increase in combustion rate.

4

Engine Modelling and Measurements

The need of modelling the combustion process of engines has several benefits when investigating the combustion performance parameters. In this thesis the importance of engine modelling is in regards to the investigation of the heat release rate from the in-cylinder pressure measurements for the operation and impact of small quantities of hydrogen, oxygen and methanol-water in the air intake area of a MAK 32E engine installed on board of Bravenes.

Property	Units	6 M 32 E	8 M 32 E
Power output	[kW]	3,300	4,400
Speed rating	[rpm]	720	720
Cylinder number	[-]	6	8
Minimum speed	[rpm]	360	360
Bore	[mm]	320	320
Stroke	[mm]	460	460
BMEP	[bar]	23.7/22.7	23.7/22.7
NO_x emissions	[g/kWh]	9.6	9.6

Table 4.1: CAT MAK M32E specifications ,[47]

The engine's characteristics are presented in table 4.1. The same engine structure with different cylinder's configuration are installed in Bravenes, 2 x 8 M 32E and 2 x 6 M 32 E, and when in normal operation the FuelSave Marine+ module will feed in each engine H_2, O and methanol-water mixtures on demand. The current engine model developed by the university supports only two engines that are not suitable for the current project thus the first adjustment to the model will be the implementation of the appropriate engine.

4.1. Measurements

For the purposes of the thesis and during the measurement program scheduled by Van Oord and FuelSave for the effects on the engine performance table 4.2 presents some of the interesting quantities which will be recorded. In the first trial the quantities will be recorded with the module on and off in order to have an accurate comparison of the performance and emissions effects. The second phase of the measuring program after the trial will continue for 12 months in normal operating conditions for Bravenes in order for Van Oord to obtain more information and conclude on the benefits of the installation.

Property	Units
Delivered Power	[kW]
Speed	[rpm]
Cylinder pressure	[Bar]
Exhaust gas temperature	[C]
Fuels flow	[l/h]
Cooling water in and out	[C]
Emissions	[g/kWh]
Electrolyzer energy consumption	[kWh]

Table 4.2: Table : FuelSave and Bravenes measurements

Worth to be mentioned is that in case the measurements are not available by the completion of the thesis the model will be based on assumptions, and measurements will be required on a later phase to verify whether these assumption were appropriate or not.

4.2. Modelling

Models can differ depending on the accuracy and the investigation of parameters required by the user. In general, in order to calculate the heat release rate experimental inputs of the cylinder pressure are needed as well as for calibration and verification of the model. Once they are known, the temperature mean value in the cylinder can be calculated from the gas law and the change of internal energy can be estimated.

Heat release rate analysis can be done by the usage of a single or double zone model. For our needs the single zone is more convenient since the behavior of the combustion can be investigated through this model, since combustion details, like flame fronts, emissions formation or hot spots are not required in our situation, [43],[40].

Single zone model

According to Stapersma [40], one way of performing heat release modelling is by considering the cylinder as a single volume with the energy released obtained using the first law of thermodynamics considering mean values. In reality often the fuel in the cylinder is in parts vapour and in parts liquid requiring the need for a second volume which is discussed further down. In the single zone model it is assumed that all the injected mass fuel is instantly evaporated and combusted almost directly in the cylinder and thus is equal to the combustion rate. Even though the simplicity of the single zone model the results often are accurate enough.

Dual fuel single zone model

Lee in his thesis [22] by adding methanol's properties to the diesel operation model managed to improve the single zone model to a dual fuel single zone model. Lee thesis was investigating the premix combustion of methanol to diesel operated engines by port injection, like in this thesis, and thus assumed that methanol is already in vapour form when entering the cylinder and pilot diesel fuel ignited the combustion. By doing so, the modelling process became simpler due to avoiding additional sub-models. R.S Tol [43] using the model of Lee experimented with the addition of methanol by direct injection to the engine cylinder along with diesel. This meant that the original assumption by Lee could not hold true anymore since methanol would be in liquid form. This change resulted in the need for an injection model, an evaporation model and spray vaporization calculation before using the single zone model.

In the current moment of the literature study, I would also assume that the methanol-water mixture since injected before the change cooler and in the hottest part of the air intake system will manage to vaporise in most of their concentration and be inserted in the cylinder as vapour phase. The same applies for the hydrogen addition but due to the already gas phase of the substance it is certain that when introduced in the cylinder will not be liquid. With all that in mind currently, I believe that there is no need for an injection model, evaporation model or spray vaporization calculation for this thesis.

Double zone model

In the double zone model it is considered more complex and if the correct assumptions and parameters are chosen a more accurate model represents more realistically the combustion process by taking into consideration that the cylinder can consist of an unburned and a burned zone with each zone having its own thermodynamics systems exchanging energy/mass to the surroundings and to each other zone. In

order to obtain the heat release from the double zone model the first law of thermodynamics needs to be applied to each of the zones using the crank angle and experimental in-cylinder pressure signals. Using the double zone model more information can be obtained for the exhaust gas composition prediction, [40], [43].

4.3. Mean Value Model

The Delft University of Technology (TU Delft) have already a mean value first principle (MVFP) diesel engine model which will be used in the current project along with the necessary changes. The model is operating in cycle time instead of crank angle thus is able to simulate the entire turbocharged diesel engine system with less computational time and output all the important engine performance parameters under the chosen conditions by the user, [29]. The MVFP model includes the operation of sub-models, some of them are:

- in-cylinder process
- gas exchange
- thermodynamic-volume
- turbo-machinery
- exhaust process

The 'in-cylinder process' includes the Seiliger process providing information between the inlet valve close (IC) to exhaust valve open (EO) process describing the combustion cycle. The Seiliger process model will be explained with detail further down, [5].

Figure 4.1 displays the engine model foundation build in simulink environment. The main input of the model are the engine speed along with the fuel rack position. More inputs include the ambient conditions in terms of pressure and temperature along with the data about the engine and fuel, [29]. The output of the model is the engine torque and brake power.

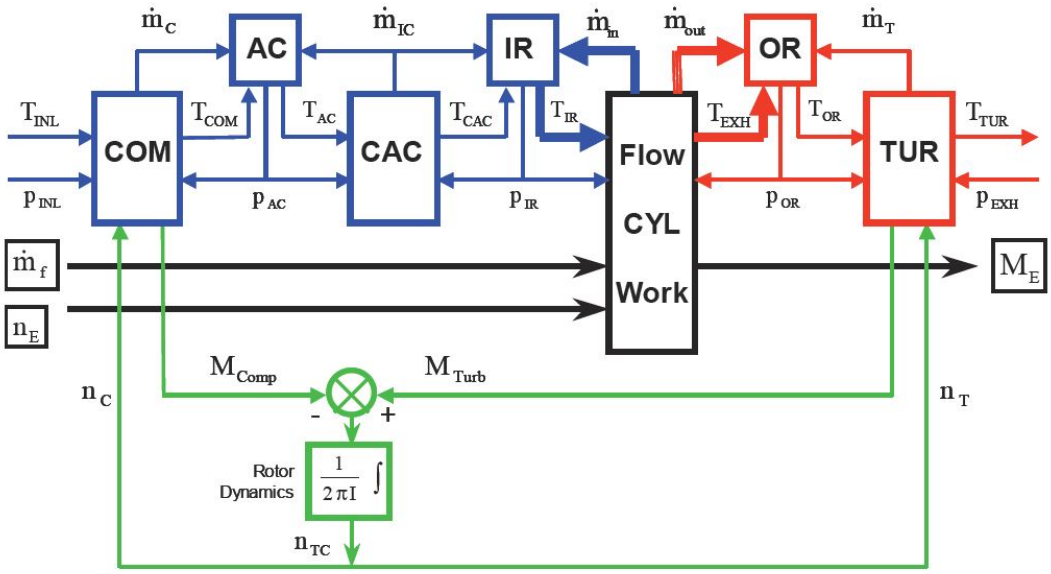

Figure 4.1: Mean value engine model, [41]

4.4. Heat release model

The heat release model is not included in the current modelling research but it contains fundamental knowledge which can be used in the mean value engine model.

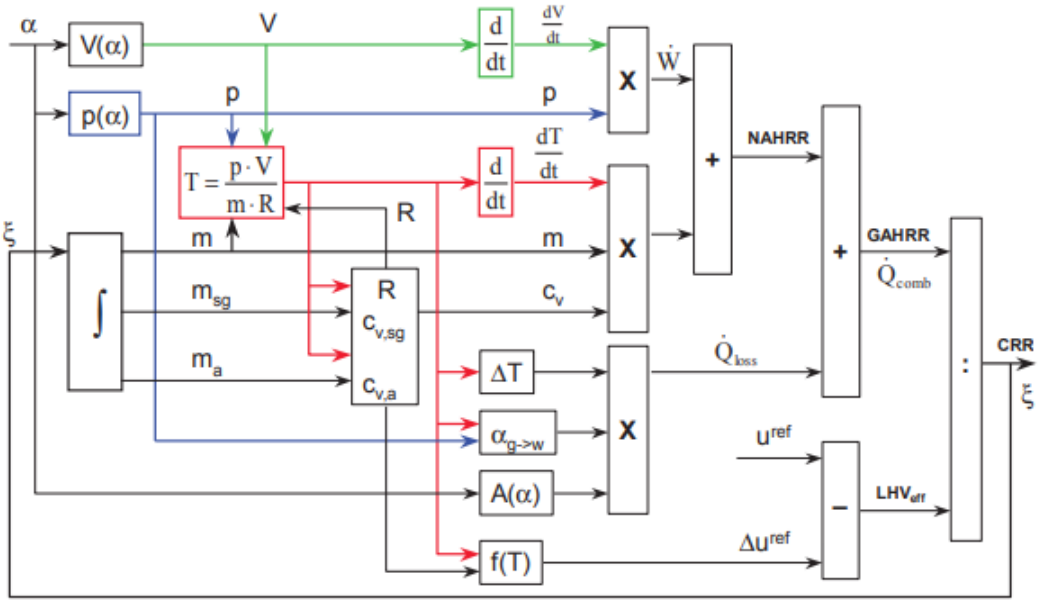

Figure 4.2: Block diagram of heat release and CRR determination, [40]

4.4.1. Cylinder volume change

$$\frac{dV}{d\phi} = \frac{\pi}{360} \cdot V_s \cdot \left\{ \sin(\alpha) + \lambda_{CR} \cdot \left(\frac{sin(\alpha) \cdot cos(\alpha)}{\sqrt{1 - \lambda_{CR}^2 \cdot sin^2(\alpha)}} \right) \right\} \tag{4.1}$$

In order to calculate the work as seen in equation 4.7 and other parameters, the change of volume in the cylinder needs to be estimated since while the engine is in operation the pistons inside the cylinders move thus the available volume changes. Equation 4.1 makes the calculation possible, where V_s is the volume stroke, α is the engine's crank angle and λ_{CR} defines the crank/rod ratio. For the volume stroke calculation the engine's geometry, bore (D_B) and stroke (L_S) are taken from the manufacturer data.

4.4.2. Gas Law

The gas law in the model is useful for the cylinder temperature calculation which is necessary for initiating the model.

$$p \cdot V = m \cdot R \cdot T \tag{4.2}$$

As described in equation 4.2 the gas law consist of the pressure of the cylinder, *p*, which is acquired by engine measurements, the engine changing volume, *V*, which is calculated by the 4.1 as mentioned above, the mass of the gasses *m*, the universal gas constant *R* and finally the temperature, *T*.

4.4.3. Mass balance

In normal diesel engines operation, fuel is injected into the cylinder to self-ignite the premixed mixture. This means that fuel injection is the way that mass of fuel is added to the cylinder after the intake and exhaust valves close. During the injection of fuel, in the current single zone model it is assumed that all the fuel is evaporated and then combustion is taking place almost directly without living any fuel vapour in the gas phase. This can conclude that the change of mass in the cylinder is equal with the reaction rate, $\frac{dm}{dt} = \xi$.

Additionally, the total mass trapped in the cylinder includes fuel, air and stoichiometric combustion gas, $m = m_f + m_a + m_{sg}$. During combustion no leakage of gas is assumed to be leaving the control volume (cylinder) nor entering in, which means that the change of mass is only due to the mass of fuel injected in the cylinder ,[40].

$$\frac{dm}{dt} = \dot{m}_f^{in} \tag{4.3}$$

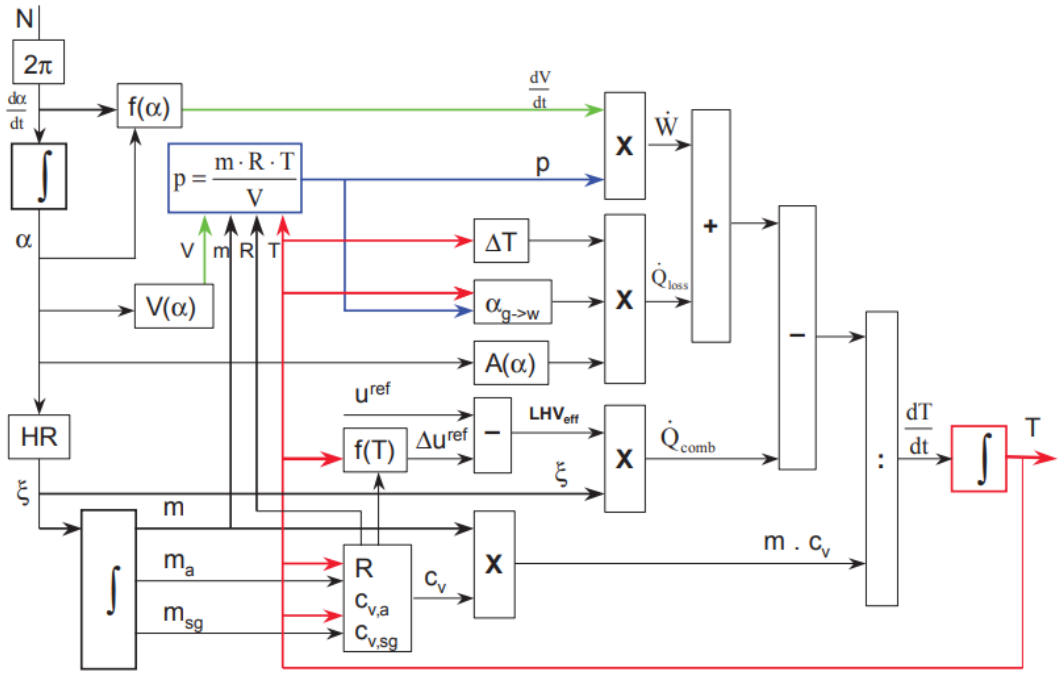

Figure 4.3: Block diagram of in-cylinder process simulation with the heat release as input, [40]

As mentioned above, in the single zone model, it is assumed that all of the injected fuel is evaporated and burned which means that the change of mass equals the reaction rate, ξ.

$$\frac{dm}{dt} = \xi \tag{4.4}$$

For the current thesis, it needs to be taken into account that although diesel is directly injected in the cylinder as in a normal operation, now the additives mixture injected in the air intake area will enter the cylinder during the intake stroke only.

4.4.4. Energy balance

The total energy change of the system can be described by the following equation 4.5:

$$m \cdot c_v \cdot \frac{dT}{dt} = \dot{Q}_{comb} - \dot{Q}_{loss} - p \cdot \frac{dV}{dt} \tag{4.5}$$

As can be seen, the total energy change of the system is structured by the combustion heat, heat losses and the indicated work. Heat of combustion can be described as the heat value of the reference conditions with a correction term which is temperature dependent multiplied by the reaction rate. The combustion heat can be found using the equation 4.6 where u_{comb}^{ref} represents the combustion value in a closed system and the Δu_{comb}^{ref} is the change in internal energy due to the temperature change from the reference conditions.

$$\dot{Q}_{comb} = (u_{comb}^{ref} - \Delta u_{comb}^{ref})\xi \tag{4.6}$$

While the combustion is taking place, heat losses to the surrounding of the cylinder, cylinder walls, head and piston crown, and due to vaporization processes can be described by the $\dot{Q}_{loss}$.

Last but not least, the indicated work can be defined as the pressure and rate of changing volume in the cylinder.

$$\dot{W} = p \cdot \frac{dV}{dt} \tag{4.7}$$

The heat release rate according to Stapersma [40], can be described by the following possible definitions,

Net Apparent Heat Release Rate

$$\dot{Q}_{comb} - \dot{Q}_{loss} = m \cdot c_v \cdot \frac{dT}{dt} + p \cdot \frac{dV}{dt} \tag{4.8}$$

The NAHRR can be estimated from the temperature and pressure in the cylinder but it neglects the heat losses in the cylinder.

Gross Apparent Heat Release Rate

$$GAHRR = \dot{Q}_{comb} = m \cdot c_v \cdot \frac{dT}{dt} + p \cdot \frac{dV}{dt} + \dot{Q}_{loss} \tag{4.9}$$

The GAHRR by taking into account the lost heat in the cylinder corrects the NAHRR term but since they are not measured but rather estimated using the Woschni model the accuracy is dependent on the model and assumptions, [40] ,[5].

Combustion Reaction Rate

$$CRR = \frac{m \cdot c_v \cdot \frac{dT}{dt} + p \cdot \frac{dV}{dt} + \dot{Q}_{loss}}{u_{comb}^{ref} - \Delta u_{comb}^{ref}} = \xi \tag{4.10}$$

The CRR takes into account the effective heat value and helps to determine the composition which along with the temperature leads to the instantaneous specific heat of the content in the cylinder. This is important because the change of internal energy can be calculated. Another difference from the GAHRR is the units of CRR which are $\frac{kg}{s}$ instead of $\frac{kJ}{s}$.

After the CRR is integrated the reaction coordinate (RCO) can be obtained for determining the Vibe parameters which at the end are the main input data for the in cylinder model [22]. CRR since is estimated using the measured cylinder pressure is fluctuating. On the other hand, the RCO since is the integration value of CRR is a monotonous function suitable to be analysed and for curved fitting which is necessary for the simulation of the in-cylinder process 4.3. For the current project the in-cylinder process will be described using the Seiliger process model which is implemented in the TU Delft engine B model.

4.4.5. Heat Losses

In the cylinder chamber while the combustion process takes place and the temperature rises heat is transferred to the cylinder's walls, cover and piston crown. Heat is lost also while fuel is injected into the cylinder in order to vaporize which can usually be seen in the small dip of the heat release diagram before the premix combustion. In order to estimate the heat loss to the cylinder's environment Woschni's heat transfer coefficients are used and the equation 4.11:

$$\dot{Q}_{loss} = \sum_{i=1}^{3} \left\{ \alpha_{g \rightarrow w,i} \cdot \left(T - T_{wall,i} \right) \cdot A_{wall,i} \right\} \tag{4.11}$$

Where:

- i=1 cylinder wall
- i=2 cylinder cover
- i=3 piston crown

Equation 4.11 contains the heat transfer coefficient, $\alpha_{g \rightarrow w,i}$, the temperature, *T*, and the area of the specific part, *A*. During the combustion process the area and the gas temperature are variable while according to Woschni the temperature of the wall can be assumed constant and approximately a mean value between the highest and lowest points.

The piston wall area is the only one changing due the piston movement and can be estimated using equation 4.12, [40]:

$$A_{wall,1} = \pi \cdot D_B \cdot L_P \tag{4.12}$$

D_B is the cylinder diameter, L_P is the length of the piston crown position from the cylinder top which is crank angle depended.

The Woschni heat transfer coefficient is defined in equation 4.13 taking also the radiation heat without an additional term due being inclusive in the convective part of the formula, [42].

$$\alpha_{g\to w} = C_1 \cdot \frac{1}{D_B^{0.214}} \cdot \frac{p^{0.786}}{T^{0.525}} \cdot \left(C_3 \cdot c_m + C_4 \cdot \frac{p - p_0}{p_1} \cdot \frac{V_S}{V_1} \cdot T_1\right)^{0.786} \tag{4.13}$$

Where V_S the volume stroke, c_m the piston speed, p_0 and T_0 describe the 'no fuel injection' condition and parameter C_1 is used to correct the reaction coordinate (RCO) to unity at different points of operation while C_3, C_4 describe the swirl velocity effects and the combustion chamber shape respectively [5].

Parameter C_3 as advised by Woschni can be estimated by two cases:

- During gas exchange: C_3=6.18+0.417 $\cdot \frac{w_t}{c_m}$
- During compression and expansion: C_3=2.28+0.308 $\cdot \frac{w_t}{c_m}$

where w_t is the swirl velocity and the ratio w_t/c_m is challenging to measure thus an estimate from literature can vary from 5 to 50 depending on the engine [5]. For this thesis although the compression and expansion is applied for the C_3.

Parameter C_4 advised by Woschni:

- Direct injection: C_4=0.00324
- Pre chamber: C_4=0.00622

In the current thesis combustion is ignited by the direct injection of diesel which makes sense to have the direct injection value for C_4.

4.5. Seiliger process model

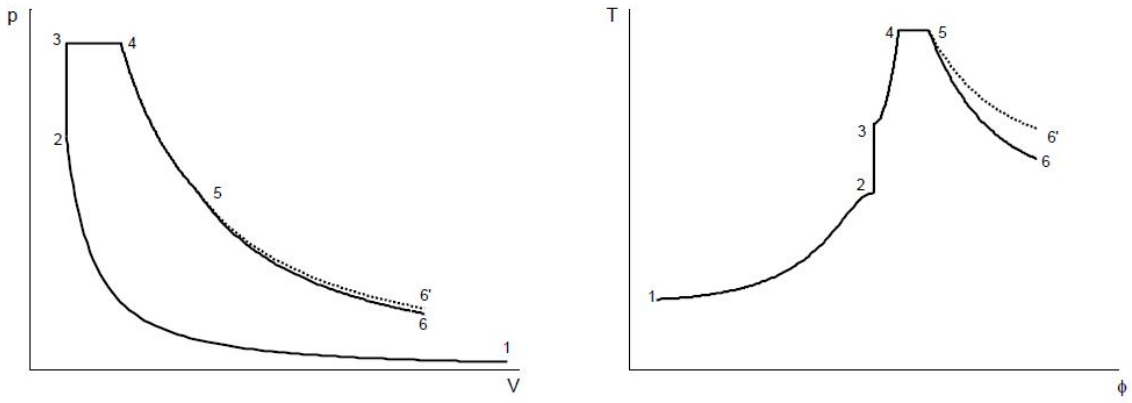

Figure 4.4: Seiliger process [5]

The Seiliger process model as mentioned above can simulate the in-cylinder combustion process of the engine based on selected parameters. Figure 4.4, presents the basic and advanced Seiliger process divided into 5 stages. The main difference between the advanced and basic Seiliger process is the the choice to have combustion or not in the last stage of the cycle respectively.

- 1-2: polytropic compression
- 2-3: isovolumetric combustion
- 3-4: isobaric combustion and expansion

- 4-5: isothermal combustion and expansion
- 5-6: polytropic expansion indicating net heat loss, no combustion
- 5-6': polytropic expansion indicating net heat input by late combustion

For the basic Seiliger process the stage are 1-6 while for the advanced Seiliger process the stages are 1-6'. Yu Ding is his research distinguished the advanced with the basic Seiliger process by whether there is combustion or not in the last stage. This could be performed by selecting the appropriate value of parameter n_{exp} in order to indicate the net heat input rather than heat loss, [5].

Stage	Seiliger difinition	Parameter definition	Seiliger parameter
1-2	$\frac{p_2}{p_1} = r_c^{n_{comp}}$	$\frac{V_1}{V_2} = r_c$	r_c, n_{comp}
2-3	$\frac{V_2}{V_3} = 1$	$\frac{p_3}{p_2} = \alpha$	α
3-4	$\frac{p_4}{p_3} = 1$	$\frac{V_4}{V_3} = b$	b
4-5	$\frac{T_5}{T_4} = 1$	$\frac{V_5}{V_4} = c$	c
5-6 (5-6')	$\frac{p_6}{p_5} = r_e^{n_{exp}}$	$\frac{V_6}{V_5} = r_e$	r_e, n_{exp}

Table 4.3: Seiliger parameters

Stages 2-3, 3-4 and 4-5 are combustion stages and can be characterised by the Seiliger shape parameters α, b and c respectively. Parameter n_{comp} describes the lost heat during the compression phase while the n_{exp} represents the net heat input during the advanced Seiliger process or the heat loss during expansion for the basic Seiliger process depending on the selected value. Together with stages 1-2 and 5-6 the pressure, temperature, net combustion heat and work of the in-cylinder process for each stage can be computed, [39], [5].

4.6. Modelling process

The completion of the literature study has helped to have a clear image of the modelling process for the next phase of the research. A rough explanation of the process which will be followed is given below. The first scenario is based on available measurements for the in-cylinder pressure along with the volume per crank angle for using the b model for diesel and FuelSave operation. The second scenario is in case no measurements are available and the proper assumptions need to be made according to the literature study and other experimental sources.

For the rest of the thesis the implementation of the M32E engine will be imported to the model and more information about the functionality of the TU Delft engine B model will be provided along with the description and investigation of the necessary modifications which need to be performed and taken into account for the model B to accommodate the hydrogen, methanol-water properties and effects on the combustion process.

It is important to confirm that the addition of the substances provide reliable results in regards to the changes to the Seiliger model and during the heat losses modelling due to their unique characteristics which are different than diesel and may not be valid for the current heat losses model taking into account their initial purpose [38].

5

Literature study conclusion

Hydrogen and water-methanol when tested individually along with the diesel operation have promising potentials as alternative fuel for emission reductions and efficiency improvements. The ability of the fuels to be produced with sustainable energy and thus further emission reductions possibilities when considering the well-to-tank emissions are another reason to consider their future usage in the marine industry.

From the research questions which were established in the introduction of the current literature study the following were given an answer and/or a rough estimate. The rest of the aimed outputs will be discussed, processed and given an answer in the main part of the thesis.

Which are the main differences of hydrogen and methanol compared to marine diesel oil?

According to the references the main differences which point out between hydrogen, methanol and marine diesel oil are the lower heating values, the cetane numbers, the heat of vaporization, flame speed, their density and storage abilities, in some cases the toxicity to humans and in other cases the safety to the humans. Some of the parameters mentioned above are more important for the current project due to their impact on the engine performance and emissions.

Which performance parameters of the diesel engine are affected by the methanol-water and hydrogen properties?

The diesel engine operation is a combination of performance parameters that ensure the safe and proper operational conditions. These parameters depending on the fuel used can affect majorly the engine. Some of the parameters that will be certainty affected by the hydrogen and water-methanol are the air excess ration, the ignition delay, the pressure and temperature in the cylinders, specific fuel consumption, brake thermal efficiency and combustion duration.

What are the effects of hydrogen, methanol-water addition on the engine's combustion parameters and emissions?

The major expected effects, based on the literature, of hydrogen and methanol-water addition will be on:

- increase of the ignition delay due to the methanol's high latent heat of vaporization which could potentially increase the cylinder pressure for the premix combustion phase
- decrease the combustion duration since the addition of hydrogen could increase the combustion reaction rate due to the higher flame speed
- the air excess ratio will change due to the injection of the methanol-water and hydrogen on the intake area which could potentially replace some of the air, oxygen in the area and reduce the amount of oxygen in the cylinder which could affect the engine performance while on the other hand the FuelSave introduces some oxygen before the compressor inlet which could potentially neutralize the issue mentioned
- cylinder temperatures reduction due to the higher latent heat of vaporization of methanol and the higher specific heat of water thus reducing the NO_x emissions produced by the engine whilst the hydrogen could increase the temperatures

- CO and CO_2 reduction is expected due to the diesel substitution by hydrogen while the methanol introduction could increase them

The literature study for the current project reveals that the combination of hydrogen and water-methanol in diesel engines could have improvements regarding the efficiency and emissions. The impacts could be quantified in the later stages of the project and the remaining of the research questions could be answered.

- How does the model's diesel results compare with the available measurements from Bravenes?
- Which modifications and assumptions are necessary for the engine B model in order to accommodate the hydrogen, oxygen, methanol-water characteristics along with the diesel operation in the combustion process?
- How does the diesel operation compare to the Fuelsave operation based on the changes and assumptions selected in terms of efficiency, fuel consumption and emissions?

II

Modelling research

6

M32E engine modelling diesel operation

6.1. Measurements of M32E engines

The initialization of the main thesis begins with the acquisition of important measurements from onboard Bravenes. The value of these data are of great importance since they are essential for the calibration and verification of the model. Out of the four engines' pressure - crank angle measurements received from the chief engineer regarding the period between 2019 and 2022 it was noticed that only one of them had the expected combustion behavior which is to have the maximum pressure after the top dead center(TDC), while the other three had the maximum pressure before the TDC.

Based on this observation it was decided to focus the research on the measurements and diagrams of the specific engine. After reviewing the available pressure-crank angle diagrams received for the specific period mentioned above, an ideal sailing trip was chosen where the engine was operating in high load conditions providing power to the thruster on the port side.

The selected pressure-crank angle diagram along with the received supporting information about engine temperatures, fuel consumption and other operational information offered similar readings with the available engine acceptance test from the manufacturer thus the decision to verify the output of the model with the specific diagram.

The information from the ship that is currently accessible that will be utilized to calibrate and validate the model is listed below:

- Pressure-Crank angle diagrams
- Indicted work, mean indicated pressure, indicated power
- Turbocharger temperatures and speed
- Temperatures and pressures in the system
- Fuel consumption

Figure 6.1 and 6.2 present the received pressure trace measurements for the two similar M32E 8 cylinder engines focusing on the TDC region since the rest of the graphs are similar and can be seen in the appendix A in full size. It is clearly visible from the two diagrams regarding the same engine type and for the same sailing trip the difference in pressure delivery. In figure 6.1 the peak temperature is after the TDC and nearly 213 bar while on the other hand figure 6.2 presents a peak pressure of nearly 220 bar and before TDC. A possible explanation can be drawn from figure 6.3 which provides an illustrative pressure curve diagram depending on the injection timing.

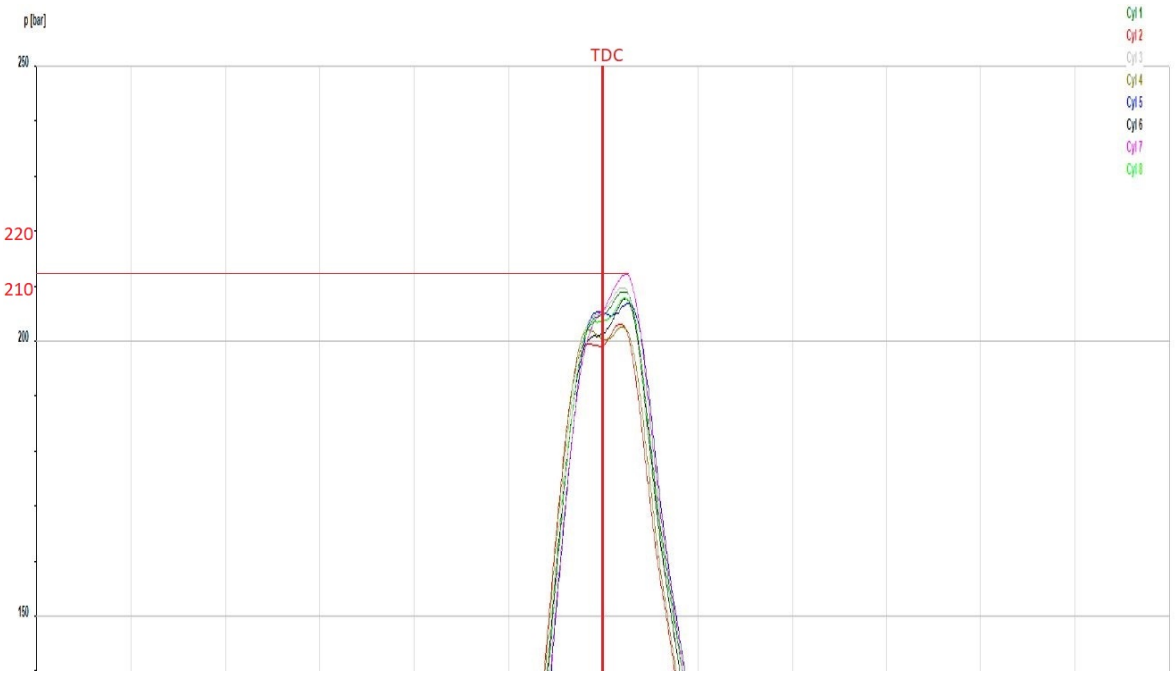

Figure 6.1: Pressure-Crank angle measurement from Bravenes DG1, [28]

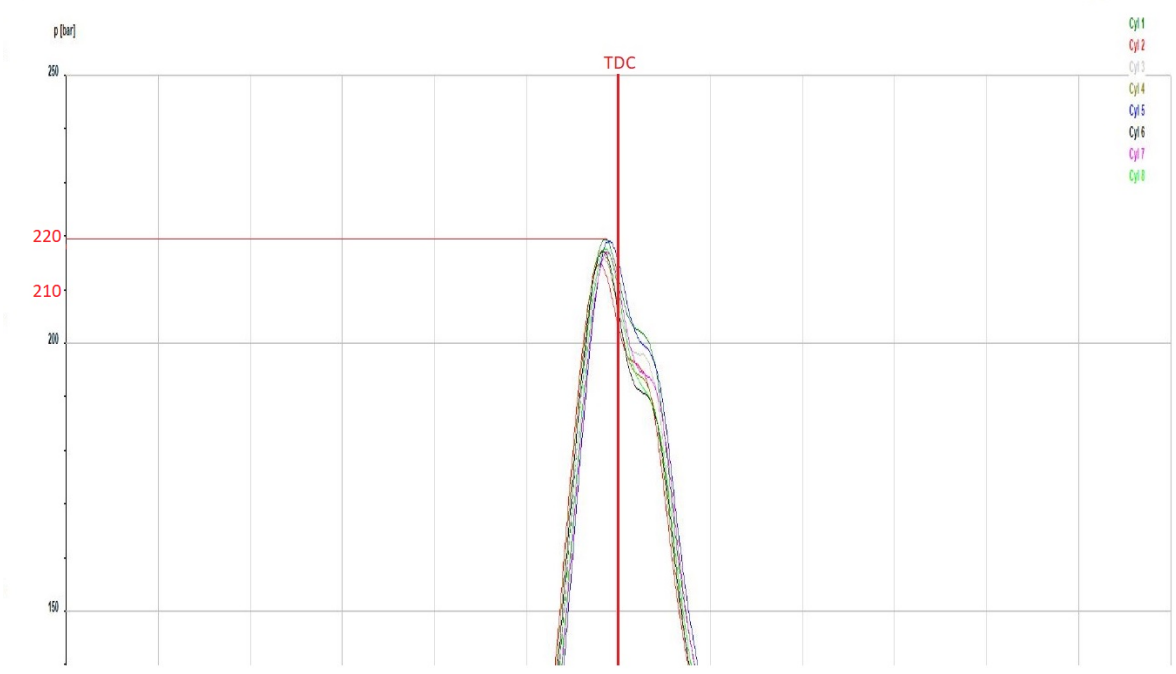

Figure 6.2: Pressure-Crank angle measurement from Bravenes DG4,[28]

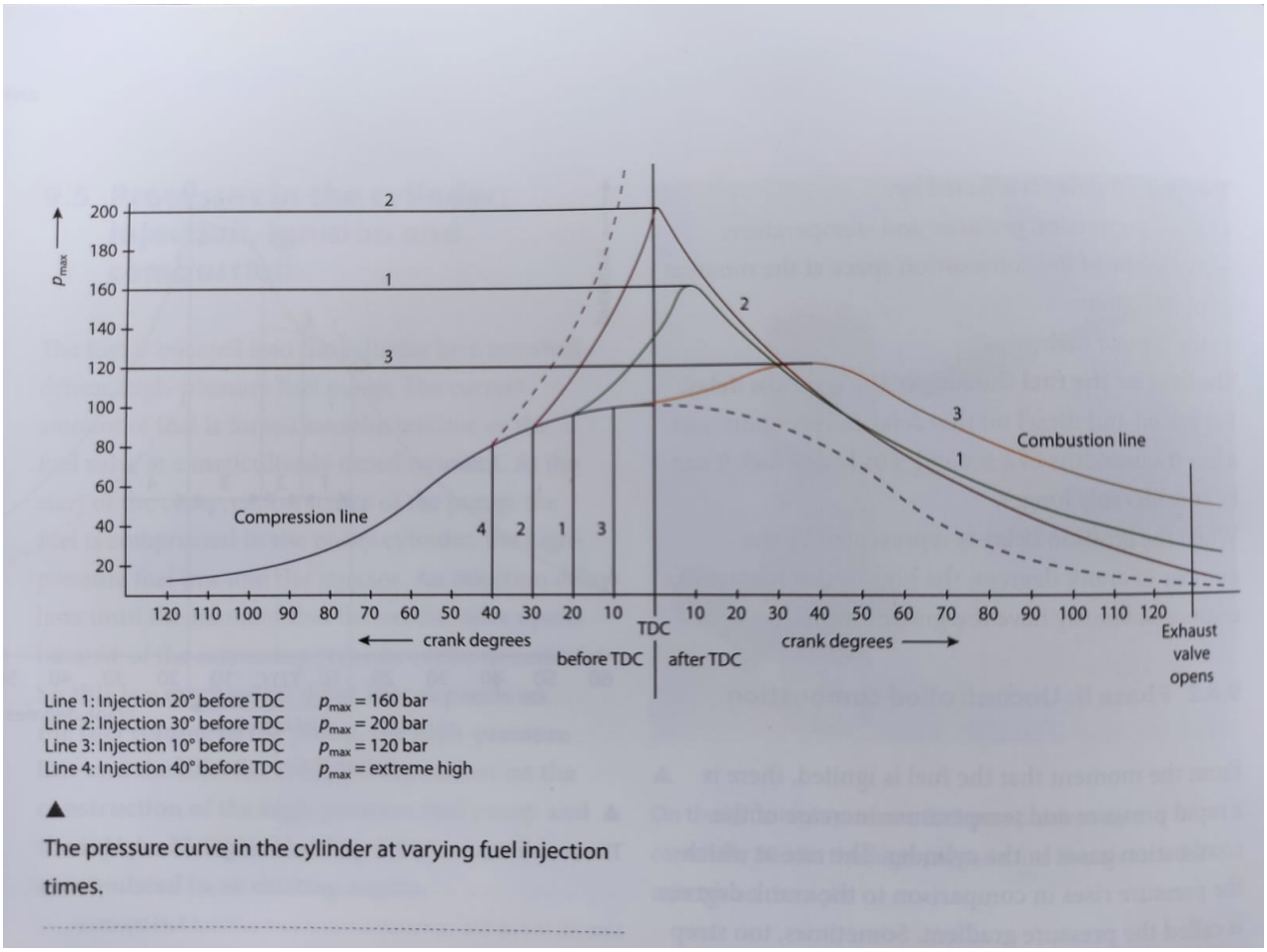

▲ The pressure curve in the cylinder at varying fuel injection times.

Figure 6.3: Illustrative cylinder pressure at different fuel injection timing, [21]

There are four cases mentioned showing how the pressure in the cylinder goes from early fuel injection until very late injection. The four case are:

- Case 1: Injection 20° before TDC p_{max}= 160 bar
- Case 2: Injection 30° before TDC p_{max}= 200 bar
- Case 3: Injection 10° before TDC p_{max}= 120 bar
- Case 4: Injection 40° before TDC p_{max}= extremely high value

An ideal normal operational injection case would be the first one since the peak combustion pressure is close after the TDC with a nice partially controlled combustion. In the second case the injection happens 10° earlier than the first case and it can be observed a large increase of the peak pressure exactly at the TDC position of the piston and may not be as effective since the piston has not yet begin the downward trajectory. Regarding the third case injection happens 10° after the first case leading in a smaller peak pressure value taking place further away from the TDC thus delivering less power to the piston while also increasing the pressure and temperature in the exhaust gasses. The forth and final case regards the injection at 20° before the first case resulting in an extreme value of peak pressure before the piston reaches the TDC position resulting in opposite forces inside the cylinder between the piston and the pressure with a high possibility of damage occurring, [21].

As can be concluded from the diagrams mentioned above and the described cases, the curves of 6.1 are very similar to the ideal case 1 of the illustrated figure 6.3 while figure 6.2 are similar to the case 3 and/or 4 which are not so ideal thus the decision to use the selected diagram.

Comparing the two diagrams 6.1 and 6.2 we can clearly see the difference in peak pressures where in the first case is around the 213 bars mark while in the second case is around the 220 bars mark with 208 bars and 218 bars averaging pressures respectively. In addition to the cylinder pressures, when comparing the available information regarding the exhaust temperatures of DG1 to DG4 engines, it can be observed that the average temperature is slightly less with 408°C compared to 411°C respectively concluding that the difference in pressures does not affect the exhaust temperatures as much as expected. Based on the aforementioned the rest of the research will focus on the available information obtained for the DG1.

6.2. Model changes for diesel operation

The existing input information in diesel B engine model needed to be changed in order to run for the M32E engine that is installed onboard of Bravenes. Most of the used data became available from the provided engine acceptance test, measurements from onboard the vessel while sailing and other documentation provided by Van Oord. Some of the parameters of the model were remained the same either due to be estimates based on the engine's stroke and bore dimensions because the exact values were not possible to be found or because the information were not available thus it was determined to alter only the things that were known to be accurate. The most important model changes are presented below:

- Dimensional measurements
- Operational information
- Seiliger parameters

6.2.1. Dimensional measurements

This part of changes is regarding the dimensional measurements of the specific engine. Changes involve the number of cylinders, the bore, stroke and connecting rod dimensions, the geometric compression ratio and the silencer and exhaust manifold diameters since they were available.

6.2.2. Operational information

The operational information of the engine is regarding the air fuel ratio, the brake specific fuel consumption, valve timing, injection timing, output per cylinder, nominal engine speed and the number of revolutions per cycle regarding if it is a two stroke or 4 stroke engine. Using the available information

the model can estimate the effective compression ratio, mean piston speed, total torque and power of the engine as well as the expected fuel consumption at nominal load. In addition to the above changes, information were also available about the measurements of water and air temperatures in and out of the charge air cooler as well as some system pressures. On top of that, data regarding exhaust and turbocharger temperatures were also included aiming to calibrate the model as close as possible to the real engine operation.

6.2.3. Seiliger parameters impact on combustion process

The Seiliger parameters are one of the most important parts of this research. Based on the parameters $n_{comp}, a, b, c and n_{exp}$ the model can describe the combustion of the cylinder process from the inlet valve close until the exhaust valve open timing providing valuable information about the engine's operation. Yu Ding in his research investigated thoroughly the Seiliger parameters and their connection to the combustion shape. Some of the most important conclusions from his research are that a large value of parameter a translates to a higher peak pressure and temperature. On the other hand a larger value of parameter b based on the results does not influence the peak pressure in stage 3 but the peak temperature and afterwards is increasing. Furthermore, the investigation on parameter c reveals that the only impact of the parameter increase is on the pressure and temperature at the exhaust valve open stage. In addition to the combustion shape parameters a,b and c, Yu Ding noticed the influence of the polytropic compression component, n_{comp} on the pressure and temperature in stage 2 which effected the rest of the Seiliger process. Last but not least, the polytropic expansion, n_{exp} is found to determine primarily the stage 5-6 and the exhaust valve open conditions, [5]. Based on the provided information a small investigation will take place for the diesel and Fuelsave technology in this thesis in order to calibrate the model to the available measurements and understand better the model.

Parameters estimation

In the current diesel B model provided by the TU Delft the parameters for the Seiliger process are estimated as described below:

Parameter a

The way that the isochoric combustion ratio a is calculated in the model is with the empirical formula derived by Schulten:

$$a = 1 + \frac{\tau_{cb} \cdot \eta_{cb} \cdot q_{f23} \cdot X_a}{c_v \cdot T_2} \tag{6.1}$$

$$X_a = X_{a,n} \cdot (\frac{n_e}{n_{e,nom}} - 1) + X_{a,c} \tag{6.2}$$

The variables mentioned in equation 6.1 include the ignition delay, τ_{cb}, the combustion efficiency, η_{cb}, the heat release fraction for stage 2-3, q_{f23}, parameter X_a indicating the heat fraction of potential heat during the stage along with the specific heat at constant volume and the temperature after compression takes place.

The parameter X_a describes the effect of fuel supply on the pressure rise. There are two equations available in order to estimate it. The difference between them is the consideration of another variable regarding the fuel injection rather than just the engine rotational speed and the constant value of $X_{a,C}$.

$$X_a = X_{a,n} \cdot (\frac{n_e}{n_{e,nom}} - 1) + X_{a,f} \cdot (\frac{m_f}{m_{f,nom}} - 1) + X_{a,c} \tag{6.3}$$

In the thesis of J.S van Duijn and Congbiao Sui there was also the addition of another variable in the X_a parameter describing the dependency of both the fuel injection mass per cycle and the engine rotational speed.

Currently in the model parameter X_a is estimated only as a function of the engine rotational speed but it would be a nice recommendation to update the way of calculation to the improved formula.

Parameter bb and b
The way of calculating parameter b involves the estimation of an intermediate variable bb which can be introduced by equation 6.4. As can be seen, a similar variable is introduced here which helps in the calculation of bb and it was introduced by Baan. Using equation 6.5 and not the updated formula parameter X_b is estimated. After the calculation of bb we can proceed with the isovolumetric combustion ratio b using equation 6.7.

$$bb = a \cdot b = 1 + \frac{X_b \cdot q_f}{c_p \cdot T_2} \tag{6.4}$$

$$X_b = X_{b,n} \cdot (\frac{n_e}{n_{e,nom}} - 1) + X_{b,c} \tag{6.5}$$

$$X_b = X_{b,n} \cdot (\frac{n_e}{n_{e,nom}} - 1) + X_{b,f} \cdot (\frac{m_f}{m_{f,nom}} - 1) + X_{b,c} \tag{6.6}$$

$$b = \frac{bb}{a} \tag{6.7}$$

Parameter c
The last parameter, the isothermal combustion ratio c describes the last stage of combustion and it is basically determined by the values of parameters a and b.

$$c = e^{\frac{w_{45}}{T_4 \cdot R_{45}}} \tag{6.8}$$

Even though parameter c cannot be directly selected by the user its purpose is significant since it determines the values of pressure and temperature for the exhaust open stage which are the main input for the gas exchange model and in the end the input to the turbine inlet temperature.

6.3. Model calibration

The received model was calibrated for two different 4 stroke engines, one CATERPILLAR 16 cylinder engine with nominal engine speed 1600 rpm and one MAN 4 cylinder engine with nominal engine speed 981 rpm. Both engines were producing less power and pressures than the specific M32E engine but they were used as a guideline and template for the calibration of the current model. The available models for the mentioned engines were both used in the beginning in order to observed which of the two offered the best foundation to extent the M32E engine in. After performing similar changes in both cases regarding the M32E engine specification without changing any information about the turbocharger, or the Seiliger combustion it was noticed that the model for the CATERPILLAR engine was more suitable for our needs as the temperatures and pressures in the system were higher and similar to the available data .

The next step after choosing the base model was to perform the changes mentioned in section 6.2 and then investigate the Seiliger parameters.

6.3.1. Cycle calibration

The calibration of the model as was mentioned above is based on information provided by the manufacturer engine acceptance test, measurements from onboard the vessel while sailing and other documents. On the other hand, as was explained in the introduction of the chapter the pressure-crank angle and sailing measurements for the DG1 were taken into account to calibrate the combustion shape for the specific engine load condition. The chosen information was for a sailing trip in November of 2019 when the DG1 engine was operating at 100 % engine load delivering 3920 kW generator load. In addition to the load reading the pressure trace diagram for the specific trip was used for the calibration of the model which resulted in some interesting findings which will be addressed in the section below.

The following procedure was followed in order to use the received data in the calibration process. To begin with, the initial pressure-crank angle measurements was processed and using the equations 6.9 and 6.10 it was possible to plot the pressure-volume diagram which then is compared to the estimated pressure-volume diagram produced by the model, [40]. The crank radius can be also be expressed as

half of the stroke length,L_s, which is known along with the connecting rod length, L_{cr}. The exact value of the result will remain hidden from this report.

$$\lambda_{cr} = \frac{R_{cr}}{L_{cr}} = \frac{L_s/2}{L_{cr}} \tag{6.9}$$

Continuing, now that the volume at each crank angle is estimated using equation 6.10 from Yu Ding, the diagram 6.4 can be drawn.

$$V(\alpha) = V_s \cdot \left[\frac{1}{\epsilon - 1} + \frac{1}{2} \cdot \left((1 + \cos\alpha) + \frac{1}{\lambda_{cr}} \cdot (1 - \sqrt{1 - \lambda_{cr}^2 \cdot \sin^2\alpha})\right)\right] \tag{6.10}$$

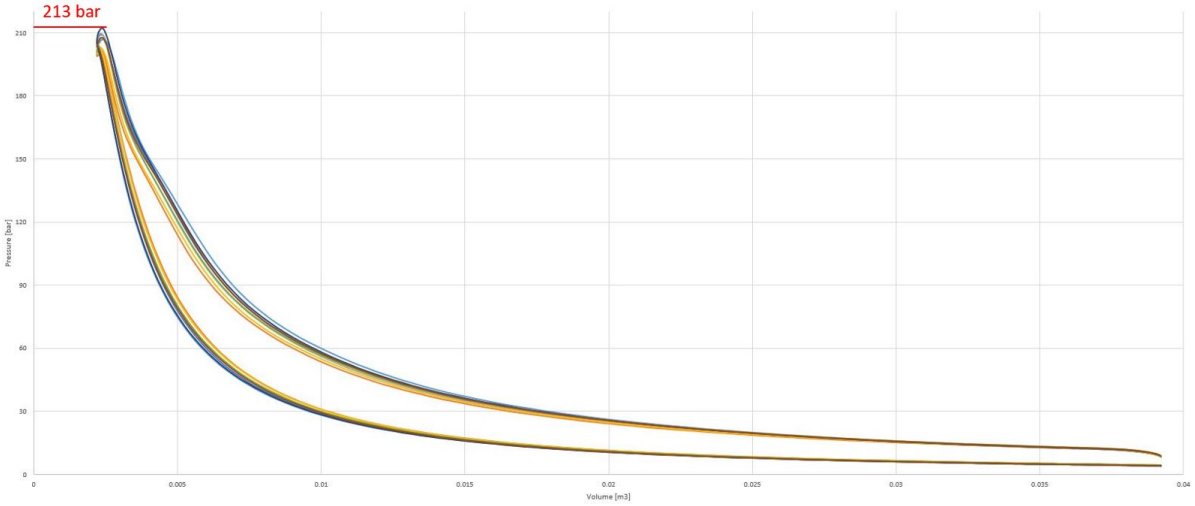

Figure 6.4: Pressure-Volume diagram DG1 8 cylinders

As can be seen from figure 6.4 the pressure traces for the 8 cylinders of the DG1 have been plotted. Interestingly a variation of peak pressures and pressure curves can be observed. The maximum recorded pressure is around 213 bars and along with the rest of the pressure-volume curve will be compared with the results from the model b.

From the pressure trace of the engine it was also possible to estimate the indicated power, indicated work as well as the mean indicated pressure which will be used later on for the validation of the model. In the process of estimating the above parameters it was noticed that the indicated power of the engine measured by the vessel in another document for the same trip resulted in 3036 kW which has a large variation from the 3920 kW generator load found initially. The rest of the investigation about the difference in the provided measurements from Van Oord is viewed in detail in the appendix B since it does not benefit the main research question of the thesis.

The next step is the research of the b model provided by the TU Delft university. The default Seiliger parameters for the 16 cylinder Caterpillar engine can be seen in table 6.1 which resulted in the following pressure volume diagram 6.5.

As can be seen from figure 6.5 the peak pressure is slightly higher than 250 bars which is not suitable for our case. Using equation 6.11 and since the desired peak pressure of 213 bars is know, an estimation for parameter a can be drawn based on the engine's effective compression ratio r_c, the polytropic exponent n_{comp} and the initial trapped pressure when the inlet valves close p_1.

$$p_{max} = p_1 \cdot r_c^{n_{comp}} \cdot a \tag{6.11}$$

With the above approximation regarding parameter a what comes next was to investigate the rest of the variables for the Seiliger process in order to have reasonable values and similar results to the measurements. Taking into consideration the remarks made in the above section regarding the difference in the engine recorded power from the pressure trace and the one from the engine's main switchboard, it was decided to ignore the pressure trace information and calibrate the model for the 3920 kW generator load. The details of that decision can be found in the appendix B.

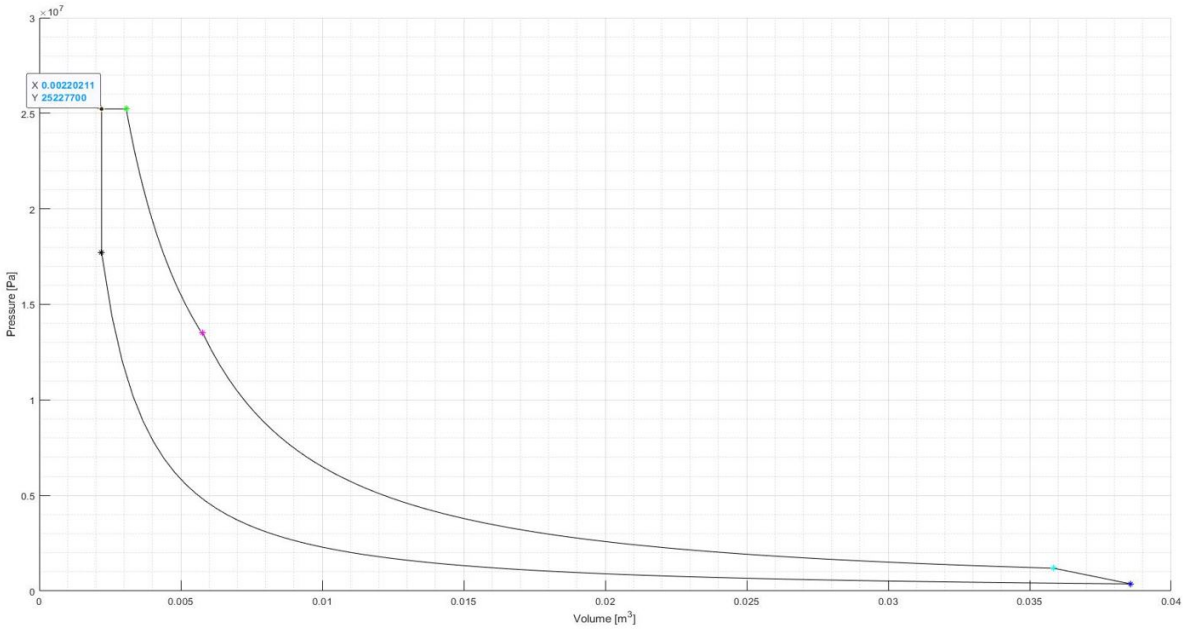

Figure 6.5: Pressure-Volume diagram using the base parameters

Parameter	Value [-]
n_{comp}	1.35
n_{exp}	1.33
$X_{a,c}$	0.3
$X_{a,n}$	-0.1
$X_{b,c}$	0.8
$X_{b,n}$	-0.4
a	1.43
bb	1.99
b	1.39
c	1.88

Table 6.1: Base Seiliger parameters from original model

Taking into account a 95% generator efficiency and a 95% mechanical efficiency leads to 4343 kW indicated power from the engine. The model cannot be calibrated for the indicated power directly but only through the brake power and then from the Seiliger the indicated power can be estimated. The results from the model will be assessed using the information at hand, and a choice will be made as to which Seiliger parameters will be carried out in the end.

To diesel b model provided by TU Delft initially was calibrated for two smaller engines. Processing the documentation provided by Van Oord regarding the M32E engines the calibration of the model for the diesel operation was completed. Taking into consideration that the main research question is focusing on the Fuelsave technology effects on the engine performance it was decided to avoid further investigation of the data contradiction that was discovered. The calibration of the model is performed for the 3920 kW generator load operation. The mentioned generator power translates to around 93.78 % load conditions for the DG1 assuming a 95% mechanical efficiency to estimate the effective power. The selected Seiliger parameters were selected aiming on matching the peak pressure of the DG1 to the model's output.

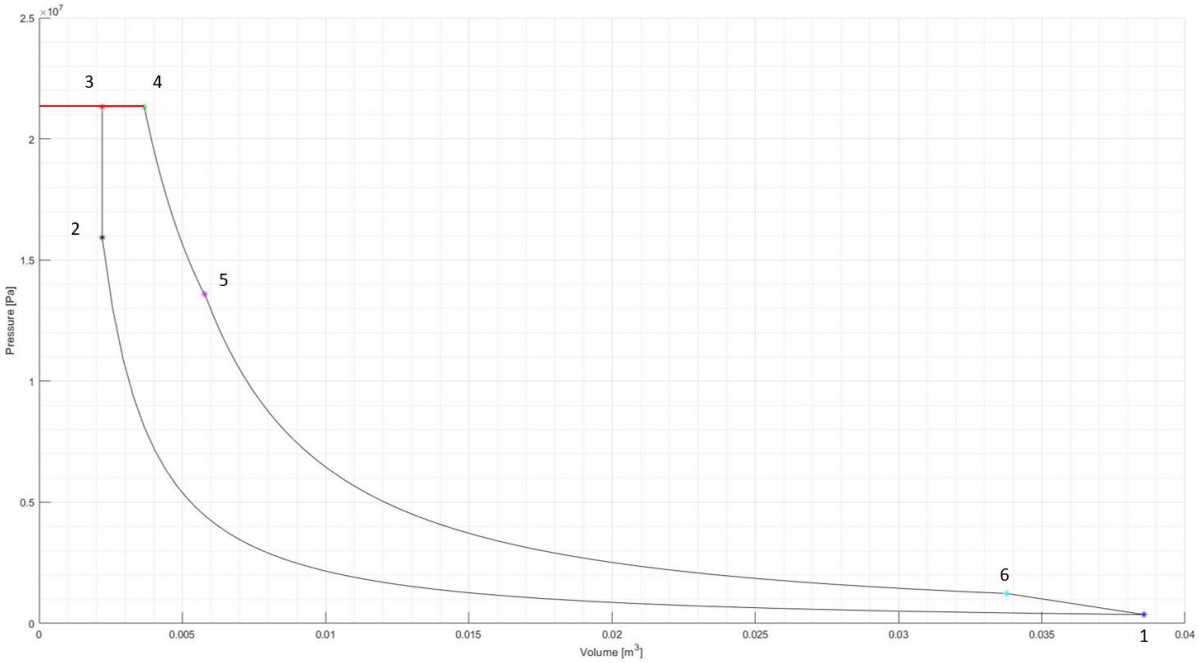

Figure 6.6: Pressure-Volume diagram for diesel operation

Parameter	Value [-]
n_{comp}	1.32
n_{exp}	1.36
$X_{a,c}$	0.205
$X_{a,n}$	-0.1
$X_{b,c}$	0.84
$X_{b,n}$	-0.4
a	1.34
b	1.67
c	1.575

Table 6.2: Calibrated Seiliger parameters for diesel operation

7

Verification and validation of model for diesel operation

The model is now configured and produces calibrated results for the M32E 8 cylinder engine of Bravenes running 4126 kW effective power. It is wise to verify that indeed the output of the model agrees with the available documentation either from the manufacturer or from operational data from onboard the vessel.

7.1. Equivalence criteria

The obtained measurements of the engine were compared to the results of the model for the same operational conditions. In order to verify that the model's outputs match with the received data the following equivalence criteria will be utilized.

- Maximum pressure
- Indicated work
- Inlet valve close pressure
- Charge pressure in the system
- Turbocharger temperature
- Charge air cooler temperature

7.1.1. Measurements

The available information received from Bravenes while sailing is the main calibration of the model since it covers most of the equivalence criteria. The maximum cylinder pressure for the 8 cylinder M32E engine, DG1, is averaging around 208 bars with the peak pressure to be 213 bars. The cylinder temperatures are not know, but information regarding the temperature before and after the turbocharger as well as before and after the charger air cooler are very useful to learn the inlet and outlet conditions of the engine.

According to Yu Ding, to fit the Seiliger process with a good approximation to the measured cycle the most important equivalence criteria are the peak pressure and the indicated work and the least important are the peak temperature and the temperature when the exhaust valve open. The temperature and the pressure for the exhaust valve open stage are related by the gas law and since the mass in constant the only one the two is necessary, [5].

First of all the peak pressure can be of great importance since it describes the mechanical load occurred on the engine which then translates to the maximum stresses applied on different components of the engine. Due to this, it is clear why the Seiliger parameters needs to be set properly in order to have an accurate representation of the cylinder pressure, [5]. As can be seen from table 7.1 the peak pressure from the model is identical to the measured peak pressure from the recorded sailing trip of

Cylinder	1	2	3	4	5	6	7	8					Average
Fuel rack position	48.5	48	48.5	48	48	48	48	48.5					48.19
Exhaust temp.	393	406	402	410	401	428	421	402					407.88
Act pos./Fuelrack pos.	8	79%											
Fresh cooling water	LTt	33	LTp	2.4	HTin	71	HTout	84	HTp	3.7			
Combustion press.	210	204	210	203	208	209	213	208					208.13
Compression press.	0												0.00

Lubricating oil			Fuel			n Engine	720	rpm
p bef. filter	bar		Type	MGO		Gen. Load	3920	kW
p aft.filter	bar	4.8	Gravity	kg/m3	0.84	Load DCU	101	%
p last main bear.	bar		Sulpher	%		Exhaust colour		
p last camsh. bear.	bar		Consumpt.	kg/h	773-907			
t inl. eng.	°C	58.5	p bef. filter	bar		**Turbocharger**		
t outl. eng.	°C	63	p aft. filter	bar	5.1	Turbine speed	rpm	23570
t inl. cool.	°C	62	p Nozzle cool.	bar	n.a	t Exhaust bef.turbo	°C	518
t outl. cool	°C	55	t Nozzle cool.	°C	n.a	t Exhaust aft.turbo	°C	321
oiler adjustm.			t Fuel service tank	°C	30	t Charge air bef.cool.	°C	229
circuit oil			t Final pre heat	°C		t Charge air aft.cool.	°C	48
consumption	kg/d		t Fuel viscotherm.	°C		t Intake air in a distance		
Cyl.lubricat. oil			Viscosity at --			of 10 cm to the filter	°C	25
consumption	kg/d		Viscotherm	Cst		t ambient	°C	
Quality			t Fuel bef.eng.	°C	39	p Charge air aft.cool.	bar	3,95
Treatment			Additives			p difference	mmWC	
Oil Qty. in system	kg		Treatment			Exhaust gas -		
Autom.Filter			Autom.filter			back pressure	mmWC	
Flushings/day			Flushings/day			p diff. air screen	mmWC	

Figure 7.1: Bravenes DG1 measurements, [28]

Bravenes for the specific diesel generator. In case of another engine or another engine load the Seiliger parameters would need to be altered for a more precise characterisation of the cylinder process.

The indicated work describe the engine output and also its ratio with the heat input provide the cycle's indicated efficiency which is key element for the engine performance. From the provided information the average indicated work per cylinder per cycle is 90.49 kJ while from the model output is 86.56 kJ which is near the estimation of the theoretical indicated work of the engine. It was not possible to match the indicated work per cycle for the current pressure trace measurements mainly due to the lack of accurate data for the engine which made it hard to calibrate the model correctly. The only available indication was the generator load value and by assuming a 95% generator efficiency and a 95% mechanical losses efficiency the indicated work was estimated and tried to be match unsuccessfully, [15]. It can be discussed that the value for the indicated work from the generator load is again estimated since no accurate data were known. In the appendix B the pressure volume diagrams between the measurements and the model output along with a discussion can be found regarding the calibration choices.

Other criteria are the T_{EO} and P_{EO} which are the last temperature and pressure for the Seiliger process and the input signals to the gas exchange process. Due to that, they have a high impact on the temperature and pressure entering the turbine side of the turbocharger affecting its performance. The cylinder pressure trace from the Bravenes were available but as mentioned above were not matching with the data on figure 7.1 thus were not used.The initial and final pressures may have been known if the graphs were going to be utilized.

Additional to the exhaust valve open pressure, the inlet valve close pressure can be also considered a criterion since is the trapped pressure where the cylinder compression begins. A different value of the

Parameter	Estimated value	Measured value
Pmax	213 [bar]	213 [bar]
Wi per cycle	86.56 [kJ]	90.49 [kJ]
P_{IC}	3.64 [bar]	3.95 [bar]
T exh before turbo	537 [C]	518 [C]
T exh after turbo	382 [C]	321 [C]
T air before CAC	194 [C]	229 [C]
T air after CAC	45 [C]	48 [C]
Fuel consumption	838 [kg/hr]	773-907 [kg/hr]

Table 7.1: Model output compared to measurements, [28]

trapped pressure could result in the change of the Seiliger process since a higher starting point would lead to an increased pressure p2 and as a reaction the increase of peak pressure. The trapped pressure for the model and the measurement is somewhat lower, according to table 7.1 but close enough.

From the measurements the before and after temperature of the turbocharger are also available and they can be compared with the results of the model. As can be seen from the table 7.1 there is quite a difference between the measured and the estimated values of the temperatures but this was expected since there were missing information about the turbocharger parameters thus were assumed to be the same with the base values from the initial model.

It can therefore be concluded that the model with the selected Seiliger parameters and the other changes based on the available information and the equivalence criteria provide sufficient results to continue with the FuelSave technology changes on the model and in the end compare the performance analysis of the two.

8

Model changes for FuelSave technology

The FuelSave Marine+ purpose as mentioned in the beginning of the report is to enhance the combustion efficiency of the engine and/or reduce emissions. In order to describe the benefits of the module the operation of the model needed to be understand with the aim to find the best way to show the capabilities of the project.

8.1. Fuel addition

The model b originally provides the choice of operating in different loads and modes like in a propeller load operation or in a generator mode. Bravenes operates in a generator mode at all times thus it was also set up this way in the model. In the generator mode the model takes as input the required engine speed by the user and then the governor using a PID controller to compare the desired and actual engine speed controls the fuel rack position. Continuing, the fuel rack position signal is sent to the fuel pump subsystem where using the nominal fuel quantity given by the user alogn with the signal for the fuel rack position by the governor the fuel injected per cycle per cylinder, $m_{f,cyc}$, is estimated and also the fuel flow into the engine is found, ϕ_f for the specific engine speed and load.

$$m_{f,cyc} = X_f \cdot m_{f,cyc,nom}\,[kg] \tag{8.1}$$

$$\phi_f = m_{f,cyc} \cdot i_{cyc} \cdot \frac{n_{eng}}{k_{cyc}}[kg/s] \tag{8.2}$$

8.1.1. Fuel addition changes

J.S van Duijn, [10], when performing his master thesis about ammonia-diesel combustion in two stroke engines due to the unknown quantity of ammonia injection he decided to convert the nominal fuel mass to a nominal fuel energy using an energy share ratio between the two fuels. The required energy would be found using the lower heating values of the fuels and the ammonia energy share ratio set by the user which in the end would determine the nominal mass quantities and flows of diesel and ammonia. In addition in the above thesis it is assumed that ammonia-diesel will be a blend mixture rather than port injected.

The difference in this thesis is that FuelSave injects the additives with a different fuel pump in the intake area of the engine and the quantities of the fuels are approximately known. To begin with, the company aims to inject 3% of the nominal diesel fuel with methanol and 7% of the nominal diesel fuel with water. As for the hydrogen, oxygen addition the quantities are based on experiments that were performed by FuelSave and would be around the 12 m^3/h. Based on the above approximations the quantities of the additives are known for now. Taking into consideration also that FuelSave considers methanol the fuel which can replace and reduce some of the diesel quantity it is possible to determine that since methanol is characterized by approximately half the lower heating value of diesel it could be possible to achieve 1.5% reduction of the primary fuel used.

In order to perform the necessary changes for the introduction of energy and quantity of additives to the model the lower heating value of methanol and hydrogen alogn with the nominal hydrogen quantity

per cycle per cylinder were added into the 'fuel_specification.m' matlab file. Using the additional terms of the additives adjustments were performed to the simulink model to account for the 1.5% primary fuel reduction, the 3% of methanol addition and the hydrogen quantity into the cylinder amongst their lower heating values.

The changes do not take into account the second fuel pump which will be needed in reality for the injection of water-methanol mixture and will consume some electricity from the main switchboard. In addition, another thing that is not taken into account is the power consumption needed for the electrolyzer to produce the hydrogen and oxygen.

8.2. Combustion efficiency

The combustion efficiency is a very important variable in the structure of the model since describes what fraction of the injected fuel is fully combusted in the combustion chamber. The majority of the diesel engines operate in lean mixture conditions to provide as much oxygen as possible in the mixture in order to help having as complete combustion as possible. An engine with poor combustion efficiency results in quantities of un-burned fuel increasing the fuel consumption of the engine and increase of emissions in the exhaust gas.

8.2.1. Original model

The combustion efficiency estimation as is in the current model is based on the empirical formula of Betz and Woschni. What they found was a linear relationship between the combustion efficiency and the air excess ratio up to a maximum value. A comparison between the air excess ratio and a specific smoke limit means that when the air excess ratio is higher than the smoke limit the combustion efficiency is complete, 100 %.

The combustion efficiency of the M32E engine was not available in order to verify that the above empirical equation could be used thus it was investigate if there was another way to calculate it. Harsh Sapra [34] while trying to find the combustion efficiency in his own dissertation used equation 8.3 to calculate it.

$$\eta_{comb} = (1 - \frac{C_{CO} + C_{UHC}}{C_{fuel}}) \cdot 100 \tag{8.3}$$

The above equation is based on emission measurements which result from incomplete combustion all measured in $\frac{Kg}{Kg}$ of fuel.

A test report was available from Van Oord with the emissions of the M32E engine thus it was possible to calculate the combustion efficiency for diesel operation based on that. The measurements were performed by ecoxy in the beginning of 2020 and was mainly focused on the NOx emissions but the CO_2 and CO emissions were also measured for four different loads as well. Unfortunately the UHC were not showing thus the combustion efficiency was only calculated with the CO measurements for the four different loads.

The results of equation 8.3 showed that the M32E engine has a very high combustion efficiency of 99.99 % for the four loads but taken into consideration that the measurements were performed in 2020 and only the CO emissions were available we can expect that indeed the real combustion efficiency of the engine could be lower. In addition to that we could argue that an operating engine over the years due to many reasons could potentially perform worse over the increase of the operational hours thus the actual combustion efficiency could drop even further.

8.2.2. Alternative calculation

The current empirical formula was not suitable for our needs due to the need of more accurate and recent measurements as stated above thus a research was performed in order to find alternative ways to calculate the combustion efficiency and present the possible improvement due to the FuelSave operation.

Two alternative formulas were able to be found but due to their nature requiring measurements they were not able to be used in our case.

The first equation is 8.3 which was used for the estimation of the combustion efficiency for the diesel operation but still the lack of measurements did not provide an accurate result.

The second equation was found in Heywood [17]:

$$H_R(T_A) - H_P(T_A) = m \cdot \left(\sum_{i,reactants} n_i \delta h_{f,i} - \sum_{i,products} n_i \delta h_{f,i} \right) \tag{8.4}$$

$$\eta_{comb} = \frac{H_R(T_A) - H_P(T_A)}{m_f \cdot Q_{HV}} \tag{8.5}$$

Equation 8.4 describes the net chemical energy release after combustion in the engine by taking into consideration the total mass, m, entering and leaving the control volume of the engine by assuming it an open system and the enthalpy of reactants (fuel and air) and products (exhaust gas). The difficulty of the above equation is that you could never know the exact composition of the fuel and again measurements of the mass flows would be necessary to calculate it.

Equation 8.5 is another way of estimating the combustion efficiency of an engine by taking into consideration the net chemical energy release as mentioned above over the supplied fuel energy entering the control volume described by the mass of the fuel, m_f, and its heating value, Q_{HV}.

8.2.3. Combustion efficiency conclusion

Taking all the above into consideration it was decided to have the current combustion efficiency model unchanged due to the estimated value of efficiency which was around 100 % based on equation 8.3 and because an alternative way to improve the modelling was not found.

8.3. Air excess ratio

The air excess ratio is linked to the engine's power delivery. Diesel engines usually are operated in lean operational conditions to make sure that enough oxygen is present in the combustion of diesel. The air excess ratio also describes the higher real amount of combustion air compared to the ideal air quantity. The actual combustion air needs to be higher than the stoichiometric in order to improve the combustion but also cool the cylinder, [15]. The increase of fuel without the necessary change in the air quantity will result in the decrease of air excess ratio in reduce power, and the rich mixture can result incomplete combustion.

$$\lambda = \frac{afr_{actual}}{afr_{theoretical}} = \frac{m_{air}}{m_f \cdot \sigma} \tag{8.6}$$

As can be seen from equation 8.6, λ is depended on the actual air quantity entering into the engine over the theoretical air quantity which is found by multiplying the fuel quantity with the stoichiometric ratio. The addition of hydrogen and methanol affect the air excess ratio since each fuel has its own stoichiometric ratio and injection quantity.

First the stoichiometric ratio of each of the additives is calculated either using the chemical structure formula or the mass fractions of the fuels as shown below [40]:

$$C_p H_q S_r + \left(p + \frac{q}{4} + r\right) \cdot O_2 \rightarrow p \cdot C0_2 + \frac{q}{2} \cdot H_2O + r \cdot SO_2 \tag{8.7}$$

$$\sigma_{da} = \frac{M_{da}}{y_{O_2}^{da}} \cdot \frac{p + \frac{q}{4} + r}{p \cdot M_C + q \cdot M_H + r \cdot M_S} \tag{8.8}$$

$$\sigma_{da} = \frac{M_{da}}{y_{O_2}^{da}} \cdot \left\{ \frac{x_C^f}{M_C} + \frac{1}{4} \cdot \frac{x_H^f}{M_H} + \frac{x_S^f}{M_S} \right\} \tag{8.9}$$

For the estimation of methanol stoichiometric air fuel ratio it is more convenient to use equation 8.9 by removing the sulphur content and adding the oxygen content of methanol resulting in equation 8.10.

$$\sigma_{da} = \frac{M_{da}}{y_{O_2}^{da}} \cdot \left\{ \frac{x_C^f}{M_C} + \frac{1}{4} \cdot \frac{x_H^f}{M_H} - \frac{x_O^f}{M_O} \right\} \tag{8.10}$$

For the hydrogen stoichiometric air fuel ratio estimation we can use the mass fraction equation again by using only the hydrogen mass fraction as shown in equation 8.11.

$$\sigma_{da} = \frac{M_{da}}{y_{O_2}^{da}} \cdot \left\{ \frac{x_H^f}{4 \cdot M_H} \right\} \tag{8.11}$$

The results of the above equations for hydrogen and methanol are 34.4 and 6.45 which are in line with the information found in literature.

The above estimations result in a change of the air excess ratio equation since the amount of hydrogen and methanol along with their stoichiometric air fuel ratios need to be taken into account. Equation 8.12 shows the modified air excess ratio which is implemented in the model to account for the additives introduction where m_{d_f} and σ_d are the diesel quantity and stoichiometric air fuel ratio, m_{h_f} and σ_h are the hydrogen quantity and stoichionetric air fuel ratio and m_{m_f} and σ_m are the methanol quantity and stoichiometric air fuel ratio.

$$\lambda = \frac{m_{air}}{m_{d_f} \cdot \sigma_d + m_{h_f} \cdot \sigma_h + m_{m_f} \cdot \sigma_m} \tag{8.12}$$

8.4. Gas mixture

Air is composed of multiple gasses. Out of the different gasses in the air only oxygen is assumed to be reacting with fuels resulting in reaction products. Depending on the fuel and the oxygen quantity in the air the reaction products are changing.

8.4.1. Air flow in engine

The composition of air can be broken down into four main element according to DIN standard, [40]. The dry air composition can be seen in table 8.1:

Element	Kmol fraction [-]	Mass [g/mol]
N_2	0.7809	28.013
O_2	0.2095	31.999
Ar	0.0093	39.948
CO_2	0.0003	44.010

Table 8.1: Dry air composition into the engine

The composition of the air can be used to estimate the molecular weight of the mixture using equation 8.13

$$M = \sum_j M_j \cdot y_j \tag{8.13}$$

$$M_{da} = M_{N_2} \cdot y_{N_2}^{da} + M_{O_2} \cdot y_{O_2}^{da} + M_{Ar} \cdot y_{Ar}^{da} + M_{CO_2} \cdot y_{CO_2}^{da} \tag{8.14}$$

In addition to the dry air composition there is also the wet air composition expressing the absolute humidity. In order to describe the quantity of water in wet air equation 8.15.

$$x_{H_2O}^{da} = \frac{m_{H_2O}}{m_{da}} \tag{8.15}$$

The default value of absolute humidity in the model b is 0.0097 g/kg dry air which leads to the calculation of the wet air mass fraction and in the end the volume fraction of each chemical element 8.2.

The introduction of oxygen, methanol-water and hydrogen happens in the air intake area of the engine. This means that the initial composition of air will be affected by the additives. Based on the quantity of the air demand of the engines and the quantities of additives the following compositions were estimated.

Table 8.1 shows the initial dry air composition which can be compared with table 8.3 presenting how the air composition in volume percentage changes for the 6 and 8 cylinder engines when the additives are introduced.

Element	Kmol fraction [-]	Mass [g/mol]
N_2	0.7689	28.013
O_2	0.2063	31.999
Ar	0.0092	39.948
CO_2	0.0003	44.010
H_2O	0.0003	18.015

Table 8.2: Wet air composition into the engine

Engine	N_2 %	O_2 %	Ar %	CO_2 %	H_2 %	CH_3OH-Water %
6M32E	77.427	20.798	0.923	0.0298	0.122	0.666
8M32E	78.085	20.949	0.930	0.030	0.101	0.552

Table 8.3: Dry air composition change with additives

According to the results the effects of additives are not significant and this makes sense since the quantities of the hydrogen, oxygen, methanol & water compared to the air demand of the engines are very small. Based on the above it was decided to leave the incoming air composition unchanged in the fluid_properties.m file of the model since it was expected that the results would not be affected.

8.4.2. Exhaust gas composition

The exhaust gasses are the result of the combustion of reactants with air. The composition of the reaction products is of great importance since it can determine the thermodynamic properties of the exhaust gasses heading toward the exhaust turbine and also some of them are remaining into the cylinder affecting the temperatures and compression in the engine. The estimation of the composition is done using stoichiometry by following the conservation of mass law in which the total mass of products equals the total mass of reactants. Diesel reaction with air oxygen results in CO_2, H_2O and SO_2 emissions with their composition calculated using the following equations:

$$x_{sg,CO_2} = \frac{M_{CO_2}}{M_C} \cdot \frac{x_C^{fuel}}{\sigma_{fuel} + 1} \tag{8.16}$$

$$x_{sg,H_2O} = \frac{M_{H_2O}}{2 \cdot M_H} \cdot \frac{x_H^{fuel}}{\sigma_{fuel} + 1} \tag{8.17}$$

$$x_{sg,SO_2} = \frac{M_{SO_2}}{M_S} \cdot \frac{x_S^{fuel}}{\sigma_{fuel} + 1} \tag{8.18}$$

The emission composition depends on the mass fraction of diesel fuel in regards of the carbon, hydrogen and sulphur content along with the stoichiometric ratio of the specific fuel.

In addition, to the diesel fuel reacting with oxygen there are some substances included in the inlet air like nitrogen and argon which can reach and result in products like the N_2 and Ar. The amount of nitrogen and argon in the exhaust gasses can be found using the following equations by taking into account the mass fraction in the air and the stoichiometric air fuel ratio of the fuel.

$$x_{sg,N_2} = x_{air,N_2} \cdot \frac{\sigma_{fuel}}{\sigma_{fuel} + 1} \tag{8.19}$$

$$x_{sg,Ar} = x_{air,Ar} \cdot \frac{\sigma_{fuel}}{\sigma_{fuel} + 1} \tag{8.20}$$

Last but not least, since oxygen is assumed that is completely reacted with diesel fuel in stoichiometry this means that the composition of oxygen is equal to zero:

$$x_{sg,O_2} = 0 \tag{8.21}$$

The b model already contains information about different types of fuels, like DMA, DMB and the selection of the fuel is straight forward. For our case the DMA is similar to the fuel that Bravenes is using thus is the more suitable option. The mass fraction composition of DMA is x_C=0.865, x_H=0.133, x_S=0.002 resulting in the product composition in table 8.4:

Element	Mass fraction [-]
N_2	0.7003
O_2	0
Ar	0.0119
CO_2	0.2023
H_2O	0.0759
SO_2	$2.5505 \cdot 10^{-4}$

Table 8.4: Diesel stoichiometric combustion composition

8.4.3. Methanol and hydrogen addition

In addition to the diesel combustion the FuelSave module will introduce methanol and hydrogen whose combustion with oxygen results in CO_2, H_2O and H_2O respectively. The estimation of the additional emissions can be found using equations 8.16 and 8.17. What changes now is the mass fraction of carbon and hydrogen contained in the fuels along with the stoichiometric air fuel ratio of the fuels. Methanol is composed of x_C=0.3749, x_H=0.1258, x_O=0.4993 which results in the following product composition in table 8.5:

Element	Mass fraction [-]
CO_2	0.1844
H_2O	0.1511
N_2	0.6476
Ar	0.0110
O_2	0

Table 8.5: Methanol stoichiometric combustion composition

Element	Mass fraction [-]
H_2O	0.2545
N_2	0.7266
Ar	0.0123
O_2	0

Table 8.6: Hydrogen stoichiometric combustion composition

The combustion of methanol and hydrogen do not produce different elements than the ones already existing from the diesel combustion with oxygen. What can be observed although is that there are no $S0_2$ emissions produce and when hydrogen is ignited there are no carbon dioxide emissions but an increase in N_2 can be seen which could possibly increase the $N0_x$ emissions.

The above impact of the methanol and hydrogen additives were not modelled into the current matlab files since the small quantities of injection were assumed that would not affect the thermodynamic properties of the mixtures.

However the additives were added in the calculation of the air composition. Initially, in each stage of the model the composition of the mixture is estimated using equation 8.22 where x is the mass fraction of the mixture and when is equal to 1 it means that only air is contained whilst when is equal to 0 means that there is only stoichionetric gas.

$$x_{air} = 1 - x_{sg} \tag{8.22}$$

The composition of the stoichiometric gas now includes the stoichionetric mass of diesel, methanol and hydrogen which can be found using equation 8.23 and its adjusted in every Seiliger stage. The model is build under the assumption that all of the fuel is combusted into stoichiometric gas and at the end of the process the combustion efficiency accounts of the percentage of fuel that in reality is not lost. The results will be discussed in the performance comparison chapter.

$$m_{sg} = m_{fuel} \cdot (\sigma + 1) \tag{8.23}$$

8.4.4. Thermodynamic properties

In the properties library of the model the estimation of the thermodynamic properties is performed. In the cylinder there are coexisting stoichiometric gas and air with the element described in the above section. For each of the elements of the air and stoichiometric gas they can be considered as non-perfect, ideal gases meaning that the mixture behaves in a similar way. For this reason the specific heat, enthalpy and internal energy of both the air and stoichiometric gas are function of temperature and element fractions [5].

Gas constant

The gas constant R in the model is estimated using equation 8.24 for both the air and stoichiometric gas by changing each time the mass fraction of the elements respectively and are constant throughout the model.

$$R = x_{N_2} \cdot R_{N_2} + x_{O_2} \cdot R_{O_2} + x_{Ar} \cdot R_{Ar} + x_{CO_2} \cdot R_{CO_2} + x_{H_2O} \cdot R_{H_2O} \tag{8.24}$$

In the simulink model there is also another gas constant estimation based on equation 8.25 and is based on the composition of air and stoichiometric gas and their gas constants.

$$R = (1 - x_{sg}) \cdot R_{air} + x_{sg} \cdot R_{sg} \tag{8.25}$$

Specific heats

The specific heats play an important role on the model since are used for the estimation of pressure and temperature in different stages. Using a power series for temperatures ranging from 200 - 2500 K based on 6 terms the specific heat at constant pressure can be estimated with sufficient accuracy.

$$\begin{aligned} c_p &= \alpha_1 + \alpha_2 \cdot \theta + \alpha_3 \cdot \theta^2 \cdot \dots \cdot \alpha_k \cdot \theta^{k-1} \cdot \dots \cdot \alpha_m \cdot \theta^{m-1} \\ &= \sum_{k=1}^{m} \alpha_k \cdot \theta^{k-1} \end{aligned} \tag{8.26}$$

$$\theta = \frac{T - T_{shift}}{T_{norm}} \tag{8.27}$$

With T$_{s}hift$ being equal to 0 K and the T$_{n}orm$ being equal to 1000K.

$$c_p = x_{N_2} \cdot c_{p,N_2} + x_{O_2} \cdot c_{p,O_2} + x_{Ar} \cdot c_{p,Ar} + x_{CO_2} \cdot c_{p,CO_2} + x_{H_2O} \cdot c_{p,H_2O} \tag{8.28}$$

The specific heat at constant volume can be found using equation 8.29 which is based on the specific heat at constant pressure and the gas constant.

$$c_v = c_p - R \tag{8.29}$$

Because it was assumed that the small amounts of fuels would not have a substantial impact on the outcomes, the thermodynamic parameters of the model were not altered to account for the specific heat of methanol.

8.5. Ignition delay

Ignition delay is important for the current thesis because it describes the time between the injection of fuel until the measurement of the pressure rise. From the literature, it is understood that methanol enhances the ignition delay because of the higher latent heat of vaporisation. The ignition delay in the model is primarily used in the estimation of Seiliger parameter a. The method of calculation was developed by Hardenberg and Hase taking into consideration the mean piston speed, the injection pressure and temperature along the energy of activation of the fuel and the gas constant, [17], [16]. J. Svan in his ammonia-diesel combustion research for the same b model used in this thesis used measurements from a smaller engine and a function to associate the ammonia energy share with the ignition delay, [10]. The formula remains unchanged in the model but is converted in ms rather than degrees since the model is operating in time-domain.

$$\tau_{id(CA)} = (0.36 + 0.22c_M) \cdot \exp\left[E_A\left(\frac{1}{R \cdot T_{ing} - \frac{1}{17190}}\right) \cdot \left(\frac{21.2}{P_{ing} - 12.4}\right)^{0.63}\right] \tag{8.30}$$

8.6. Safety on board of the vessel

The usage of hydrogen and methanol on board of vessels requires some measurements in order to guarantee the safety of the crew and the equipment. More specifically, it is know that the lower flammability limits of hydrogen and methanol are quite low compared with diesel. This means that if FuelSave injects enough quantities that are above the lower flammability limits of methanol, 6 % in air volume, and for hydrogen 4 % in air volume there is the possibility to have unexpected explosions in the system which are not desirable. Based on the M32E air requirements and the additives quantities the following table 8.7 shows the percentages of hydrogen and methanol in the system for the worst and best case scenarios. The worst case being when the 6 and 8 cylinder engines are operating in very low loads, around 25% were the air demand in minimum, and the best case when the engines are operating at 100 % load and the air demand in maximum.

Engine	Load %	Methanol %	Hydrogen %
6ME2E	25	2.07	0.38
6ME2E	100	0.67	0.12
8M32E	25	1.8	0.3
8M32E	100	0.6	0.10

Table 8.7: Flammability limits of hydrogen and methanol in air

As can be seen in table 8.7 in all of the cases the flammability limits of both methanol and hydrogen are well below the concerning limits for undesirable explosions in the system, thus we can conclude the operational safety of FuelSave in terms of flammability limits. It is also worth mentioning, that FuelSave has also made the necessary changes for the required fuel lines to accommodate methanol and sensors that guaranty the safety of the crew and the vessel.

8.7. Seiliger parameters

In section 6.2.3 it was described how the original Seiliger is defined into the model. Taking into account the available literature and more specifically the experimental results provided by FuelSave and FVTR some assumptions were able to be made in order to describe the change in the combustion shape expectations due to Marine+ operation. Originally this thesis would have experimental results comparing the operation of the vessel with and without the FuelSave module working but unfortunately it would not possible to be made in time. Due to this change in plans assumptions were made based on the only experimental results available from FVTR on a smaller engine but still showing the possible effects.

8.7.1. FVTR measurements

First, the FVTR results for FuelSave will be introduced as they provide evidence on what can be expected as well for the M32E engines, [32]. We have to keep in mind the difference although that the two engine have in terms of cylinders, dimensions, power delivery and cycle frequency.

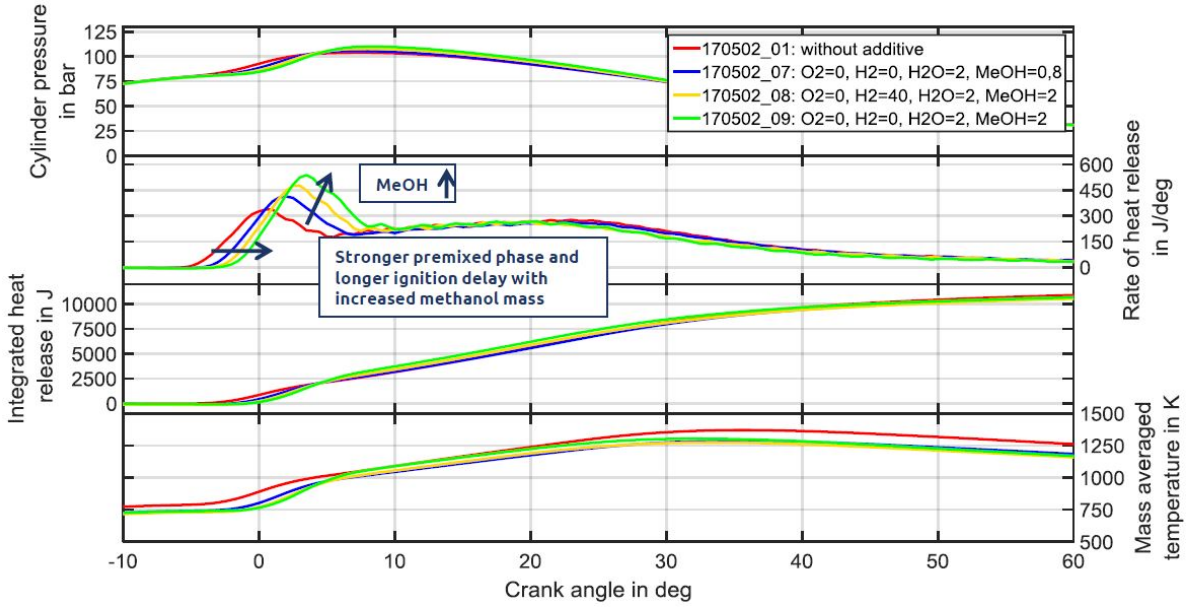

Figure 8.1: FVTR-FuelSave experiments, [32]

In the specific experiments a one cylinder engine named VDS 18/15 was used with a 180 mm stroke and 150 mm bore which is almost half of the bore of the M32E engine. Another important difference between the two engine is the nominal speed which was 1500 rpm for the experimental engine and 720 rpm for the M32E engine. The nominal speed plays an important role in the cycle frequency, $f_{cyl} = \frac{i \cdot N}{k}$ where N is the nominal speed and k is the number of revolutions per cycle. A higher cycle frequency means that the engine requires a higher fuel injection frequency. All in all, some conclusions can be drawn from the results of the experiments which can be useful.

As can be seen in figure 8.1 the red line provides the information for the diesel operation of the engine for 75 % load. We can focus our attention on the first part of the figure where the cylinder pressure is shown, the second part of the figure provides the rate of heat release and the last part the average mass temperature which is the cylinder temperature.

It is noticeable that when methanol and water are introduced into the engine the temperatura reduced and the ignition delay increased as can be seen from the pressure and heat release diagrams. The ignition delay increase as was expected resulted in a higher retarded peak pressure and heat release rate.

An interesting comparison between the blue and the green line indicates that the methanol quantity increase from 0.8 $\frac{l}{h}$ to 2 $\frac{l}{h}$ enhanced the ignition delay even further and as a result the peak heat release and peak pressure increased even more. On the other hand, once the hydrogen is injected as well, as can be seen by the yellow line, the ignition delay reduced slightly as well as the peak heat release, peak pressure, and temperature.

What is also crucial to highlight are the temperature measurements, where the use of the additives described with the yellow line compared to the original case with the red line the peak temperature never becomes larger than the diesel operation. The initial temperature drop can be explained by the methanol's high latent heat of vaporisation and the lower temperature in the late combustion stage could be justified by the less diesel quantity in the cylinder. It is interesting to notice that in the diffusive combustion phase the temperatures remained under the original case values in all the other three cases. Moreover, even though the hydrogen is characterized by high flame speed and heating value it can be seen that it helped the reduction of temperatures compared the diesel and pure methanol-water mixture addition combustion which is promising for the NO_x emissions reduction expectations.

In addition to the above measurement, FVTR also measured the emissions and efficiency effects of the additives to the engine. It is clear that the introduction of the additives can increase the indicated efficiency of the engine around 2-3 % in this situation and regarding the NOx emissions there can be a decrease when the proper quantities of methanol, water and hydrogen are used. In the specific

measurement the oxygen was not included as an additive but on a previous measurements on the same report it was seen that oxygen helps in the further increase of the indicated efficiency but with an increase of the NOx emissions as well.

All of the measurements above cannot be considered as the conclusive effects that will also occur in the M32E engines but can be a good indication of what to expect because of the difference in the cycle frequency, the bore and stroke dimensions and in general, there is no comparison between them since the one is performed in an experimental facility while the effect which we want to investigate will be about a real life condition. In the case of the experiments no charge air coolers were noticed in the experimental configuration and also it was noticed that the hydrogen and oxygen injection took place very near the cylinder while in this research the goal is to inject before the charge air cooler. With all the above in mind the purpose of the measurements will be to assist in making more accurate assumptions and expectations of the impacts of the module on the actual combustion shape of the engine through the Seiliger process.

8.7.2. Assumptions for the M32E engine modelling

Based on the above experiments and the available parameters that can be altered in the Seiliger model some assumptions can be concluded about the FuelSave operation on the combustion shape of the Bravenes' engines. J.S van Duijn in his thesis used equations 6.3 and 6.6 for the estimation of the Seiliger combustion parameters which included an additional term in order to include the different ammonia properties to the Seiliger process, [10]. The new terms are $X_{a,d}\&X_{b,d}$ along with the energy share ratio of ammonia x_f which then used measurements from a smaller engine to calibrate.The new equations used in the ammonia-diesel combustion in J.S van Duijn thesis are showed below:

$$X_a = X_{a,n} \cdot \left(\frac{n_e}{n_{e,nom}} - 1\right) + X_{a,f} \cdot \left(\frac{m_f}{m_{f,nom}} - 1\right) + X_{a,d} \cdot x_f + X_{a,c} \tag{8.31}$$

$$X_b = X_{b,n} \cdot \left(\frac{n_e}{n_{e,nom}} - 1\right) + X_{b,f} \cdot \left(\frac{m_f}{m_{f,nom}} - 1\right) + X_{b,d} \cdot x_f + X_{b,c} \tag{8.32}$$

In the current research for the FuelSave project, no changes were performed in Seiliger equations since it would require more time for the calibration of the diesel operation and then additional time for the FuelSave operation calibration which would be again based on speculations since there are no available measurements yet from the M32E engines.

Concluding the results of FVTR and the aimed expectations a preview of the combustion effects can be written. First of all, it is anticipated to have an enhanced ignition delay which will increase parameter a. An increase in parameter a will effect the peak pressure $p_3 = p_4 = p_{max}$ value. Due to the fact that the equation for the ignition delay estimation is not altered in any way nor the combustion efficiency, changes will be mainly made on the X_a parameters in regards the ignition delay effect. In addition to parameter a, parameter b and c will also be effected since an assumption will be made for reduced combustion duration. This is because of the added oxygen and hydrogen addition which can improve the combustion. It needs to be considered as well that the quantity of hydrogen which will be injected is not yet final since the module has not been fine tuned for Bravenes' operation but the aim of the company is to restrict the peak pressure enhancement to a minimum since the hydrogen with the higher flame speed is to compensate the higher ignition delay caused by the methanol and provide a more complete combustion. Nevertheless some increase in pressure is still expected due to the rapid combustion of the additives in the premix phase. After the premix phase, it is assumed that all of the additives are ignited and less diesel quantity will be injected in the cylinder for the diffusion and late combustion stages. The temperatures could be reduced and the same can apply for the heat loss since the temperature difference between the gas and the cylinder is less.

9

FuelSave technology impact

In this section the Seiliger parameters were investigate on how they can represent the impact of FuelSave operation on the model b. Based on conclusions from literature and experiments performed by Fuelsave and FVTR appropriate values will be selected to calibrate the model after the initial impact investigation.

9.1. Seiliger parameters

In section 6.2.3, a small introduction was performed about the research of Yu Ding and his focus on the Seiliger parameters and the combustion cycle. Some predictions could already be made based on his findings, but it was decided to do a modest impact research to further understand the effects of the parameters and also because the model had been modified for the Fuelsave operation.

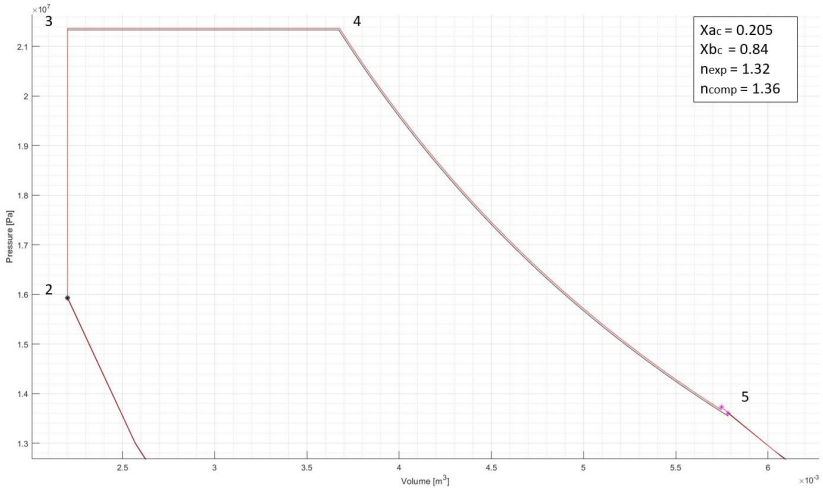

Figure 9.1: Pressure-Volume diagram comparison using the diesel calibrated parameters

To begin with, figure 9.1 presents the change in peak pressure when the adjustments for the FuelSave technology took place in the model with red colour compared to the diesel operation. This means that the additives result in slightly higher peak pressure during the combustion stage 3-4 while also decreasing parameter c in stage 5. The figure can be used to confirm that indeed the model has been adapted without changing the Seiliger parameters just yet.

The next step is to investigate which changes in the parameters can provide satisfying results which then will be used to analyze the performance of the FuelSave compared to the diesel operation.

9.1.1. Parameter Xa

Parameter Xa is very important as was introduced in section 6.2.3 since for this thesis is one of the variables which can be changed by the user to estimate parameter a for the Seiliger process. The value

of parameter Xa can be calculated by the combination of $X_{a,c}$ and $X_{a,n}$ as can be seen in equation 6.2, but because this investigation is performed under generator load conditions where constant load is applied, the constant part of the equation $X_{a,c}$ equals parameter Xa. For the diesel operation, the calibrated chosen value is $Xa_c = 0.205$. Figure 9.2 compares different values of the variable to observe the change in pressure by comparing the pressure-volume curves to the initial diesel value.

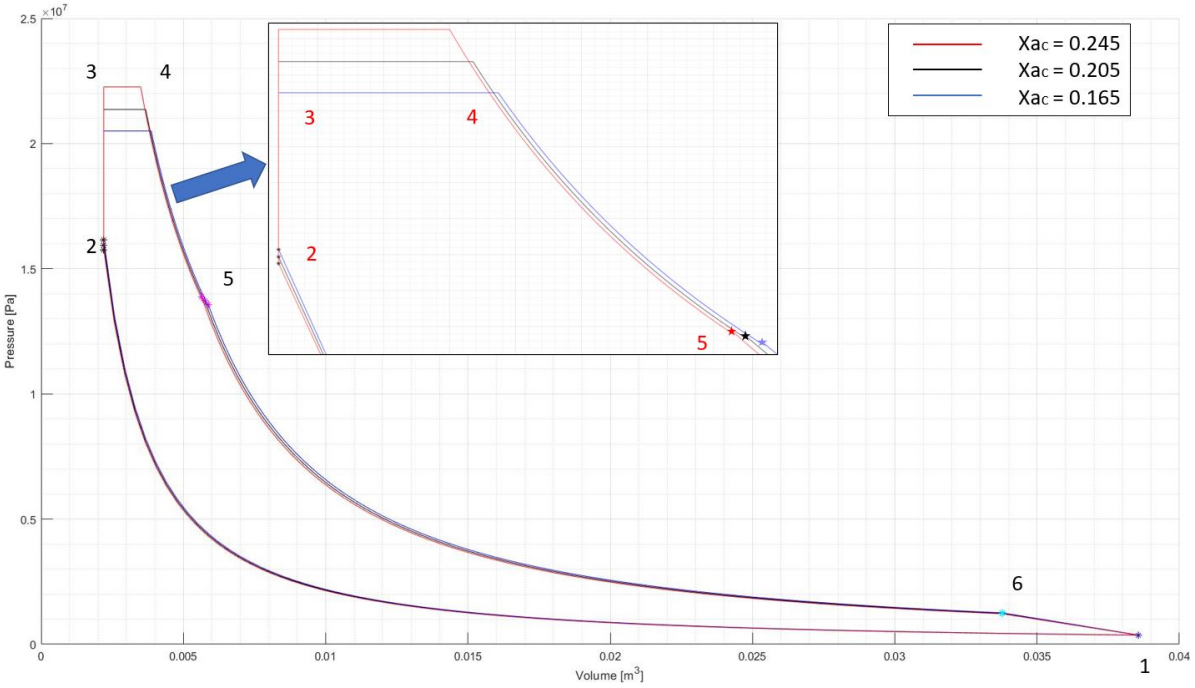

Figure 9.2: Pressure-Volume diagram with different Xa values

As can be seen in figure 9.2, the increase of parameter Xa from 0.205 to 0.245 resulted in the increase of peak pressure to 222 bar from 213 meaning that parameter a has increased as well. A further increase of parameter Xa above 0.245 could exceed the safe operational pressure limits in the cylinder thus it was decided to stop there since the results could represent the effect. The reverse effect can be seen with the decrease from 0.205 to 0.165. Table 9.1 summarizes the increase of cylinder pressure along the change of parameter $X_{a,c}$. It can be highlighted that the most obvious consequence of the parameter is in the peak pressure value $p3 = p4 = pmax$ and also the duration of stage 3-4. The increase of the stage 3-4 duration means that parameter b increased as well, while the decrease in duration signifies the parameter b decrease. A more subtle notice is the change in parameter c in stage 5. From figure 9.2 it appears that parameter c is increasing for the decrease of parameter Xa and the reverse. The decrease of parameter c indicates that less heat is distributed in stage 4-5 and this is reasonable since more heat has already been released in stage 2-3. The same applies for the increase of parameter c translating in a higher late combustion phase since stage 2-3 reduced but stage 3-4 increased. The total heat released from the fuel is being distributed in stages 2-5 through the combustion shape parameters a,b and c thus the changes in different stages based on the selection of values.

Parameter Xa,c	Pressure [bar]	Change %
0.165	205	- 4.03
0.205	213.6	0
0.245	222.6	4.21

Table 9.1: Peak pressure increase due to parameter $X_{a,c}$

9.1.2. Parameter Xb

A similar research was performed for parameter Xb with figure 9.3 and table 9.2 presenting the results. The estimation of parameter Xb is similar to parameter Xa which was explained already. The calibrated value for the variable Xb in diesel operation is 0.84 and is represented by the black curves in figure 9.3. The decrease from 0.84 to 0.78 resulted in the duration reduction of stage 3-4 as well as parameter a and b reduction, the increase of peak pressure from 213 to 215.9 bars and lastly the increase of parameter c. The reverse effects were recorded with the increase of Xb to 0.90 with the parameters a and b increasing while parameter c decreased as well as the peak pressure to 212.4 bars.

The increase of parameter c translates in higher late combustion stage and this can be verified by the figure 9.3 where the stage 4-5 is longer. The increase of c raises the pressure and temperature in the last stage where the exhaust valve opens which then increases the pressure in the inlet valve close stage before compression begins. The higher the initial pressure, p1, starting the compression the higher the pressure in stage 2. Interestingly even though parameter a decreased, due to the increase of pressure p2 the peak pressure of the cycle raised.

Table 9.2 collects all the recorded pressures for the different values of parameter Xb. Worth to be mentioned is the difference in stage 5 where the increase of parameter c results in a higher late combustion phase enhancing the duration of 4-5 and thus noting a low pressure at point 5. The reverse effect is also noticed for the decrease of parameter c where the duration of stage 4-5 is reduced and a higher pressure compared to the rest is estimated.

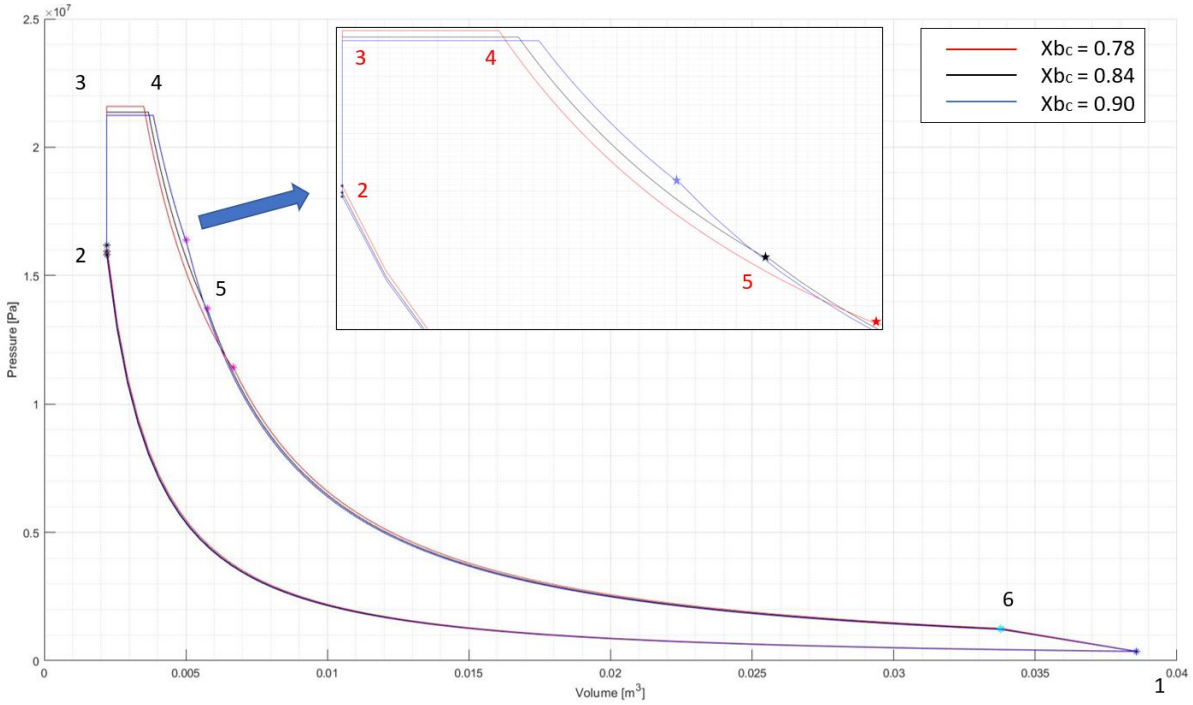

Figure 9.3: Pressure-Volume diagram comparison with different Xb values

Parameter Xb,c	Pressure [bar]	Change %
p1		
0.78	3.7	2.8
0.84	3.6	0
0.90	3.6	0
p2		
0.78	161.8	1.5
0.84	159.4	0
0.90	158	-0.9
p3=p4=pmax		
0.78	215.9	1
0.84	213.7	0
0.90	212.4	0.6
p5		
0.78	113.7	-16.8
0.84	136.7	0
0.90	163.4	19.5
p6		
0.78	12.6	2.4
0.84	12.3	0
0.90	12.2	-0.8

Table 9.2: Seiliger pressure increase due to parameter $X_{b,c}$

9.1.3. Parameters combinations

In the previous figures 9.2 and 9.3 a small research was completed to gain knowledge regarding the effects of the parameters Xa and Xb on the Seiliger and combustion cycle process. According to that information some possible parameter combinations were examined and presented in figure 9.4.

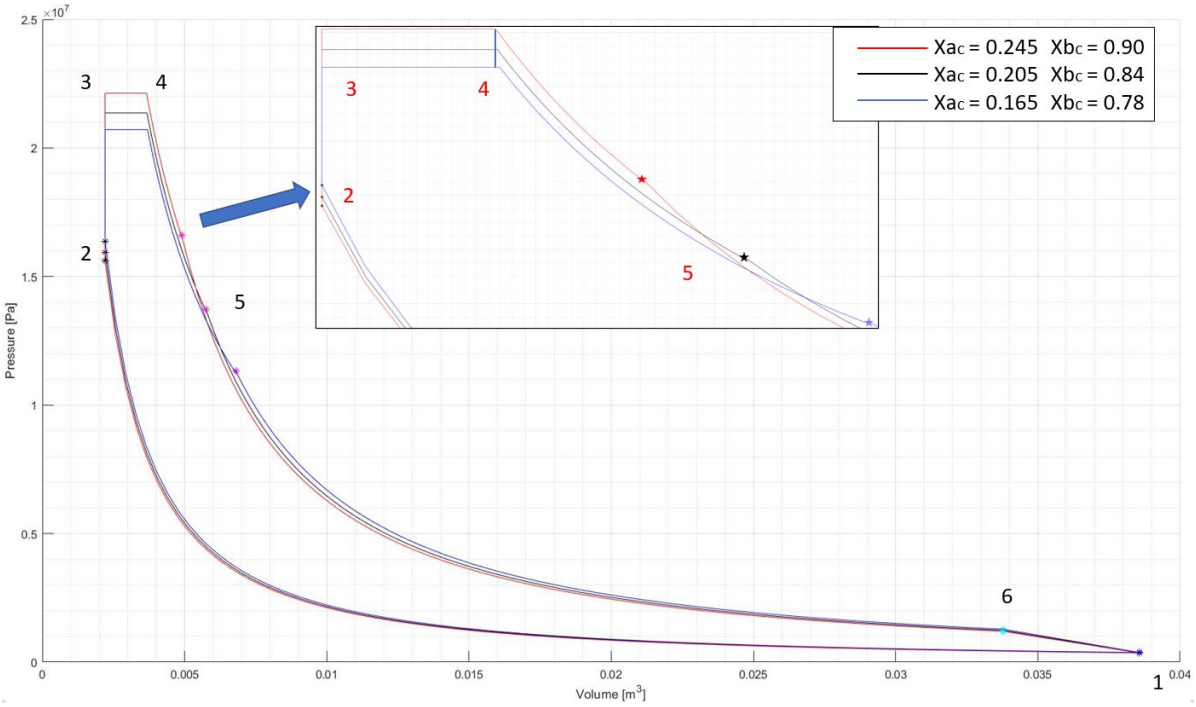

Figure 9.4: Pressure-Volume diagram with different Xa & Xb values

First, compared to the base operation, the first scenario, which centers around the values $Xa = 0.245 \& Xb = 0.90$, has the highest peak pressure of roughly 221 bars and the shortest time of stages 3-4. In addition, it decreased the late combustion stage duration since parameter b and c reduced resulting in lower pressures from stage 5 and after. Additionally, it should be noted that point 2's starting pressure is lower than it is in the other examples. This is due to the pressure dropping from stages 5-6 as a result of the decrease in parameter C.

The second scenario around parameters $Xa = 0.165 \& Xb = 0.78$ provided a peak pressure of 207 bars compared to the 213 bars of the base parameters values and an enhanced duration of the stage 3-4. Additionally, the late combustion stage is higher than it is in the other examples, which makes sense given that the late combustion phase and subsequent pressures were increased as a result of the heat distribution moving from stages 2-3 to stages 3-4 and 4-5 based on the decrease of parameter a but increase of parameter b and c compared to the base values.

With the above investigation in mind, it was decided take into account also the polytropic expansion, n_{exp}, which role's is to demonstrate the heat loss or heat input in the last stage of the cycle based on its selected value. The n_{exp} parameter was tested for the different values of 1.33 and 1.39 in order to demonstrate the reduced heat loss that could occur in the last stage. The explanation for the desire of the reduction is based on the FVTR experiments where the measured temperature is indeed reduced in the cylinder, [32]. Since there is less of a temperature difference between the cylinder and the fluid, lowering the gas temperature would also reduce heat loss to the surroundings around the cylinder.

Interestingly, the reduction of the n_exp meant the increase of the pressure and temperature in stage 6 where the exhaust valves open which is the opposite of what was desired. Based on this, it was preferred to restore the value of the polytropic expansion to 1.36.

Figure 9.5 describes the different values for n_{exp}. It can be seen that the decrease of the parameter to 1.33 from 1.36 raised the peak pressure while also reducing the parameter c. The decrease of parameter n_{exp} below a certain value can translate into heat input based on equation 9.1 and this can also be seen in the figure 9.5 in stage 6 and 1 where the pressures are higher meaning less heat loss compared to the other examples, [39]. On the other hand the increase of parameter resulted in the

decrease of peak pressure and the increase of parameter c enhancing the late combustion phase. Regarding the pressures in stage 6 and 1 they were reduced due to the increase in heat loss.

$$\frac{n_{exp} - 1}{[}\gamma - 1] > 1 \tag{9.1}$$

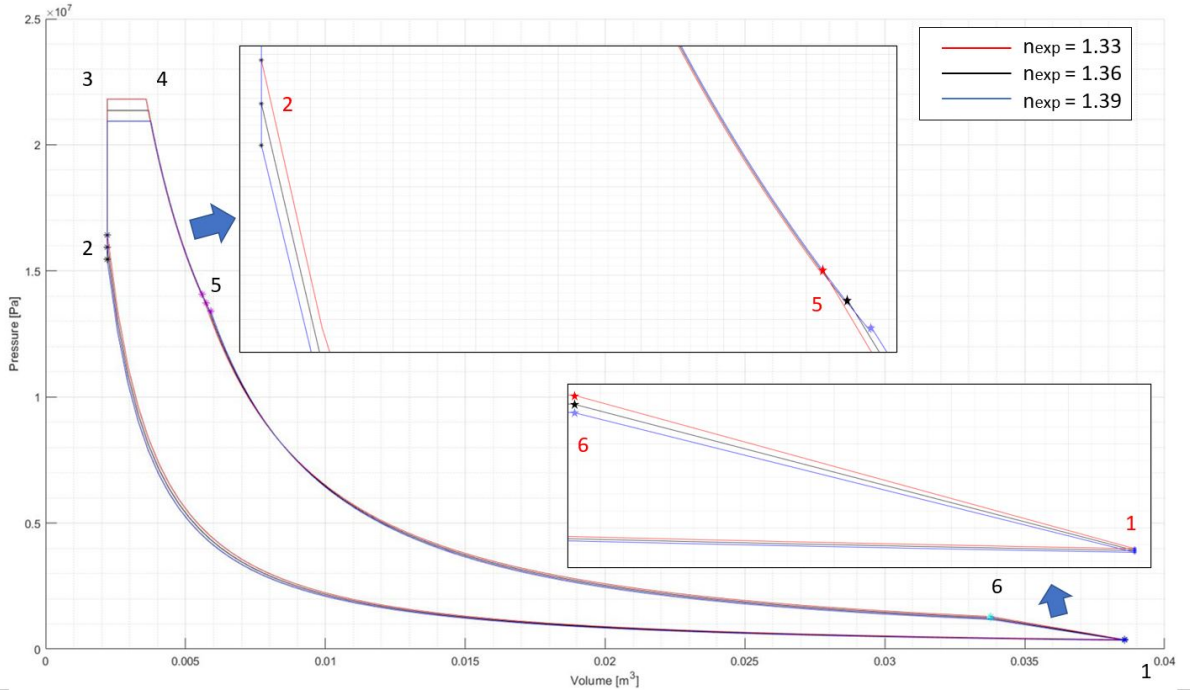

Figure 9.5: Pressure-Volume diagram with n_{exp} variation

9.1.4. Final parameters selection

The previous section helped in creating a solid understanding of the Seiliger parameters and their effects on the process. Based on FVTR measurements and the gained knowledge of the above investigation it was preferred to concentrate just on the parameters Xa and Xb and leave the rest of the Seiliger parameters similar. By doing this it would be easier to check in the next chapter the true comparison of the combustion shape parameters a,b and c and assuming that the rest of the compression and expansion stages of the process will be unaffected. Figure 9.6 demonstrates the difference between the diesel and Fuelsave technology operation. As can be seen the peak pressure increased from 213 to 221 bars while also lowering the pressure in the exhaust valve open stage. Finally, parameters b and c have been reduced meaning a reduction of the late combustion stage.

9.1.5. Seiliger parameters conclusion

In summary the aim of this chapter was to calibrate the model for the FuelSave operation based on expectations from the FVTR experiments. It was desired to show an increase of the peak pressure while remaining near the 220 bars which is around the operational limit of the engine to guarantee the safety of the components. Worth to be mentioned is that, Fuelsave once finishes with the installation will measure as well the peak pressure in the cylinders and fine tune the module's additives quantity in order to not exceed the manufacturer's limitations. The increase in peak pressure can be succeeded by the increase of parameter a which can be due to the addition of hydrogen and its higher flame speed which can decrease the combustion duration thus increasing the combustion rate at constant volume.

In addition, the stage 3-4 is assumed to be similar to the diesel operation since from the FVTR measurements the duration of the peak pressure before and after the additives are approximated to be the same. Last but not least, parameter c which demonstrates the late combustion stage is reduced, representing also the increase of combustion rate, [34], [32].

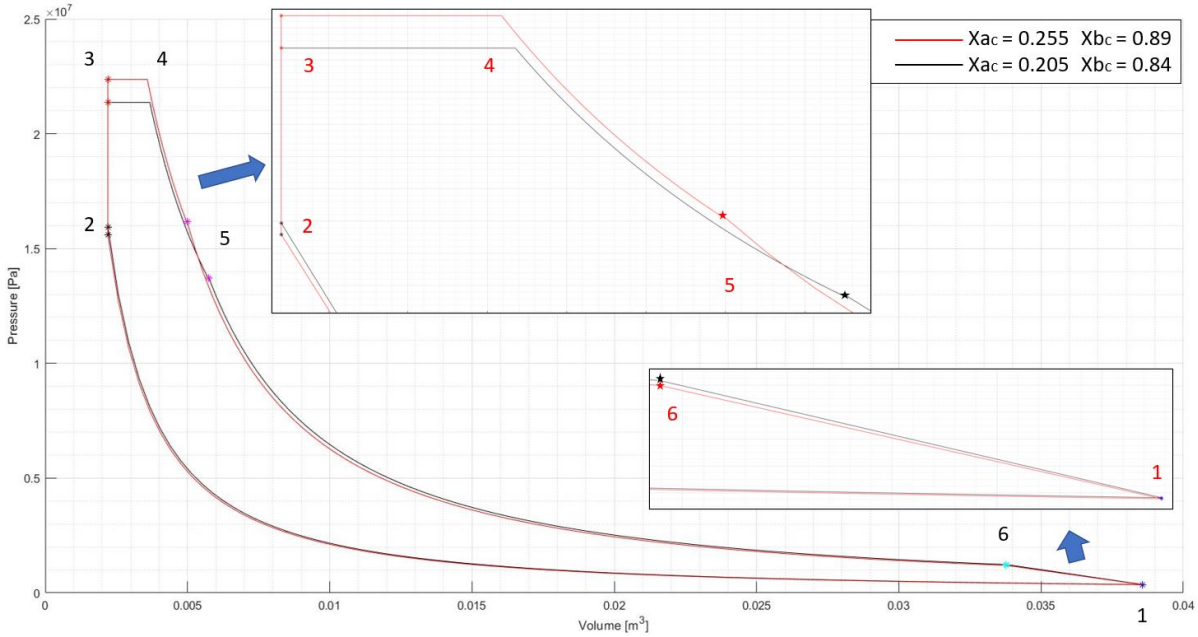

Figure 9.6: Pressure-Volume diagram with final selected Seiliger values

Furthermore, since methanol replaces some of the diesel injection in the cylinder and assuming that all of the additives will burn in the premix phase of combustion it makes sense to have a reduce late combustion phase with slightly lower pressure. The FuelSave impacts were able to be described using the parameters $Xa = 0.255 \& Xb = 0.89$, and once the available measurements are done one can confirm the validity of the expectations.

10

Diesel and FuelSave operation performance comparison

This chapter will provide a comparison between the diesel calibrated model and the FuelSave technology operation in terms of performance. Fuelsave is aiming to improve the efficiency and the emissions of the engine, thus some of the most important aspects which will be investigated are related to the combustion cycle of the engine which will result in the estimation of efficiencies along with temperatures and pressures in the cylinder which can be used to draw some potential conclusions about the emissions since the simulation does not support it.

10.1. Seiliger parameters

The first comparison between the diesel and Fuelsave operation will be in regards of the Seiliger parameters. In order to determine whether the model is capable of simulating the anticipated impacts of the technology, it is possible to analyze the temperatures and pressures inside the cylinder based on the parameters that have been chosen. Figure 10.1 presents the Seiliger parameters for the two cases. From the previous chapter the major changes on the parameters were the increase of parameters Xa and Xb. Those changes resulted in the increase of parameter a and the decrease of parameters b and c. The chosen values appear to produce results meeting the expectations. Parameter's a increase describe the premix combustion of the diesel and the additives resulting in the increase of the peak pressure compared to the initial conditions. The reason for the enhanced premix combustion was already seen in the FVTR experiments where the increase of ignition delay due to the methanol and water evaporation took place. The same conclusion can be drawn also from figure 10.2 where the q_{23} heat fraction increases presenting as well the increase of combustion rate at constant volume, [34].

According to Yu Ding's research, [5], Seiliger parameter a is associated with the premix combustion while parameters b, c and n_{exp} have effects on the diffusive and late combustion stages. This can also be confirmed by figures 10.1 and 10.2 where the reduction of b and c provided less heat in stages 3-4 and 4-5. When this is compared to the FVTR experiments it can be confirmed that the peak increase of heat release near the TDC can be associated with stage 2-3 and parameter a, the diffusive phase can be matched with stage 3-4 which can be seen to be similar between the two operations in the model and the measurements and lastly the reduction of heat release in the late combustion stage 4-5 is described by the q_{45} heat fraction decrease. The decrease of parameter c and thus q_{45} was anticipated due to the release of heat mainly taking place in the premix combustion stage assuming that all of the additives were combusted in that stage while less diesel quantity would be injected in the later stages. This was also seen in the FVTR experiments in figure 10.3 and was successfully simulated with the selected Seiliger parameters in the model.

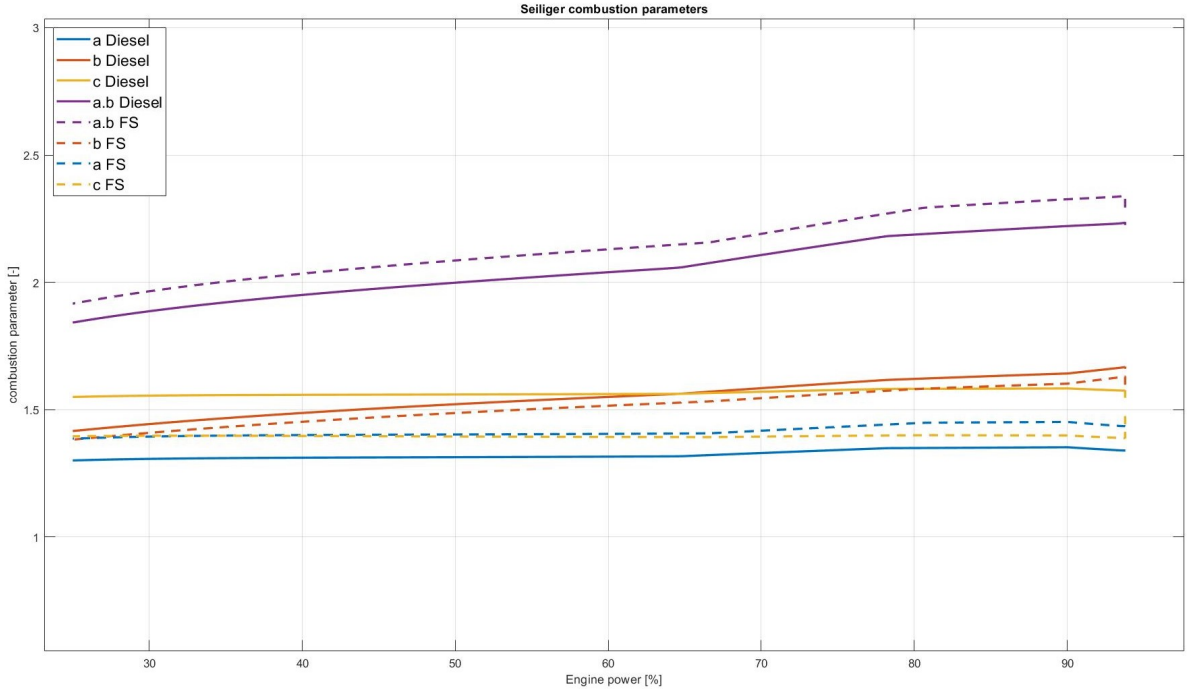

Figure 10.1: Seiliger parameters comparison

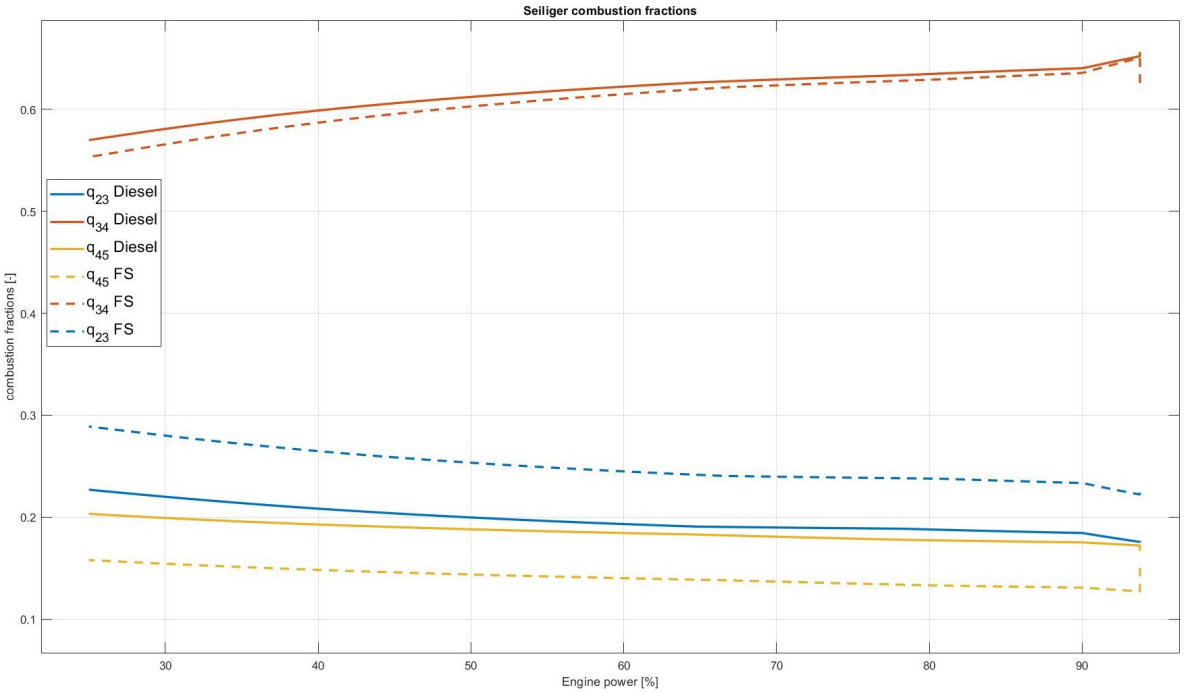

Figure 10.2: Heat combustion fraction comparison

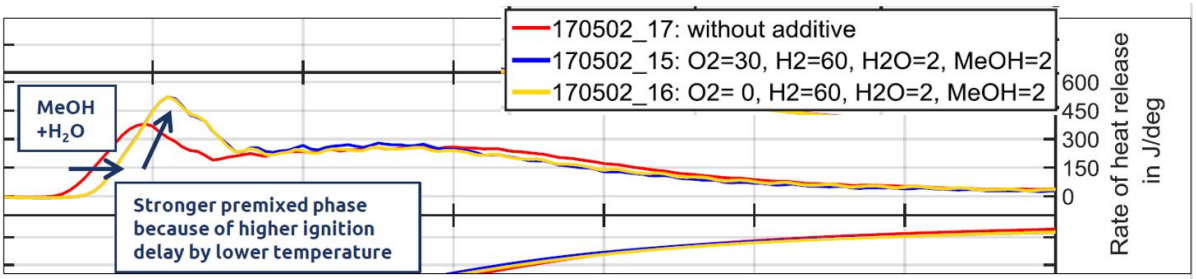

Figure 10.3: FVTR heat release measurement,[32]

10.2. Temperatures and pressures in cylinder

The selected Seiliger parameters for the diesel and the Fuelsave technology operation changed the combustion shape of the engine respectively. Those changes aimed to initially calibrate the diesel operation as close as possible to the available documentation and then investigate the possible improvements or drawbacks of the technology. The results of the parameters will be presented in the following sections and based on the FVTR experiments which are the closest available experimental confirmations of the additives effects it will be possible to discuss them and draw some conclusions.

10.2.1. Temperatures in cylinder

One of the most important parameters which will be compared are the cylinder temperatures. Temperatures are highly connected to the NO_x emissions produced by the engines as well as the thermal load [5]. Figure 10.4 presents the temperatures in points 2, 3, 4 and 5. Temperature T_2 is where the compression phase ends and the premix combustion phase begins, T_3 is where the first stage of combustion ends, followed by the temperatures in stage 4-5 where the isothermal combustion takes place described also by the highest temperatures of the process. The dotted line indicates the Fuelsave operation while the solid line the diesel operation. The figure makes it obvious how the peak temperature rises as the additives are inserted into the cylinder. Since the temperature never exceeded the nominal diesel operation according to the FVTR data, this is not what can be expected to happen in practice. It is worth mentioning although that the experiments where performed for 75 % load conditions and it could be possible to have different results with the increase of load. In the specific case, the increase of peak temperature can be a result of the Seiliger parameters a and b selection as can be seen in the equation 10.1. Since most of the other parameters are the same the effects are due to the $a \cdot b$ parameters increase which is seen in figure 10.2.

One thing that needs to be taken into consideration is the assumption that the thermodynamic properties of the additives will not be considered due to their small quantities compared to the air consumption. In reality the properties of the added water, hydrogen and methanol could reduce the temperatures since methanol is characterised by high latent heat of vaporisation which could drop the inlet temperatures, and the same applies for the higher specific heat of water compared to air even in vapour phase possibly dropping the temperatures in the cylinders as well.

$$T_{max} = a \cdot b \cdot r_c^{n_{comp}-1} \cdot T_1 \tag{10.1}$$

Figure 10.5 displays the rest of the cylinder temperatures T_1, T_6 and T_7 representing the trapped condition, the exhaust valve open and the blowdown stages respectively. The diagram shows that the Fuelsave operation succeeded in modestly lowering the majority of the temperatures, which was necessary based on the measurement predictions in figure 10.12.

10.2.2. Pressures

The cylinder pressures recorded from the Seiliger parameters selection can be seen in figures 10.7 and 10.8. It can be noticed in figure 10.7 that the maximum pressure when operating the engine at high loads % exceeds the 220 bars for the Fuelsave operation. This is a result of the parameter a increase representing the premix combustion phase enhancement. Figure 10.6 presents the in-cylinder pressure measurement with and without the additives injection. From the figure it was possible to estimate the increase percentage occurred by the additives to around 6%. The model output for the peak pressure without and with the additives increased from 213.7 to 223.7 indicating a 4.7 % raise which is reasonable.

In addition, the diagram shows for the Fuelsave operation a drop in pressure p_2 which is the point after the compression stage and an increase of pressure p_5 which is the ending point for the late combustion stage. The increase of p_5 can be explained by the decrease of parameter c for the additives' operation which shorted the late combustion phase duration nearer the TDC instead of retarding it into the expansion stroke [34]. The decrease of p_2 can be explained by the figure 10.8 where the pressure p_6 and p_1 are reduced for the Fuelsave operation. The reduction of p_6 is the result of the parameters b and c reduction since the polytropic expansion, n_{exp} remained the same for the two models. It would be wise to argue whether the p_2 after the compression stage will be affected in reality since the additives'

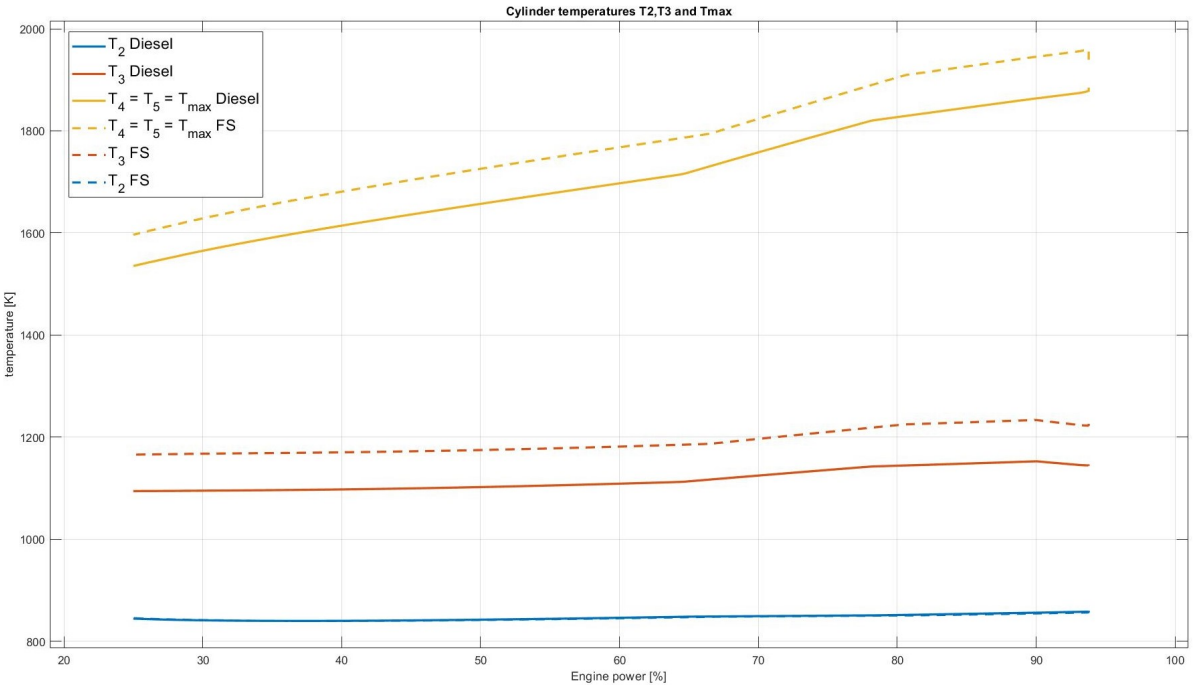

Figure 10.4: High cylinder temperatures comparison

quantities are small compared to the air demands especially in the 8 cylinder M32E engine but this can be found when the project is finished, calibrated and tested.

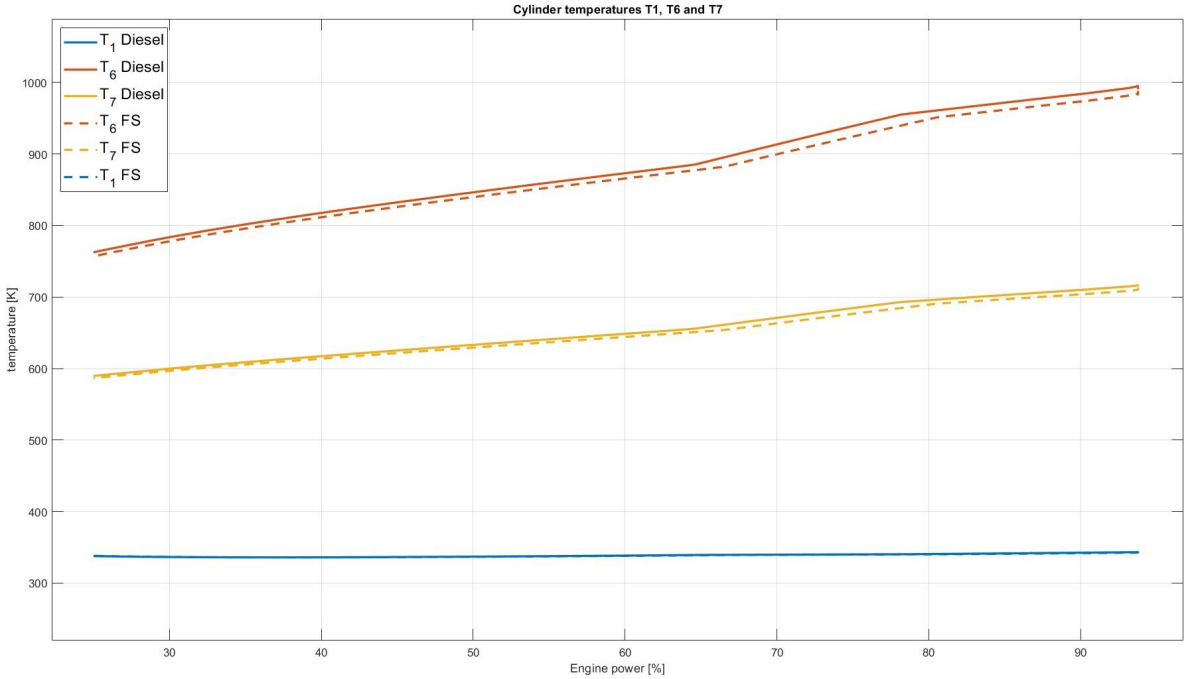

Figure 10.5: Low cylinder temperatures comparison

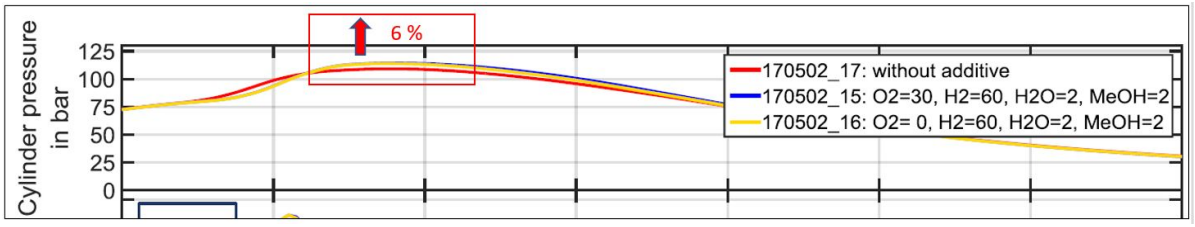

Figure 10.6: FVTR cylinder pressure measurement

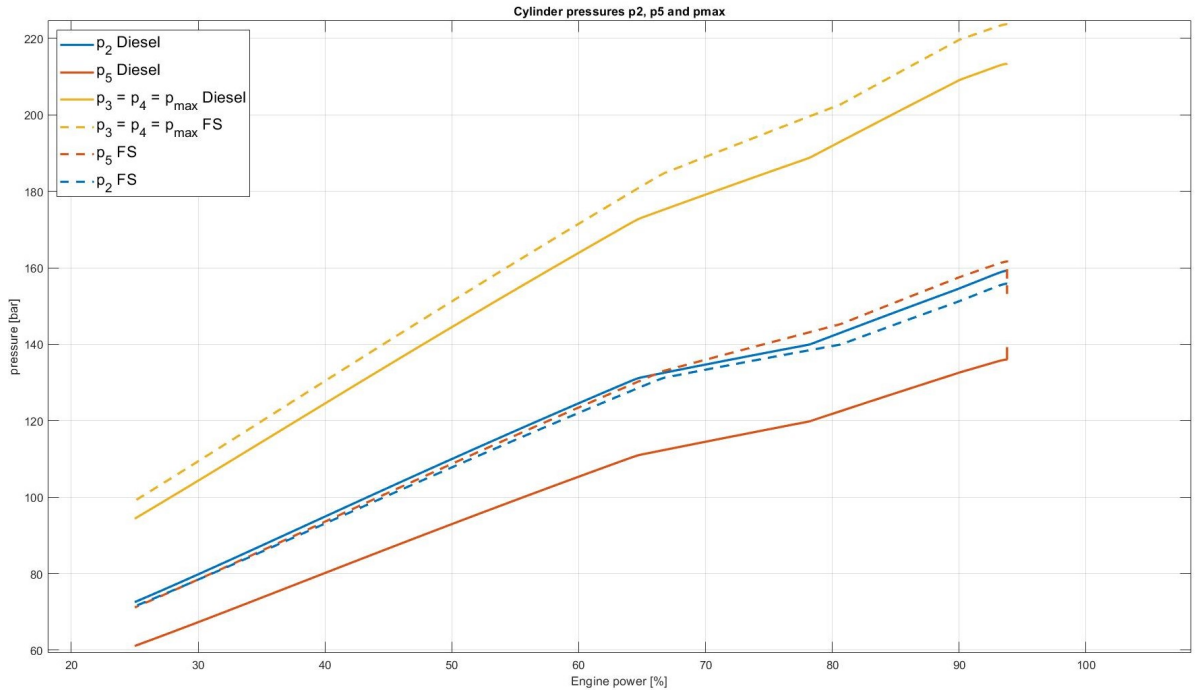

Figure 10.7: High cylinder pressure comparison

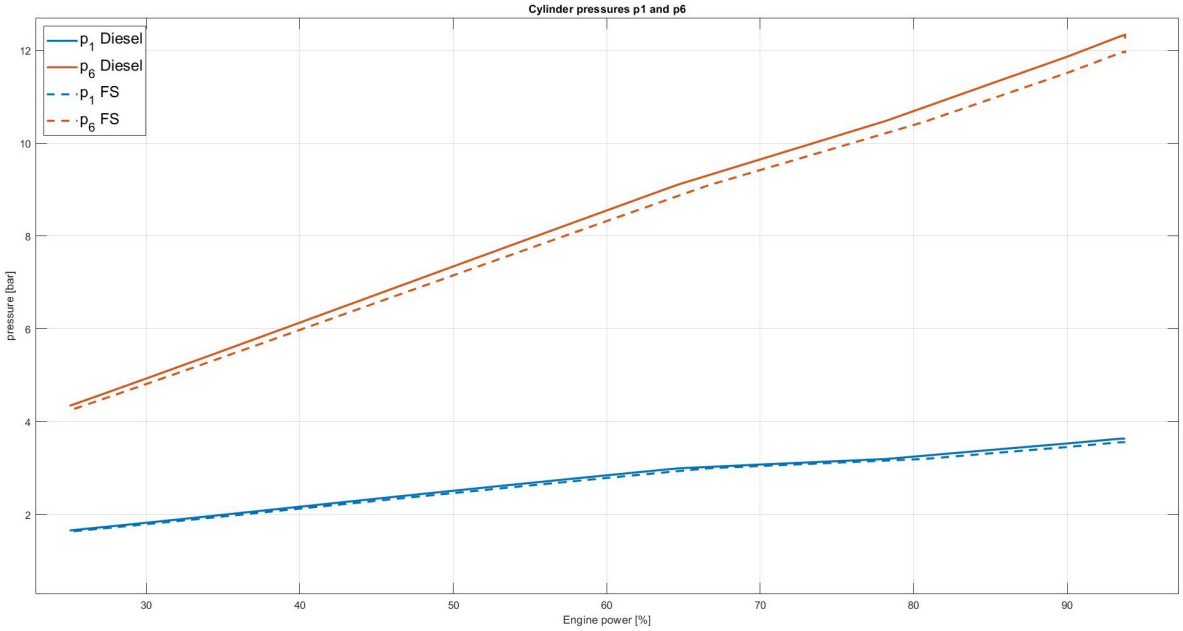

Figure 10.8: Low cylinder pressure comparison

10.3. Engine efficiencies, fuel consumption and emissions

One of the most important aspects that must be compared between the Fuelsave and the conventional diesel operation of the engine is the efficiency. The improvement of efficiency, fuel consumption, and emissions through a cleaner and more complete combustion are the primary goals of the Fuelsave technology, so it is crucial to stress these goals. Although the model does not allow for the estimation of emissions, certain conclusions can be made from the other results.

The engine's overall efficiency can first be divided into components, which will be covered below. When the fuel is ignited, the chemical energy that is stored in it releases into the cylinder. The combustion efficiency determines how much of the injected fuel actually ignites and can release that energy. The next step is to determine how much of the heat released is "lost" to the environment outside the cylinder and does not contribute to the combustion process itself by the ratio of the indicated heat over the combustion heat. The thermodynamic and mechanical efficiencies are the last two efficiencies. The mechanical efficiency is the ratio of the effective work over the indicated work while the thermodynamic efficiency is described by the indicated work over the indicated heat. Last but not least the effective efficiency of the engine can be determined once all of the aforementioned computations have been made or either by the effective work over the heat input from the fuel. In addition to the effective efficiency there is also the theoretical indicated efficiency with the difference that the mechanical efficiency is not considered, thus the name theoretical, [39].

$$\eta_e = \eta_m \cdot \eta_{comb} \cdot \eta_{hl} \cdot \eta_{td} = \frac{W_e}{Q_f} \tag{10.2}$$

$$\eta_i = \eta_{comb} \cdot \eta_{hl} \cdot \eta_{td} = \frac{W_i}{Q_f} \tag{10.3}$$

$$\eta_m = \frac{W_e}{W_i} \tag{10.4}$$

$$\eta_{comb} = \frac{Q_{comb}}{Q_f} \tag{10.5}$$

$$\eta_{hl} = \frac{Q_i}{Q_{comb}} \tag{10.6}$$

$$\eta_{td} = \frac{W_i}{Q_i} \tag{10.7}$$

Figure 10.9 and 10.10 compare some of the estimated efficiencies in the model for the diesel and Fuelsave operation. The analysis of whether the results in the diagram are indicative of the expectations will be undertaken for the various efficiencies in the sections below.

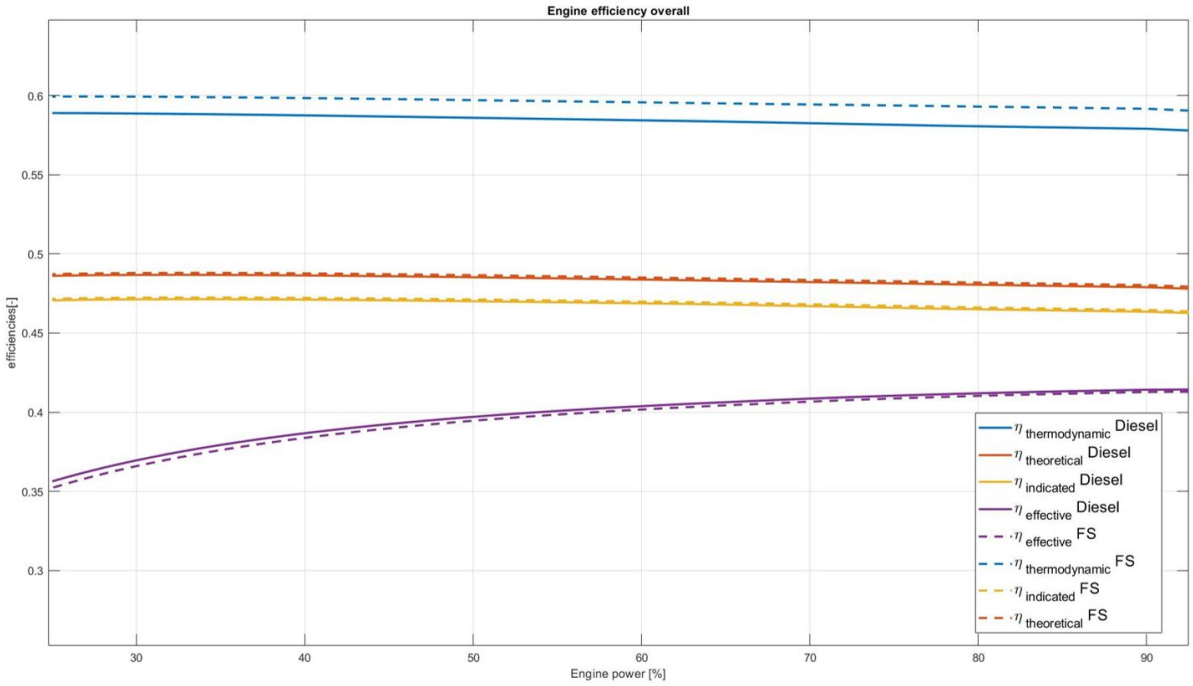

Figure 10.9: Engines' efficiencies comparison

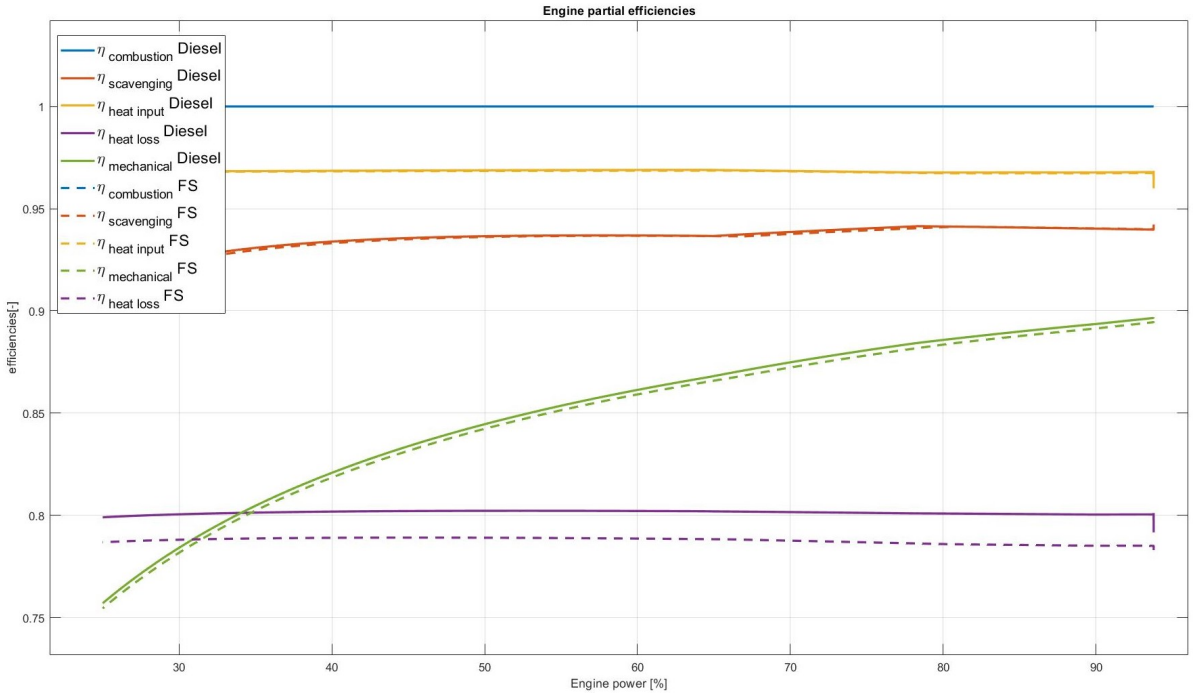

Figure 10.10: Engines' partial efficiencies comparison

10.3.1. Combustion efficiency

The combustion efficiency as is in the model was analysed in section 8.2. The limitations and the way of operation can be summarised here. First of all, the estimation of the current combustion efficiency in the model is a comparison of the air excess ratio to a constant smoke limit value determined by the user. In case the air excess ratio is greater than the smoke limit then combustion efficiency equals to 100 %. This means that all of the chemical energy stored in the fuel is converted to released heat in the cylinder without any losses. Alternatives methodologies were investigated without any success due to missing experimental information. Based on the aforementioned in both operations the combustion efficiency does not change and is 100 % as can be seen in figure 10.10. This result is not something which is expected and it can be even argued that over the years of operation the engine's combustion efficiency can deteriorate.

Figure 10.11 shows the comparison of the air excess ratio between the two operations. It can be seen that the Fuelsave technology lowers the air excess ratio meaning that the actual combustion air quantity is reduced. Equation 8.12 describes the evaluation of the air excess ratio for the additives operation. The estimated air excess ratio is still greater than the smoke limit thus the combustion efficiency is not affected.

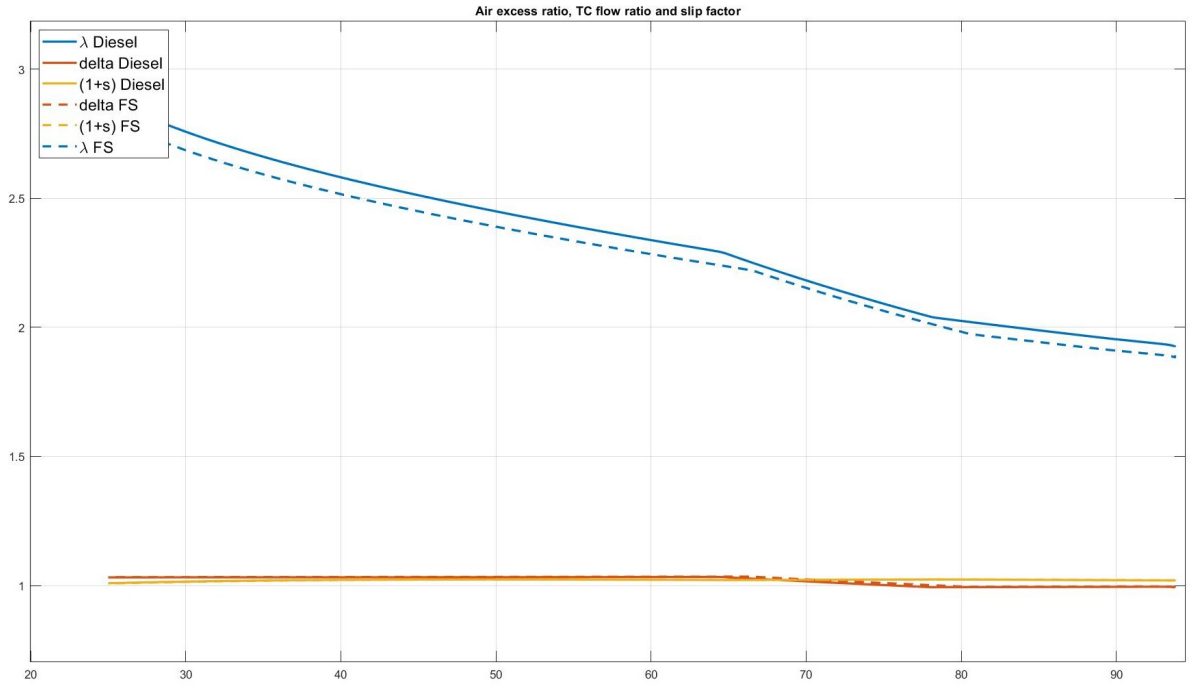

Figure 10.11: Air excess ratio comparison

The Fuelsave technology main contribution can potentially improve the combustion efficiency of the engine by a more complete combustion introduced by the hydrogen properties. The FVTR measurements provided evidence of the indicated efficiency improvement as can be seen in figure 10.15 which indeed shows the benefit of the technology. In the specific research, it was not possible to demonstrate any effects on the combustion efficiency due to the mentioned reasons.

10.3.2. Heat input efficiency and heat loss efficiency

The heat input efficiency η_q has the same meaning as the $\eta_h l$ efficiency which is approximating the amount of heat dissipated from the combustion heat in the cylinder chamber to the cylinder cooling pockets based on the cylinder wall area, the temperature, the heat transfer coefficient and the time available for heat transfer. The main difference between the two in the model is that the heat loss efficiency also takes into account the heat loss during compression and expansion while the heat input is focused on the combustion heat. Based on the FVTR experiments in figure 10.12, the cylinder temperature throughout the combustion process was reduced in comparison with the diesel operation. This reduction in temperature difference between the cylinder and the gasses in reality can result in the

increase of the heat input efficiency since less heat will be dissipated from the cylinder.

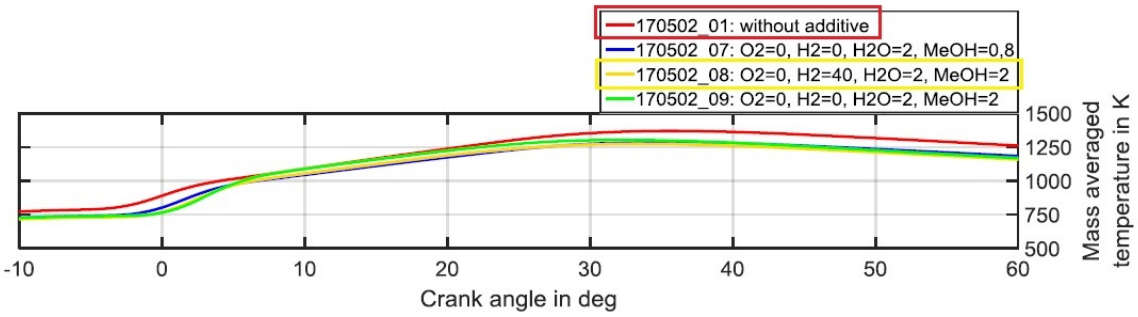

Figure 10.12: FVTR temperature measurement, [32]

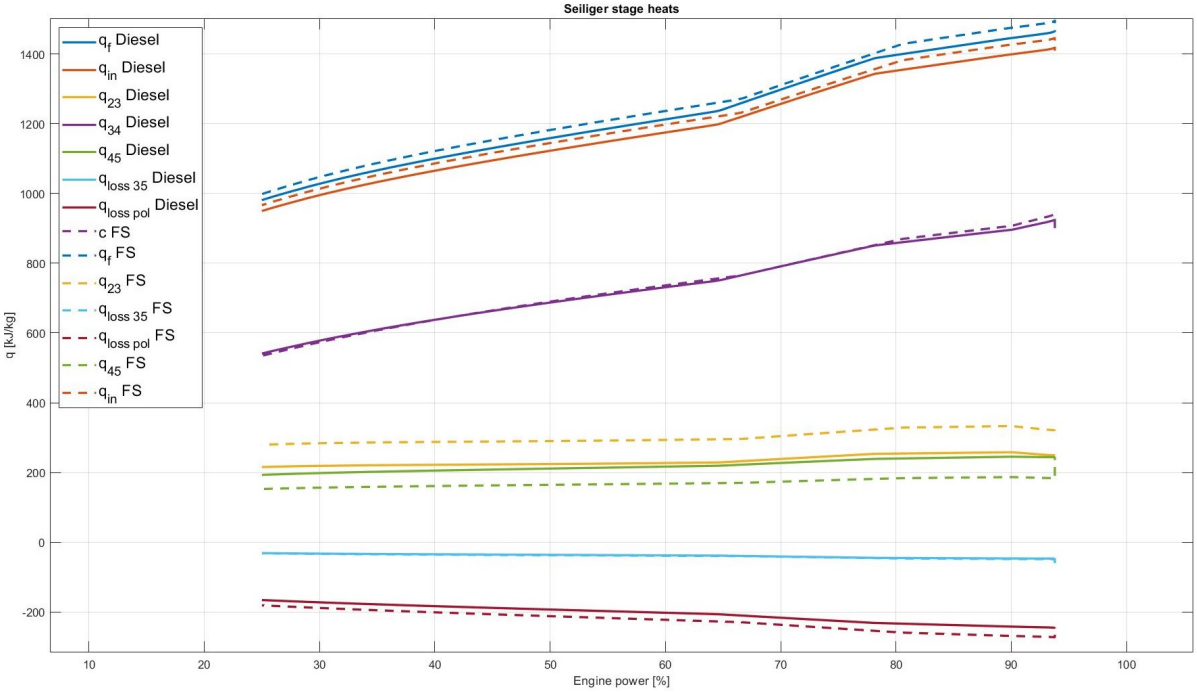

Figure 10.13: Heat stage comparison

In the model results in figure 10.10 there was not visible change in the heat input efficiency when comparing the two operations. The heat input efficiency in the model is estimated using the Woschni model. Main inputs of the model are the temperatures T_1 and T_2, the Seiliger parameters as well as the engine rotational speed. Since the temperatures T_1 and T_2 are similar between the two operations and the changes in the Seiliger parameter increase parameter a while reducing parameter b and c it seems to produce a comparable outcome. On the other hand it appears that the heat loss efficiency has dropped for the Fuelsave technology meaning that the losses during compression and expansion have increased as can be seen in figure 10.13. This is mainly attributed in the selected Seiliger combustion parameters and is not expected in reality. This effect might be readily fixed by lowering the $nexp$ parameter to show less heat loss during expansion stages 5 and 6, but this is not anticipated in practice because the temperatures in the cylinders will be lower, resulting in a smaller final temperature difference.

It can be noted that, since one of the purposes of methanol and water addition is to act as a cooling agent the temperature T_1 which takes place when the inlet valve closes could be reduced. The trapped condition will be the temperature and pressure from the inlet manifold which could potentially be slightly

lower in case the latent heat of vaporisation and the higher specific of water are taken into account.

It is important to note that FuelSave has not yet made a final choice regarding the injection location because the module has not yet been fine-tuned. There is the possibility that the injection location of water-methanol prior to the charge air cooler would not be as beneficial as assumed and lots of the additives are condensed in the charge air cooler and then rejected out of the system. In the event that something like this indeed occurs the location of injection would need to be moved after the charge air cooler and then the temperature reduction would be even greater since the water-methanol would be liquid or very small droplets after the injection. On the other hand one needs to be aware that water if not evaporated fully and injected in large quantities could be harmful for the engine's cylinders since it could effect the oil film on the surface and result in potential engine damage [26]. Nevertheless the final results from the model about the heat input and heat loss efficiencies do not represent the effects of the Fuelsave technology.

10.3.3. Thermodynamic efficiency

The thermodynamic efficiency is estimated using equation 10.8 which approximates how much of the net indicated heat input is becoming indicated work during the combustion process. In figure 10.9 the thermodynamic efficiency of the engine has increased with the Fuelsave operation. Figures 10.13 and 10.14 present the inputs for the thermodynamic efficiency estimation which can provide a better explanation for its increase.

To begin with 10.13 includes the total heat release, q_f, and after the combustion efficiency and the heat input efficiency are taken into account the heat input is estimated, q_{in}. It is obvious in the diagram the increase of both the total heat release and the heat input for the Fuelsave operation even though the combustion efficiency and the heat input efficiency are identical in both cases. This means that the additives alogn with the diesel provide higher heat to the system. On the other hand, the Fuelsave operation has a greater heat loss in the stages 1-2 and 5-6 which can be due to the selected Seiliger parameters.

$$\eta_{td} = \frac{W_i}{Q_{in,net}} = \frac{w_{12} + w_{34} + w_{45} + w_{56}}{q_{loss} + q_{in}} \tag{10.8}$$

Continuing with figure 10.14 it can be noted that Fuelsave indicated work, W_i, is slightly greater compared to diesel which can justify the increase in the thermodynamic efficiency.

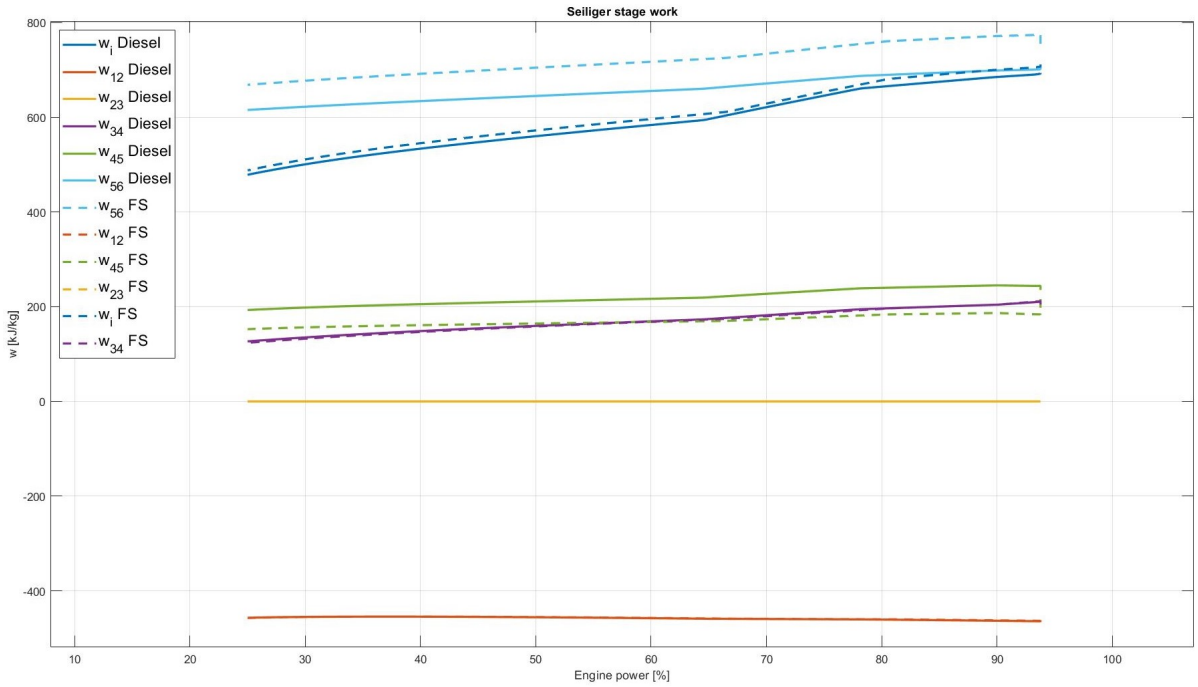

Figure 10.14: Seiliger work comparison

H. Sapra, [34] in his research with hydrogen blending in a natural gas engine concluded that the increase of peak pressure in the cylinder chamber during the hydrogen increase correlates to the increase of thermal efficiency, which is highly connected with the thermodynamic efficiency. In conclusion, the model can demonstrate the gain in thermodynamic efficiency using the chosen parameters.

10.3.4. Indicated efficiency

Indicated efficiency can be defined by the ratio of indicated work over the total heat release contained in the fuels as depicted in equation 10.9. The indicated work estimation is analysed in equation 10.8 while the total heat release is the amount stored in the diesel and the additives together in case of the Fuelsave operation. In figure 10.9 the indicated efficiency of Fuelsave is slightly increased compared to the diesel operation and this can be explained by the increase of the indicated work. The same can be confirmed by the FVTR experiments for 75 % load presented in figure 10.15, [32]. Case 1 is without the additives included while case 3 includes the methanol-water and hydrogen injection.

$$\eta_{th,i} = \frac{W_i}{Q_f} \tag{10.9}$$

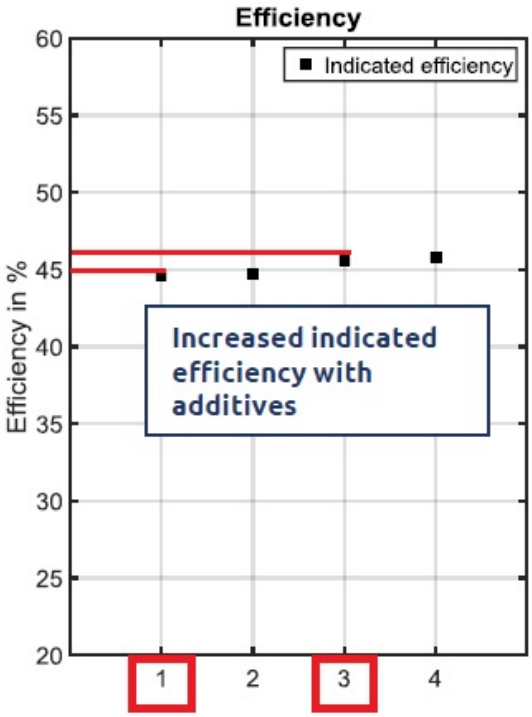

Figure 10.15: FVTR indicated efficiency, [32]

10.3.5. Effective efficiency

The effective efficiency of the engine can be estimated using equation 10.10 compared to the total heat released. When comparing the indicated work to the effective work, the effective work includes consideration for the mechanical efficiency. The mechanical efficiency takes into account the friction losses in the engine using the Chen and Flynn model, [37], based on the engine speed and the maximum pressure and the losses due to the pumps. It needs to be mentioned that Fuelsave will include two additional pumps for injecting the methanol-water mixture into the air intake area of the engines which will increase the mechanical losses but this is not included in the current model.

Figure 10.9 shows a minor increase of the effective efficiency when comparing the Fuelsave with the diesel operation for high loads, then becomes identical and drops somewhat for low loads. The increase of effective efficiency is probably due to the increase of thermodynamic efficiency but a conclusion cannot be drawn about the actual effect of the project since some mechanical parts will be included which have an immediate impact.

$$\eta_e = \frac{W_e}{Q_f} \tag{10.10}$$

10.3.6. Fuel consumption results and discussion

Figure 10.16 displays the specific fuel consumption for the diesel and Fuelsave operation. There are two curves for the Fuelsave function, one regarding the amount of diesel and the other about the overall quantity with the additives. The diagram indicates that the additives slightly raised the overall sfc, indicating that more fuel is needed for the engine to deliver the same brake power.

On the other hand, it is evident that the amount of diesel is decreased, which is related to the technology's primary goals of fuel savings. The project's second primary goal, a reduction in CO_2 emissions, can be achieved in part by using less diesel.

The sfc from the model accounts for the substitution of some diesel with methanol in an effort to give a comparable overall heating value and the addition of hydrogen to increase the potential heat in the combustion. The amount of hydrogen utilized in the model might be lower than the amount that will actually be used, which might be able to reduce the sfc since it will provide more energy due to the higher heating value enabling for more diesel reduction. Overall, it appears that the Fuelsave technology can minimize the amount of diesel, which meets the research's objectives.

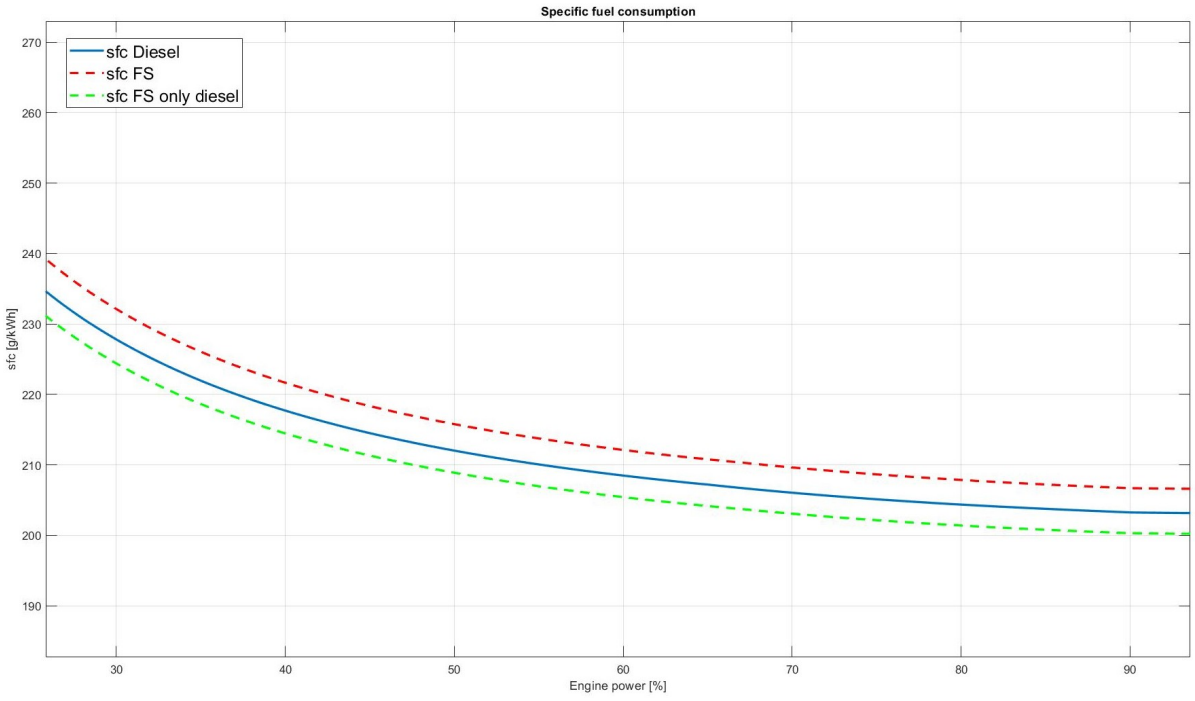

Figure 10.16: Fuel consumption comparison

10.3.7. Emissions and discussion

The current section will discuss some of the Fuelsave technology potential for the Bravenes and provide a summary of the aforementioned sections.

The engine's fuel consumption is one of the key areas that Fuelsave wants to enhance. This could be accomplished by a more complete combustion aiming to enhance the engine's combustion efficiency.The potential effects of injecting additives into the M32E engine's intake on efficiency were covered in the sections prior.Additionally, measurements of partially unburned emissions were used to determine the M32E's combustion efficiency, yielding a figure that was quite close to 100%. An engine's efficiency could decrease with time, but Fuelsave could stop that from happening. The precise impact could be demonstrated by measurements of incomplete combustion emissions with and without the technology, but it is not yet possible to provide a firm response. Another way of achieving the fuel consumption reduction is by replacing more diesel fuel with methanol. The current plan is to substitute 1.5 % diesel mass with 3% methanol mass depending on the load of the engine. By doing so, the CO_2 emissions could further reduce since methanol contains less carbon content compared to diesel.

The methanol and water could also reduce the temperatures in the cylinder when injected in the proper location. Fuelsave initial plan was to inject the mixture before the charge air cooler where the highest temperature takes place in order for them to evaporate and lower the incoming temperatures. One possibility of that could be that inside the two stage air cooler some of the quantities could condense and be rejected out of the system thus being a waste. The methanol and water mixture by lowering the inlet temperatures could lower the NO_x emissions as was already seen from literature [2].

Furthermore, the addition of hydrogen and oxygen gas in the cylinder not only aims for a more complete combustion but also to provide additional heat into the chamber. The higher flame speed of hydrogen and the much greater heating value could indeed increase the combustion rate, decrease the combustion duration and if calibrated correctly have the same amount of power with less diesel injection thus decrease fuel consumption. In the current research the quantity of hydrogen cannot be taken for granted that will be used as well in the real tuning of the engine since the company requires more experimentation for the specific engine.

Taking all of the above in mind with the available information M32E engines when combined with the Fuelsave techology could potentially improve the combustion cycle, reduce emissions and save fuel.

11

Conclusion, Recommendations and Future work

11.1. Conclusion

The main research question of the thesis is if the Fuelsave Marine+ installation aboard Bravenes can improve engine efficiency, fuel consumption and/or minimize hazardous emissions, with a particular focus on NO_x, which is also the main area of interest for Van Oord. During the investigation the effects of the technology on the performance of the engine were also researched. The research question can be answered by the the following sub-sections separately.

How does the model's results for diesel operation compare with the available engine measurements from Bravenes?

The model used in this research is capable of modelling each component of the engine from the air filter until the exhaust silencer using information from the specific engine. Part of the information that were required by the model was preferred to remain the same either due to data lack or because the model uses approximations based on known values.

In chapters 6 and 7 the detailed changes and available measurements are listed along with the verification of the models' output. Based on the information received from the chief engineer of Bravenes the calibration of the model was performed and later on compared to the actual values.

The engine's received pressure crank angle diagram was transformed into a pressure volume diagram, which was simpler to evaluate with the model's produced pressure volume diagram. As was discovered during the investigation the indicated work from the pressure crank angle diagram and the recorder generator load did not match. This led to research to continue without the pressure trace information and thus not matching the indicated work from the measurements to the model. Even though the indicated work was not confirmed, the peak pressure which is also important since is associated with the mechanical loads in the engine's components was validated. The same applies for the pressure and temperature at point p_1 providing similar results along with the rest of the pressures in the system. In addition, the estimated fuel consumption and the engine output were again in the margin's provided by the measurements. On the other hand the temperatures before and after the turbocharger were offset by small margins but this is somewhat acceptable since some information were incomplete and assumptions needed to be made.

All in all, it can be concluded that the model for the diesel operation provides a solid base in order to proceed with the research and have a performance comparison with the Fuelsave operation.

Which modifications and assumptions are necessary for the engine B model in order to accommodate the hydrogen, oxygen, methanol-water characteristics along with the diesel operation in the combustion process?

To implement the Fuelsave technology operation on the model an investigation was performed to determine which changes would be indeed significant. The first modification was a decrease in the amount

of diesel fuel mass quantity and replacement with the appropriate methanol mass aiming to achieve the same energy release. In addition, the properties of fuels such as the lower heating value for methanol and hydrogen were implemented to the model along with the addition of hydrogen's quantity. The substitution of diesel with methanol were assumed to be 1.5 % and 3% mass wise respectively since this is also the current aim of Fuelsave. Since oxygen and water do not contribute to the total heat release in the cylinder they were not added in this part.

The next step was to research the air and gas mixture into the engine. Since the additives are injected in the air intake area of the engine some of the air could be reduced. Based on the amount of water-methanol, hydrogen and oxygen addition compared to the air quantity required by the engine, the amounts were deemed too low in order to have significant effects on the air or stoichiometric gas composition thus were not changed. Furthermore, it was also assessed whether the flammability limits of methanol and hydrogen were reached and was confirmed that with the current quantities the additives were not hazardous.

The combustion efficiency currently in the model is dependent on the air excess ratio compared to a constant smoke limit. An alternative way of estimating the combustion efficiency was tested but due to missing emissions' measurements it was not managed thus was remained the same. The air excess ratio did change though taking into account the additives quantities and their stoichiometric air fuel ratio.

Last but not least, the Seiliger parameters provided the most important change to demonstrate the combustion impact of the Fuelsave Marine+ to the M32E engine. The parameters were explored and using the FVTR measurements they were adjusted to describe the combustion shape change. Since Bravenes uses the DG1 and DG4 while sailing, it was assumed that all of the additives from the two Fuelsave pumps are put into each of them without dividing the quantities into the DG2 and DG3, respectively.

How does the diesel operation compare to the Fuelsave operation based on the changes and assumptions selected in terms of efficiency, fuel consumption and emissions?

To begin with, it needs to be mentioned that no validation took place for the model's results thus the below comparisons are expectations. According to the selection of parameters X_a and X_b, the Seiliger combustion shape parameters had the following changes for the Fuelsave operation compared to the diesel:

- Increase of parameter a
- Decrease of parameter b
- Decrease of parameter c

The model based on the selected Seiliger parameters and the rest of the changes estimates an increase of peak pressure but not over the operational limit provided by the engine's manufacturer acceptance test. In addition, the peak temperature also increased but this could be due to the increase of the combustion shape parameters $a \cdot b$. Such increase can not be taken for granted since the FVTR measurements provide evidence that the peak temperature was similar between the diesel and the additives operation but not greater. On the other hand the tests were performed for 75 % load on a single cylinder engine and a different result could be expected for higher loads and difference engines.

Continuing, the engine's thermodynamic and indicated efficiency increased for the Fuelsave operation while the effective efficiency showed a slightly decreased. FVTR indeed measured a gain in the indicated efficiency which matches the results of the model. The increased peak pressure of the cylinder could potentially have an effect on decreasing the mechanical efficiency of the engine therefore reducing the effective efficiency. On the other hand, Fuelsave needs to install two pumps for injecting the water-methanol mixture that will add mechanical losses in the system but was not taken into account for this research.

The total specific fuel consumption increased with the Fuelsave operation and this could be the result of the reduced lower heating value of methanol which replaces some of the diesel and also the quantity of hydrogen used in the model could not be enough to compensate the reduction. The specific fuel consumption for only the diesel quantity indeed was reduced compared to the conventional operation

which could also lower the greenhouse emissions produced by the engines. In reality, Fuelsave with the correct amount of additives in the engine could reduce the total specific fuel consumption but a conclusion cannot be drawn now without any experimental confirmations.

Although the model does not estimate the emissions of the engine some conclusions can be drawn from the model and literature. Emissions like CO_2 and $S0_x$ are fuel dependent. Since Fuelsave aims in replacing around 1.5% of diesel with 3 % methanol mass wise a reduction of those emissions could be expected since methanol contains less carbon than diesel and no sulphur. Emissions which are related to the combustion of the engine like CO and UHC in case the combustion efficiency of the engine is improved due to the hydrogen and oxygen addition it can be expected to have lower emissions as well. Emissions like NO_x are dependent on the high temperatures in the cylinder and the residence time which is constant since the engine speed is the same [34]. The FVTR experiments showed that the evaporation of water-methanol managed to reduced the cylinder temperature resulting in lower NO_x while the hydrogen addition increased the emissions but not as much as originally which is still an improvement. The model showed an increase in peak temperature but this could be a modelling error since it is highly associated with the Seiliger parameters.

11.2. Reflection, recommendations and future work

11.2.1. Thesis reflection

The investigation's goal is to learn more about the performance effects of Fuelsave Marine+ technology on-board of Bravenes. The initial plan was to have the technology installed by the halfway point of this study and initialise a measuring program to compare the Bravenes' operation by monitoring emissions, power production, and fuel consumption with the module on and off. Information about the combustion efficiency could be obtained by measuring emissions related to incomplete combustion both with and without the additives and record the actual benefits of the technology. Unfortunately another route had to be chosen because the installation is still in progress due to supply chain delays and other issues.

Measurements from onboard Bravenes that could offer adequate data to calibrate a mean value first principle model provided by TU Delft capable of representing the combustion process of the diesel engine was an alternate option that was also pursued. It was difficult to calibrate the model accurately because the data from onboard the ship included information that did not correspond substantially to the rest of the documentation. This lead to focus the calibration of the model on more general data rather than the pressure trace which could help in the estimation of the indicated work which is the main indicator of the engine's output. Since there were no engine measurements available for the Fuelsave operation, the model was attempted to be calibrated using literature sources as well as some experimental data supplied by FVTR.

11.2.2. Recommendations

The model's outputs could be improve by considering the following recommendations. The current Seiliger parameters which are used in the model do not take into account the different fuels properties. Considering the thesis of J. Svan, [10] where the adjusted parameters take into account the injected fuel per cycle it would be a nice comparison between the two. Furthermore, since no measurements were available for the Fuelsave operation on the M32E engine the results of the model are validated based on the FVTR experiments and from literature. To improve the accuracy of the model it would be interesting to have real data and compare the exact effects of the technology with the current approximations.

The combustion efficiency as it is in the model provides a fine estimation but it does not provide the freedom for the Fuelsave technology to show the possibility of improved efficiency since the result is 100 %. It would be possible to have a more appropriate calculation of the combustion efficiency by using equation 8.3 which takes into account the emissions related to incomplete combustion. Based on the measurements a conclusion would be possible to be drawn and the model would be able to take into account a better combustion efficiency estimation.

The thermodynamic properties of the additives were not taken into account in the model due to the assumption of being very small quantities compared to the rest. Even-though the quantities were small it would be more suitable to include methanol's specific heats since it could alter the gas constant of

the air which is associated with the ideal gas law thus resulting in a more accurate output of pressures and temperatures. In addition, the water properties could be further examined on how they can change the humidity of the incoming air and notice the impact in the model.

The engine B model does not provide the freedom of defining the flame speed of each fuel. Therefore when the methanol, hydrogen and diesel are ignited there cannot be a prediction of how the peak pressure and temperature will be impacted in the cylinder due to the difference in flame speed.

Last but not least, in case there are available measurements from emissions about the M32E engines it would be beneficial to implement an estimation of emissions in the current model. By doing so, the recommended combustion efficiency equation could be also tested and a further investigation of the Fuelsave technology by changing the quantities of the additives could be performed.

11.2.3. Future work

In this section some of the suggestions for future work will be discussed for the improvement of the research. The model was calibrated with data during sailing of the Bravenes, with the DG1 engine functioning at 100% load conditions according to the documentation. As was noticed some of the measurements between the received data produced contradicting results which made the calibration and some of the conclusions more challenging. It would be recommended for Van Oord to examine the mentioned issue so more accurate data could be used in the continuation of the research in the future.

Bravenes is a subsea rock installation vessel meaning that it is operating in low load conditions during projects. It would be recommended to analyse the operational profile of the vessel and combined with correct measurements for the engines operation, create different calibration scenarios in the model with the proper Seiliger parameters. This will help to create calibrated pressure-volume diagrams for different operational points, enabling a more accurate comparison with the Fuelsave technology effects on the combustion shape when the measuring program takes place.

Last but not least, it would be an interesting research to process the data from the Fuelsave measuring program when this takes place and model the change to the engine's performance with the increasing replacement of diesel fuel to methanol-water and hydrogen for different operational points. In order to successfully model such scenario proper information are required. In case the model needs to be used for another engine the whole procedure will need to be repeated since only when the correct values the results will be accurate.

A

Bravenes M32E 8 cylinder measurements

Figures A.1 and A.2 display the two 8 cylinder engines onboard of Bravenes for the same operational conditions.

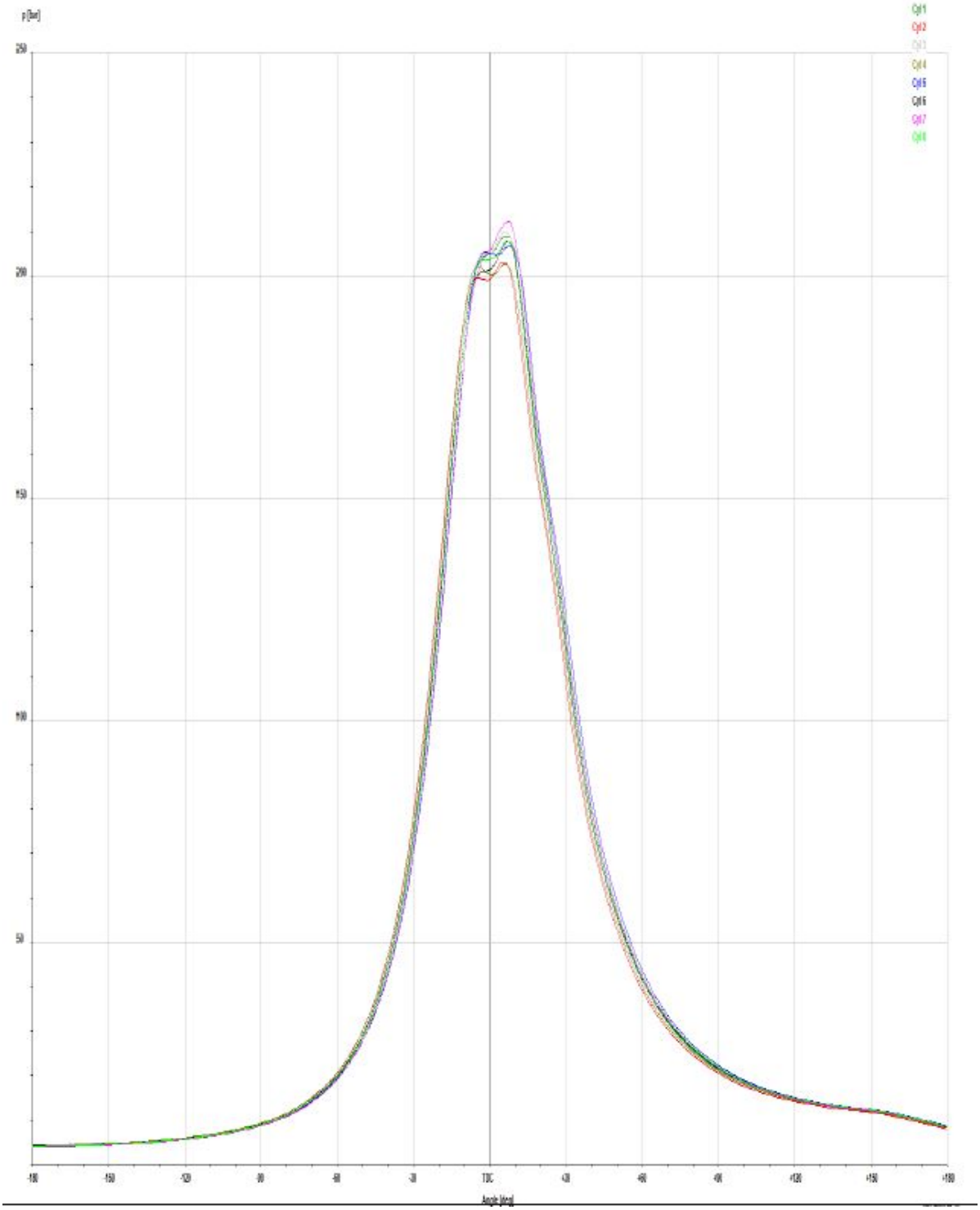

Figure A.1: Pressure-Crank angle measurement from Bravenes DG1, [28]

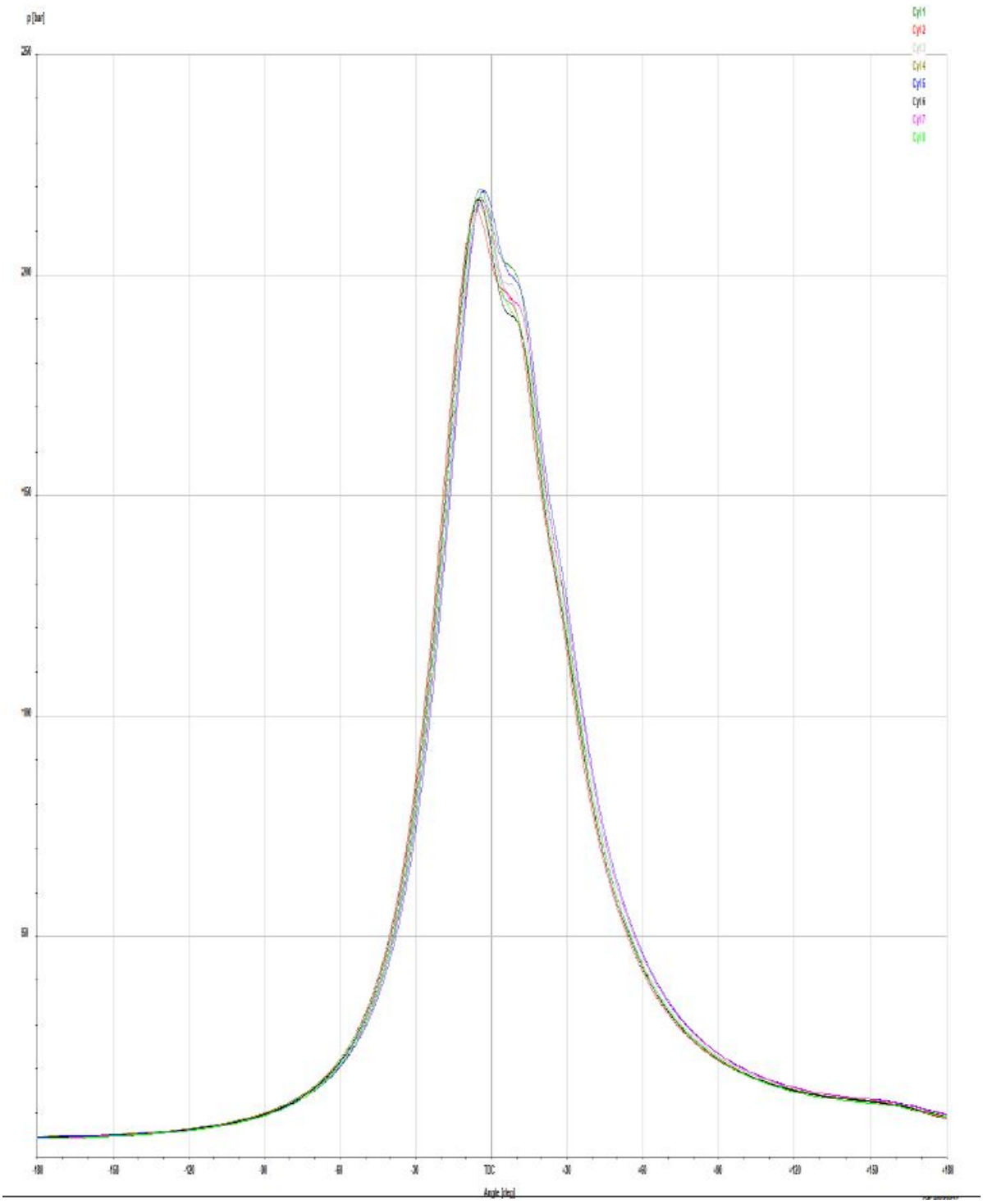

Figure A.2: Pressure-Crank angle measurement from Bravenes DG4, [28]

B

Bravenes measurements investigation

To further investigate the data contradiction issue, using equation B.1 the estimation of the indicated work was performed. Instead of deriving the change in volume in time $\frac{dV}{dt}$, since the data were measured in crank angle it was easier to find the $\frac{dV}{d\phi}$ using equation B.2 to estimate the change in volume, [40].

$$Wi = P \cdot \frac{dV}{dt} \tag{B.1}$$

$$\frac{dV}{d\phi} = \frac{\pi}{360} \cdot V_s \cdot \left\{ \sin\alpha + \lambda_{CR} \cdot \left(\frac{\sin\alpha \cdot \cos\alpha}{\sqrt{1 - \lambda_{CR}^2 \cdot \sin^2\alpha}} \right) \right\} \tag{B.2}$$

The estimation of the indicated work per cylinder per cycle can result in the approximation of the indicated power using equation B.3 which then can be compared to the measured indicated power available in the documentation.

$$Pi = Wi \cdot f_{cyl} \tag{B.3}$$

The results of the estimated indicated work, estimated indicated power and measured indicated power can be seen in table B.1. From the table it can be seen that the calculations based on the pressure trace measurements confirm the data found in documentation. On other hand this result does not match with the 3920 kW generator power found in another data-sheet about the same trip. In addition, there are more data which contradict with the values of the pressure traces. To begin with, the fuel rack position at the current time of the trip is near the maximum available position meaning that there is enough diesel injected in the cylinders to produce nearly the nominal 4400 kW power of the DG1. Furthermore, at the time of the sailing trip the only engines in operation are the DG1 and DG4, which according to figure B.1 the DG1 and DG4 provide independently nearly 3400 kW to each of the main thrusters powering Bravenes to travel at around the designed speed at full load.

Cylinder number	Wi estimated [kJ]	Pi estimated [kW]	Pi measured [kW]
1	65.76	394.55	394
2	51.81	310.84	310
3	60.72	364.34	363
4	55.41	332.44	332
5	73.73	442.35	441
6	63.27	379.61	379
7	70.50	423.02	422
8	66.01	396.36	395
Total	507.25	3043.50	3036

Table B.1: Indicated power and work based on pressure trace

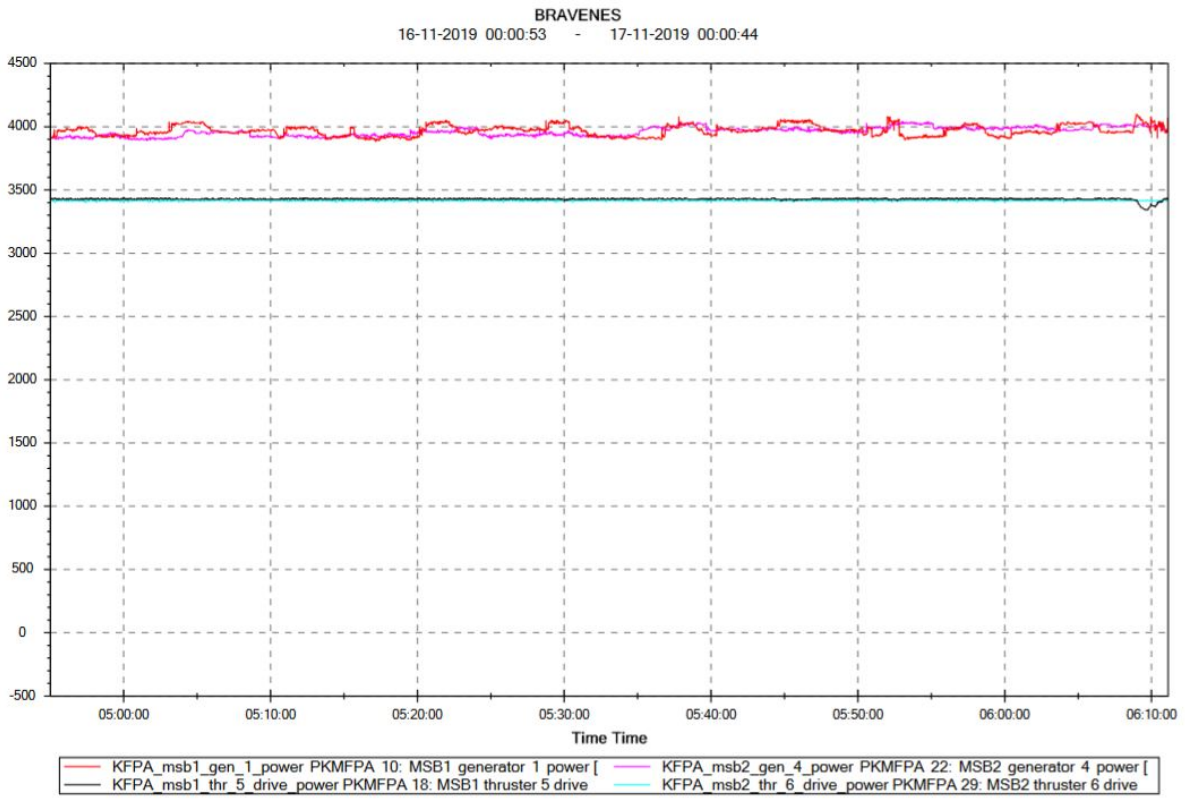

Figure B.1: Generator and thruster loads,[28]

The model was calibrated based on the two available indicated powers in order to indentify which of the two is more appropriate to be used.

Measurements for 3036 kW indicated power The first model calibration is about the engine running at around 65.5 % load conditions producing around 2884 kW brake power. The pressure-volume diagram of the model will be compared to the measured diagram along with the peak pressure and indicated work in order to conclude in the continuation of the research.

Parameter	Value [-]
n_{comp}	1.36
n_{exp}	1.285
$X_{a,c}$	0.175
$X_{a,n}$	-0.1
$X_{b,c}$	0.78
$X_{b,n}$	-0.4
a	1.16
bb	1.65
b	1.42
c	1.66

Table B.2: Calibrated Seiliger parameters for diesel operation 3036 kW

From the two diagrams 6.5 and B.2 and the related tables including the parameter values 6.1, B.2 it can seen that the peak pressure decreased from 250 bars to around 213 bars which is near the initial aim. In addition, it can be seen that changes in the parameters include the increase of n_{comp} and the decrease of $X_{a,c}$, $X_{b,c}$ and n_{exp}.

Furthermore, the polytropic compression, n_{comp} was increased from 1.35 to 1.36 while parameter a decreased from 1.43 to 1.16. The combination of the two parameters resulted in a peak pressure of 213

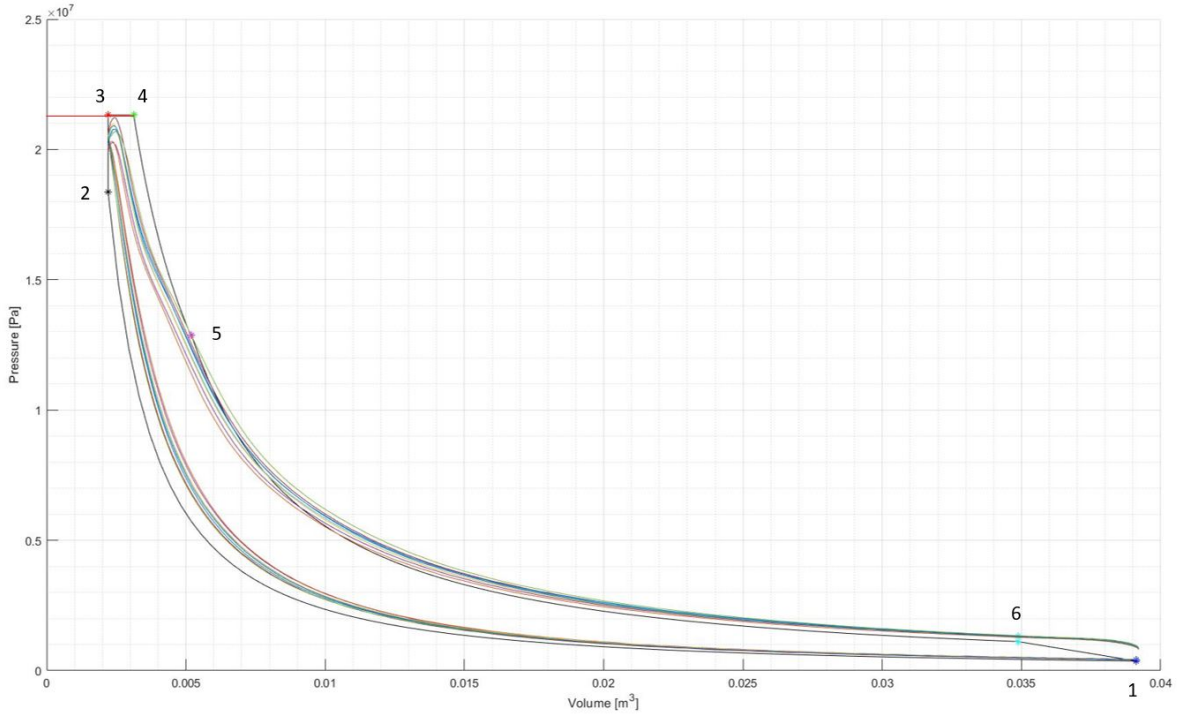

Figure B.2: Pressure-Volume diagram for 3036kW indicated power compared to measurements

bars while also providing as close as possible values to the measurements for the compression stage 1-2. As Yu Ding mentioned in his research the n_{comp} needs to be chosen wisely so it can describe heat loss process in that stage, [5]. This can be explained because during the compression stage the cylinder wall's have a greater temperature compared to the trapped fluid which means heat input, but whist the piston moves to the TDC the temperature of the fluid increases greater than the cylinder walls translating to heat loss which. Last but not least, parameter b increased from 1.39 to 1.42 and parameter c decreased from 1.88 to 1.66.

The above changes from the initial Seiliger parameters can be noticed in diagram B.2 where also the measurements of the DG1 8 cylinders pressure-volume trace are also included. The peak pressure for the measured and the estimated diagram are nearly identical. On the other hand the compression stage 1-2 from the model shows that less work is needed to be inputted for that stage. This means that the estimated indicated work for stage 1-2 will be higher than the actual work. In addition, for the stage 5-6 the estimated delivered work is less compared to the actual measured work. In total the averaged estimated indicated work for the 3036 kW operation of the engine is 64.88 kJ per cylinder per cycle compared to the average indicated work found from the documentation 63.41 kJ per cylinder per cycle. The two values are close enough indicating that the selected Seiliger parameters are suitable to describe the M32E engine combustion for the 3036 kW indicated power.

Measurements for 3920 kW generator power The second calibration is about the engine running at around 94% load producing around 4126 kW brake power or around 4343 kW of indicated power which is the second measurement available in the documentation.

The pressure volume diagram in figure B.3 compared to figure B.2 clearly shows a difference between the indicated work delivered per cycle. For the 4320 kW operation the indicated work from stage 4 and afterwords is greater compared to the 3036 kW. The estimated indicated work for the 3920 kW operation is 77.5 kJ per cylinder per cycle which is much higher compared to the measured 63.41 kJ.

This leads to the conclusion that the available pressure trace measurements are more consistent with the engine functioning near the 3036 kW rather the 4320 kW measurement. The issue raised out of this conclusion is that the pressure trace measurements or the readings from the engine display unit is not accurate since the results have significant deviation. From the pressure trace information it was possible to estimate the indicated work and power of the engine confirming the 3036 kW reading in that

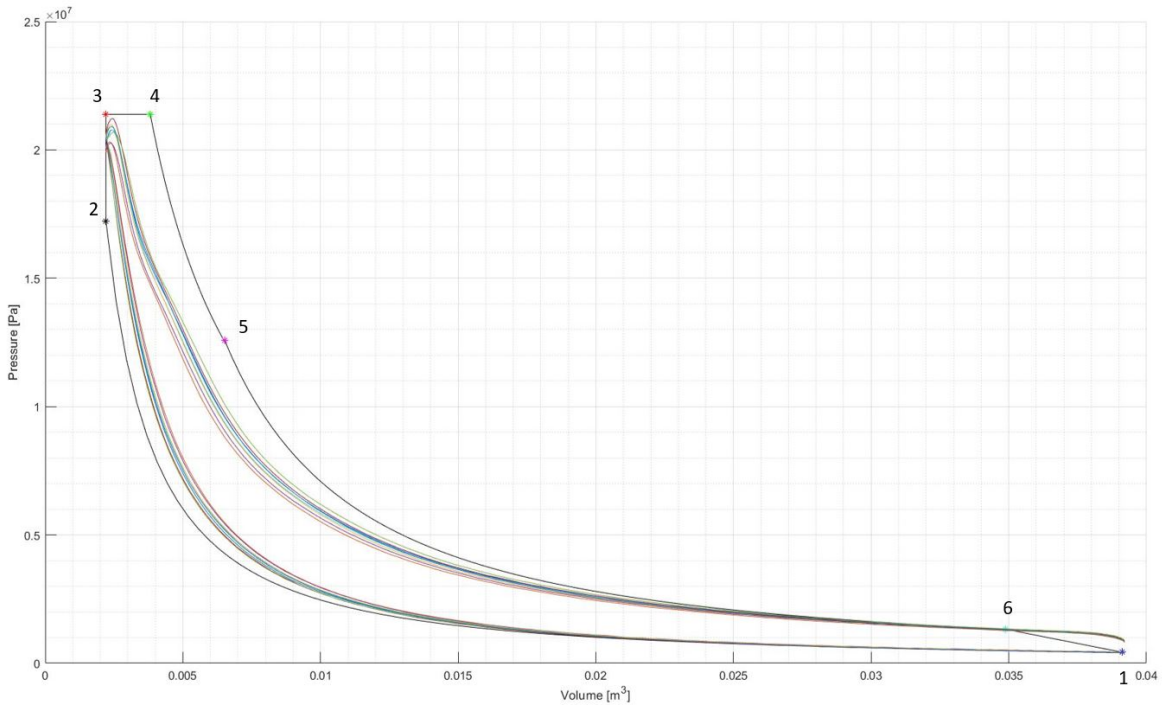

Figure B.3: Pressure-Volume diagram for 4343kW indicated power compared to measurements

Parameter	Value [-]
n_{comp}	1.285
n_{exp}	1.34
$X_{a,c}$	0.15
$X_{a,n}$	-0.1
$X_{b,c}$	0.80
$X_{b,n}$	-0.4
a	1.24
bb	2.15
b	1.73
c	1.71

Table B.3: Calibrated Seiliger parameters for diesel operation 3920 kW

document. On the other hand, the 4320 kW value it was not possible to confirm from the measurements but based on the load reading in the engine display unit which is 100 %, the fuel rack position of the cylinders compared to the engine acceptance test along with the provided diagram B.1 from Van Oord confirming the generator load and thruster load seams to provide more accurate readings compared to the 3036 kw indicated power.

Keeping in mind all of the aforementioned it was decided to try another scenario with measurements from 2018 where the indicated power reading was the highest with 3407 kW. The outcome was the same. The pressure trace measurements did not match with the recorded generator load.

The above investigation was necessary and took some valuable time of the project in order to identify the problem and decide which load to calibrate the model for. In the end it was clear that the pressure trace measurements from the engine do not match with the data found in B.1. This means that the Seiliger parameters will be chosen based on the peak pressure measurement mostly and avoiding the matching of the engine combustion indicated work. The calibration of the model for the 3920 kW generator load can be seen in chapter 6 and the verification and validation of the model in chapter 7.

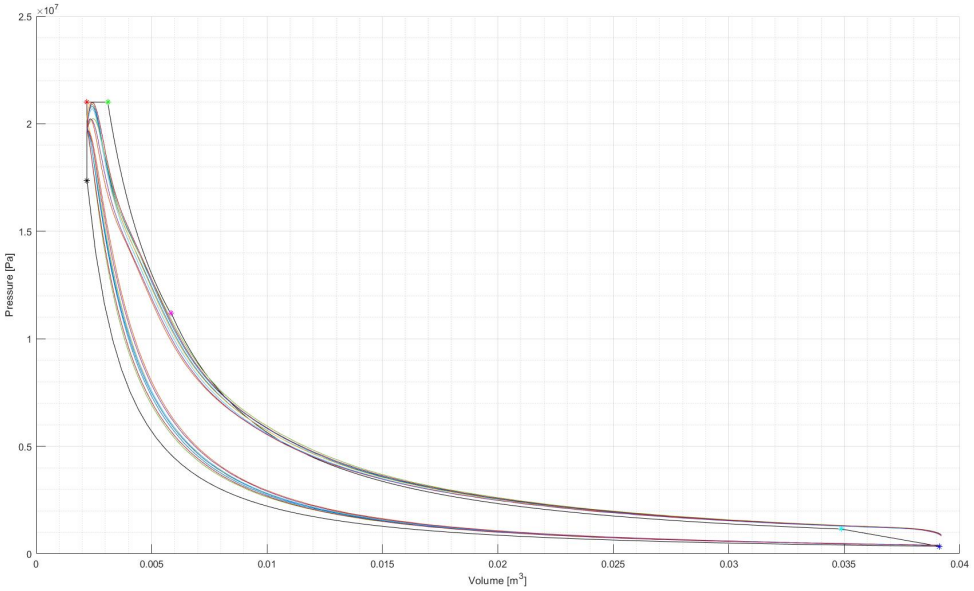

Figure B.4: Pressure-Volume diagram for 3407kW compared to measurements

Parameter	Value [-]
n_{comp}	1.36
n_{exp}	1.275
$X_{a,c}$	0.205
$X_{a,n}$	-0.1
$X_{b,c}$	0.75
$X_{b,n}$	-0.4
a	1.21
bb	1.70
b	1.41
c	1.88

Table B.4: Calibrated Seiliger parameters for diesel operation 3407 kW indicated power

Bibliography

[1] T.L. Chan C.H. Cheng C.S. Cheung et al. “Comparison of emissions of a direct injection diesel engine operating on biodiesel with emulsified and fumigated methanol”. In: *FUEL* 87 (2008), pp. 1870–1879. ISSN: 0016-2361. DOI: 10.1016/j.fuel.2008.01.002.

[2] Haengmuk Cho Changchun Xu. “Effect of Methanol/Water Mixed Fuel Compound Injection on Engine Combustion and Emissions”. In: *Energies* 14 (2021), p. 4491. ISSN: 1996-1073. DOI: 10.3390/en14154491.

[3] Yejian Qian Changchun Xu Yuan Zhuang and Haengmuk Cho. “Effect on the performance and emissions of methanol/diesel dual-fuel engine with different methanol injection positions”. In: *Fuel* 307 (2022). ISSN: 0016-2361. DOI: 10.1016/j.fuel.2021.121868.

[4] Anren Yao Chunde Yao Wang Pan. “Methanol fumigation in compression-ignition engines: A critical review of recent academic and technological developments”. In: *FUEL* 209 (2017), pp. 713–732. ISSN: 0016-2361. DOI: 10.1016/j.fuel.2017.08.038.

[5] Yu Ding. “Characterising Combustion in Diesel Engines using parameterised finite stage cylinder process models”. In: *MSc Thesis* (2011).

[6] DNV. “IMO REGULATIONS”. In: (). URL: https://www.dnv.com/maritime/hub/decarbonize-shipping/key-drivers/regulations/imo-regulations/index.html.

[7] DNV. “KEY DRIVERS”. In: (). URL: https://www.dnv.com/maritime/hub/decarbonize-shipping/key-drivers/regulations/imo-regulations/index.html.

[8] DNV. “Maritime Forecast to 2050”. In: *Energy Transition Outlook 2021* (2021).

[9] DNV. “Maritime Forecast to 2050”. In: *Energy Transition Outlook 2022* (2022). URL: www.dnv.com/maritime-forecast.

[10] J.S van Duijn. “Modelling diesel-ammonia two-stroke engines”. In: *MSc thesis* (2021).

[11] *FuelSave Marine+*. https://fuelsave-global.com/losungen/fs-marine/.

[12] Osama H. Ghazal. “Performance and combustion characteristic of CI engine fueled with hydrogen enriched diesel”. In: *International journal of hydrogen energy* 38 (2013), pp. 15469–15476. ISSN: 0360-3199. DOI: 10.1016/j.ijhydene.2013.09.037.

[13] M. Ciniviz H. Köse. “An experimental investigation of effect on diesel engine performance and exhaust emissions of addition at dual fuel mode of hydrogen”. In: *Fuel processing technology* 114 (2013), pp. 26–34. ISSN: 0378-3820. DOI: 10.1016/j.fuproc.2013.03.023.

[14] Guanglan Xu Hanjun Xu Chunde Yao. “Chemical kinetic mechanism and a skeletal model for oxidation of n-heptane/methanol fuel blends”. In: *FUEL* 93 (2012), pp. 625–631. ISSN: 0016-2361. DOI: 10.1016/j.fuel.2011.09.048.

[15] Douwe Stapersma Hans K. Wood. *Design of Propulsion and Electric Power Generation Systems*. Vol. IMarEST. 2002. ISBN: 1-902536-47-9.

[16] Hase F. W Hardenberg H. O. “An Empirical Formula for Computing the Pressure Rise Delaynof a Fuel from its Cetane Number and from the Relevant Parameters of Direct-Injection Diesel Engines”. In: *SAE Technical Paper 790493* 88 (1979).

[17] John B. Heywood. *Internal Combustion Engine Fundamentals*. Vol. 26. 02. 1988. 1988. ISBN: 0-07-028637-X. DOI: 10.5860/choice.26-0943.

[18] Ghazi A. Karim. *Dual-Fuel Diesel Engines*. 2015. ISBN: 978-1-4987-0309-3.

[19] Willem Kes. “The effect of hydrogen addition on turbocharged marine diesel engines”. In: *MSc Thesis* SDPO.16.024 (2016).

[20] H. Koten. “Hydrogen effects on the diesel engine performance and emissions”. In: *International journal of hydrogen energy* 43 (2018), pp. 10511–10519. ISSN: 0360-3199. DOI: 10.1016/j.ijhydene.2018.04.146.

[21] Kees Kuiken. *Diesel Engines for ship propulsion and power plants*. Vol. Book I: Principles. 2017. ISBN: 978-90-79104-05-5.

[22] Byungjoo Lee. “The effects of methanol fuel on combustion in premixed dual fuel engine”. In: *MSc Thesis* (2016).

[23] C. Liew et al. “An experimental investigation of the combustion process of a heavy-duty diesel engine enriched with H2”. In: *International journal of hydrogen energy* 35 (2010), pp. 11357–11365. ISSN: 0360-3199. DOI: 10.1016/j.ijhydene.2010.06.023.

[24] Guopeng Han Lijiang Wei Chunde Yao and Wang Pan. “Effects of methanol to diesel ratio and diesel injection timing on combustion, performance and emissions of a methanol port premixed diesel engine”. In: *Energy* 96 (2016), pp. 223–232. ISSN: 0360-5442. DOI: 10.1016/j.energy.2015.12.020.

[25] Gregory K. Lilik et al. “Hydrogen assisted diesel combustion”. In: *International journal of hydrogen energy* 35 (2010), pp. 4382–4398. ISSN: 0360-3199. DOI: 10.1016/j.ijhydene.2010.01.105.

[26] W. Addy Majewski. “Water in Diesel Combustion”. In: *DieselNet Technology Guide* (2002). URL: https://dieselnet.com/tech/engine_water.php#fumi.

[27] Prashant Mishra Mohit Raj Saxena Rakesh Kumar Maurya. “Assessment of performance, combustion and emissions characteristics of methanol-diesel dual-fuel compression ignition engine: A review”. In: *Journal of Traffic and Transportation Engineering* 8(5) (2021), pp. 638–680. ISSN: 2095-7564. DOI: 10.1016/j.jtte.2021.02.003.

[28] van Oord. “Bravenes engine measurements”. In: ().

[29] Schulten P.J.M. “The interaction between diesel engines, ship and propellers during manoeuvring”. In: *TU Delft* Doctoral thesis (2005).

[30] Taku Tsujimura Pavlos Dimitriou. “A review of hydrogen as a compression ignition engine fuel”. In: *International journal of hydrogen energy* 42 (2017), pp. 24470–24486. ISSN: 0360-3199. DOI: 10.1016/j.ijhydene.2017.07.232.

[31] Atul Dhar Priybrat Sharma. “Effect of hydrogen fumigation on combustion stability and unregulated emissions in a diesel fuelled compression ignition engine”. In: *Applied Energy* 253 (2019), p. 113620. ISSN: 0306-2619. DOI: 10.1016/j.apenergy.2019.113620.

[32] Michael Reska. “INVESTIGATION OF ADDITIVE INJECTION IN THE INTAKE PORT OF A SINGLE CYLINDER RESEARCH ENGINE”. In: (2018).

[33] M. Mohammad Esmaeil S. Bari. “Effect of H2/O2 addition in increasing the thermal efficiency of a diesel engine”. In: *FUEL* 89 (2010), pp. 378–383. ISSN: 0016-2361. DOI: 10.1016/j.fuel.2009.08.030.

[34] Harsh D. Sapra. “Combined Gas Engine-Solid Oxide Fuel Cell Systemsfor Marine Power Generation”. In: *PhD dissertation* (2020).

[35] American Bureau of Shipping. “Hydrogen as Marine Fuel”. In: *Sustainability whitepaper* (2021).

[36] American Bureau of Shipping. “Methanol as Marine Fuel”. In: *Sustainability whitepaper* (2021).

[37] Patrick F. Flynn Simon K. Chen. “Development of a Single Cylinder Compression Ignition Research Engine”. In: *SAE Technical Paper* 650733 (1965). ISSN: 2688-3627. DOI: 10.4271/650733. URL: https://doi.org/10.4271/650733.

[38] “Special fuels engines, Going clean and green”. In: *SWZ Maritime* 141 (2020).

[39] D. Stapersma. *Diesel Engines Volume 1, Performance Analysis*. Vol. 3. 2010. ISBN: 06934860001.

[40] D. Stapersma. *Diesel Engines Volume 3, Combustion*. Vol. 3. 2010. ISBN: 06934850003.

[41] D. Stapersma. *Diesel Engines Volume 3, Turbocharging*. Vol. 2. 2010. ISBN: 06934860002.

[42] D. Stapersma. *Diesel Engines Volume 4, Emissions and Heat transfer*. Vol. 4. 2010. ISBN: 06934850004.

[43] R.S Tol. “Combustion of methanol/diesel blends in a compression ignited engine”. In: *MSc Thesis* (2020).

[44] *Vermindering van de emissies van de scheepvaartsector*. https://ec.europa.eu/clima/eu-action/transport-emissions/reducing-emissions-shipping-sector_nl.

[45] Ir. K. Visser. “Internal Combustion Engines B”. In: *Fuels: properties* ().

[46] Guopeng Han Wang Pan Chunde Yao, Hongyuan Wei, and Quangang Wang. “The impact of intake air temperature on performance and exhaust emissions of a diesel methanol dual fuel engine”. In: *FUEL* 162 (2015), pp. 101–110. ISSN: 0016-2361. DOI: 10.1016/j.fuel.2015.08.073.

[47] *WE TAKE CARE OF POWER*. https://www.makmed.fr/en/moteurs/moteurs-mak/m-32-ce-generator-set-2/.

[48] Sarah Whiteford. “What is the difference between DP1, DP2, and DP3 vessels?” In: *OneStep Power Solutions Inc* (2021). URL: https://www.onesteppower.com/post/difference-dp1-dp2-dp3-vessels.

[49] C.D.Yaoc Z.H.Zhang C.S.Cheunga. “Influence of fumigation methanol on the combustion and particulate emissions of a diesel engine”. In: *Fuel* 111 (2013), pp. 442–448. ISSN: 0016-2361. DOI: 10.1016/j.fuel.2013.05.014.

[50] Jiangtao Li Zhiqing Zhang Jie Tian et al. “Effects of Different Mixture Ratios of Methanol-Diesel on the Performance Enhancement and Emission Reduction for a Diesel Engine”. In: *Processes* 9(8) (2021), p. 1366. ISSN: 2227-9717. DOI: 10.3390/pr9081366.

Nomenclature

Roman variables

a	Isovolumetric Seiliger combustion shape parameter
b	Isobaric Seiliger combustion shape parameter
c	Isothermal Seiliger combustion shape parameter
c_p	Specific heat at constant pressure
c_v	Specific heat at constant volume
E_A	Activation energy
i_{cyl}	Engine Cylinder numbers
LHV	Lower Heating Value
n_e	Engine rotational speed
n_{comp}	Polytropic compression exponent
n_{exp}	Polytropic expansion exponent
R	Gas constant

Greek variables

η_{cb}	Combustion Efficiency
η_{hl}	Heat loss efficiency
η_q	Heat input efficiency
η_{th}	Thermodynamic efficiency
λ	air excess ratio
ϕ_f	Fuel flow
σ	stoichiometric air/fuel ratio

Abbreviations

BDC	Bottom Dead Center
$BSFC$	Brake specific fuel consumption
CI	Compression Ignited
CO	Carbon oxide
CO_2	Carbon dioxide
CR	Compression Ratio
DCU	Display Control Unit
DP	Dynamic positioning

EC	Exhaust Valve Close
EO	Exhaust Valve Open
HC	Hydro Carbon
IC	Inlet Valve Close
IC	Inlet Valve Open
ICE	Internal Combustion Engine
ID	Ignition Delay
IMO	International Maritime Organisation
$MVFP$	Mean Value First Principle
PM	Particulate Matter
sfc	Specific Fuel Consumption
TDC	Top Dead Center